**US Army Corps
of Engineers**
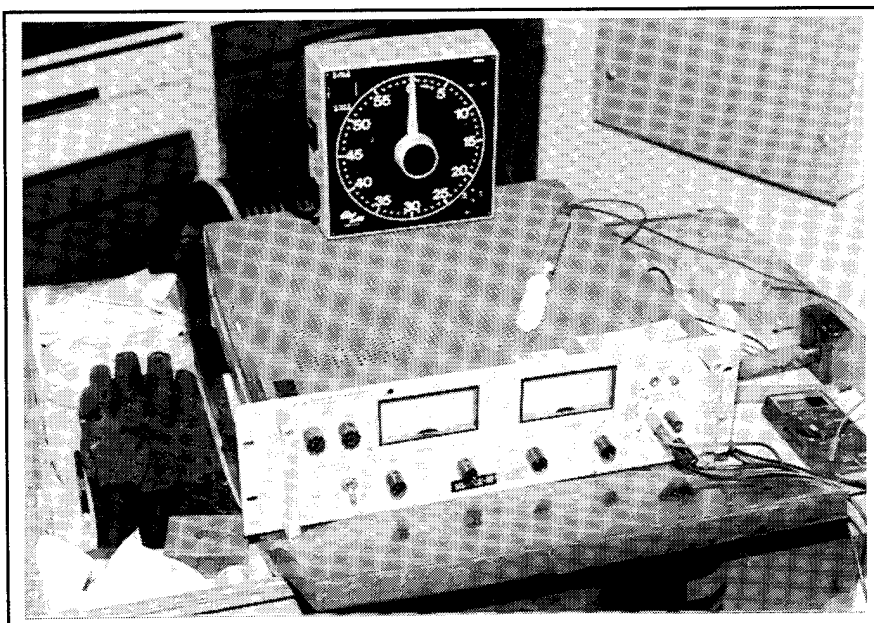Construction Engineering
Research Laboratories

Field Application of EMI Coatings

Investigation of Coating Materials and Stylus Electroplating Protocols for Shielded Facilities

by
L.D. Stephenson and L.H. Donoho

1996O426 074

To maintain reliable electromagnetic interference (EMI) shielding for electronic equipment shelter interfaces, mating surfaces such as doors and interfaces must provide low contact resistances and be resistant to excessive amounts of corrosion and mechanical wear that would tend to degrade their shielding integrity. The objective of this research was to establish the efficacy of stylus electroplating as a potentially viable field maintenance/repair technique for application of corrosion resistant, wear resistant coatings in order to help maintain the shielding integrity of those interfaces.

Aluminum alloy (6061-T6) knife-edge and channel test pieces were stylus electroplated with tin or tin-lead

coatings with nickel or copper underlayers. A custom-designed electroplating tool developed for electro-plating the complex geometry of a knife-edge substrate appears to provide better control of the plating process and circumvents possible interference with previously deposited areas.

This research has resulted in an optimized procedure for producing coatings that exhibit greater adherence, better uniformity, less scarring, and fewer blisters and ridges compared to those previously reported. An optimum electroplating strategy is suggested, which includes applying tin or tin-lead top layers over a thick layer of copper and a thin nickel strike.

DTIC QUALITY INSPECTED 1

USER EVALUATION OF REPORT

REFERENCE: USACERL Technical Report 96/55, *Field Application of EMI Coatings: Investigation of Coating Materials and Stylus Electroplating Protocols for Shielded Facilities*

Please take a few minutes to answer the questions below, tear out this sheet, and return it to USACERL. As user of this report, your customer comments will provide USACERL with information essential for improving future reports.

1. Does this report satisfy a need? (Comment on purpose, related project, or other area of interest for which report will be used.)

_____

_____

_____

2. How, specifically, is the report being used? (Information source, design data or procedure, management procedure, source of ideas, etc.)

_____

_____

3. Has the information in this report led to any quantitative savings as far as manhours/contract dollars saved, operating costs avoided, efficiencies achieved, etc.? If so, please elaborate.

_____

_____

4. What is your evaluation of this report in the following areas?

   a. Presentation: _____

   b. Completeness: _____

   c. Easy to Understand: _____

   d. Easy to Implement: _____

   e. Adequate Reference Material: _____

   f. Relates to Area of Interest: _____

   g. Did the report meet your expectations? _____

   h. Does the report raise unanswered questions? _____

i. General Comments. (Indicate what you think should be changed to make this report and future reports of this type more responsive to your needs, more usable, improve readability, etc.)

_____

_____

_____

_____

_____

_____

5. If you would like to be contacted by the personnel who prepared this report to raise specific questions or discuss the topic, please fill in the following information.

Name: _____

Telephone Number: _____

Organization Address: _____

_____

_____

6. Please mail the completed form to:

Department of the Army
CONSTRUCTION ENGINEERING RESEARCH LABORATORIES
ATTN: CECER-TR-I
P.O. Box 9005
Champaign, IL 61826-9005

REPORT DOCUMENTATION PAGE

1. AGENCY USE ONLY *(Leave Blank)*	2. REPORT DATE March 1996	3. REPORT TYPE AND DATES COVERED Final

4. TITLE AND SUBTITLE

Field Application of EMI Coatings: Investigation of Coating Materials and Stylus Electroplating Protocols for Shielded Facilities

5. FUNDING NUMBERS

MIPR
FY7620-94-AVM03

6. AUTHOR(S)

L.D. Stephenson and L.H. Donoho

7. PERFORMING ORGANIZATION NAME(S) AND ADDRESS(ES)

U.S. Army Construction Engineering Research Laboratories (USACERL)
P.O. Box 9005
Champaign, IL 61826-9005

8. PERFORMING ORGANIZATION REPORT NUMBER

TR 96/55

9. SPONSORING / MONITORING AGENCY NAME(S) AND ADDRESS(ES)

Air Force Shelter Technology Office
ATTN: ESC/AVMS
20 Schilling Circle
Hanscom AFB, MA 01731

10. SPONSORING / MONITORING AGENCY REPORT NUMBER

11. SUPPLEMENTARY NOTES

Copies are available from the National Technical Information Service, 5285 Port Royal Road, Springfield, VA 22161.

12a. DISTRIBUTION / AVAILABILITY STATEMENT

Approved for public release; distribution is unlimited.

12b. DISTRIBUTION CODE

13. ABSTRACT (Maximum 200 words)

To maintain reliable electromagnetic interference (EMI) shielding for electronic equipment shelter interfaces, mating surfaces such as doors and interfaces must provide low contact resistances and be resistant to excessive amounts of corrosion and mechanical wear that would tend to degrade their shielding integrity. The objective of this research was to establish the efficacy of stylus electroplating as a potentially viable field maintenance/repair technique for application of corrosion resistant, wear resistant coatings in order to help maintain the shielding integrity of those interfaces.

Aluminum alloy (6061-T6) knife-edge and channel test pieces were stylus electroplated with tin or tin-lead coatings with nickel or copper underlayers. A custom-designed electroplating tool developed for electroplating the complex geometry of a knife-edge substrate appears to provide better control of the plating process and circumvents possible interference with previously deposited areas.

This research has resulted in an optimized procedure for producing coatings that exhibit greater adherence, better uniformity, less scarring, and fewer blisters and ridges compared to those previously reported. An optimum electroplating strategy is suggested, which includes applying tin or tin-lead top layers over a thick layer of copper and a thin nickel strike.

14. SUBJECT TERMS		15. NUMBER OF PAGES 126
electromagnetic shielding field tests electroplating coatings		16. PRICE CODE

17. SECURITY CLASSIFICATION OF REPORT Unclassified	18. SECURITY CLASSIFICATION OF THIS PAGE Unclassified	19. SECURITY CLASSIFICATION OF ABSTRACT Unclassified	20. LIMITATION OF ABSTRACT SAR

Foreword

Contents

List of Figures and Tables

Tables

Figures

Introduction

Background

Tactical shelters that are used to protect sensitive electronic equipment require electromagnetically shielded interfaces (i.e., mating surfaces) that provide low contact resistances around doors, hatches, conduits, etc. Also, if these mating surfaces are not wear- and corrosion-resistant, the shielding integrity is easily compromised. Traditionally, these mating surfaces have required depot-level maintenance to maintain the shielding integrity.

Aluminum alloy (6061-T6) knife-edge and channel test pieces are often used as interfaces of tactical shelter doors. These aluminum alloy surfaces have adequate strength and electrical conductivity; however, they are susceptible to surface degradation from oxidation (corrosion) and other contamination, especially when exposed to a highly humid, salt-laden atmosphere. These contaminating films, which form on the surfaces of the interfaces, have lower electrical conductivities than their substrates, thus compromising the electromagnetic interference (EMI) shielding integrity. For example, shielding effectiveness may be reduced by 30 decibels (dB) simply because of corrosive or contaminating films.

To solve this problem, stylus or "brush" electroplating for environmentally-compatible field maintenance of components for tactical and strategic shelters requiring EMI shielding has undergone some rudimentary field testing. Results of previous laboratory trials revealed quality control problems with the stylus electroplating technique. For example, attempts to electroplate components similar to the interface bars for the U.S. Air Force's Deployable Strategic Mission Data Preparation Shelter (DSMDPS) resulted in blistering, flaking, burning, and poor adherence of the coating. The cause of poor quality stylus-electroplated coatings is often the improper usage or control of electroplating parameters. Furthermore, the choice of proper coating materials (e.g., single element, alloys, or mixed layers) and the thicknesses to which each are applied are critical to the coating quality.

If it is found that using stylus electroplating is suitable for application of the metal coating, it may be considered as a method for maintenance of tactical shelter interfaces based on its cost and transportability.

Much literature exists for bath (or conventional) electroplating, but little has been published on stylus electroplating. A few references indicate that stylus electroplating originated as a form of "doctoring" (or touching up) previously electroplated areas and was later modified to become a standard procedure for initial application of coatings onto parts that cannot be easily immersed into an electrolyte bath (e.g., because of substrate size or difficulty in moving the part from its service location, or because of possible interference with previously coated areas) (Byrne 1993; DOD 1988; ASMI 1994).

Objective

The objective of this research was to evaluate the effectiveness of the stylus or brush electroplating method as a function of different control parameters and coatings materials. Subsequently, a materials selection and parameter control protocol would be established for stylus electroplating of corrosion resistant EMI coatings on electronic equipment shelter components with special emphasis on adapting the coating process for (1) joining or "complexing" shelters as in the case of the DSMDPS and (2) field "repair" of shelter components.

Approach

The research was divided into four phases, and the lessons learned in each phase were integrated into the subsequent phases. The tables in this report present data on selected coating properties, appearance, thickness, adherence, and contact resistance vs. cycles behavior obtained in each phase. Micrographs (both optical and SEM) are presented for selected coating samples illustrating a series of typical coatings obtained.

The substrate (i.e., the base metal to be plated) was 6061-T6 aluminum, which is generally used in tactical shelters. Aluminum alloy knife-edge test pieces were stylus electroplated with various thicknesses of selected corrosion-resistant electrically conductive coatings at varying current densities. These pieces were electroplated on either the broadface or the knife-edge depending on the test performed; adherence tests were performed on the broadface specimens, while EMI gasket cycler tests were performed on the knife-edge samples. The coating material systems for this project were:

1. 95 percent tin - 5 percent lead (95%Sn/5%Pb) over a layer of 60%Sn-40%Pb over a thin layer of 100 percent nickel (100%Ni)
2. 100%Sn over a thin layer of 100%Ni

3.   100%Sn over a thin layer of 100 percent copper (100%Cu).

Tin and tin alloys were chosen as protective coatings because they are relatively "noble" (i.e., they do not corrode as easily as aluminum alloys), primarily because of the galvanic potential of tin (-0.14 V) compared to that of aluminum (-1.66 V) (Van Vlack 1977). Also, the tin oxide (SnO_2) that may form on the tin surface is many orders of magnitude more electrically conductive than the native oxide Al_2O_3 (Table 1.1) that may be formed on aluminum alloys under the same conditions (CRC 1972; Ben-Shalom et al. 1993). Such an SnO_2 layer would be expected to promote a significantly lower contact resistance.

Coating microstructures and thicknesses were verified before and after the tests by optical and scanning electron microscopies. Electrical resistance vs number of cycles of the coating-substrate system was ascertained by exposing test samples to 21,000 cycles in U.S. Army Construction Engineering Research Laboratories' (USACERL's) EMI Gasket Cycler Test System. Also, coating adherence to the 6061-T6 substrate was determined by the Sebastian[*] adherence test method. Flaws in the form of scratches of controllable widths and depths were introduced into the aluminum alloy test samples by an engraving device mounted on a fixture that controlled the force applied to the engraving apparatus. The scratches ranged from 0.45 mil (11.43 μm) deep × 5.62 mil (142.7 μm) wide to 6.75 mil (171.45 μm) deep × 9.75 mil (247.7 μm) wide across the width of the back sides of the test samples and along the knife-edge contact surfaces.

Scope

A complete description of the principles of electroplating is beyond the scope of this report; however, a brief review of some electroplating fundamentals is provided in the next section.

This report addresses the lessons learned during this research effort to optimize stylus electroplating technology for field application of electrically conductive corrosion-resistant, wear-resistant coatings to electromagnetic pulse (EMP) and EMI shielding interfaces, shelters, gasket mating surfaces, and other similar components. Where feasible, major developments and data are reported in chronological order.

---

[*]Sebastian Adherence Tester: Quad Group, 1815 S. Lewis Street, Spokane, WA 99204.

Fundamentals of Electroplating

Both bath electroplating and stylus electroplating are based on electrochemical reactions in which metal atoms in the form of ions are removed from the anode (positively biased electrode) to the cathode (negatively biased electrode).

In bath electroplating, the substrate (i.e, the piece to be plated) is immersed in an electrolyte solution, with the substrate electrically connected to the negative terminal (cathode) of a direct current (DC) power supply. The positive terminal (anode) of the power supply is connected to the source metal, and the power supply is adjusted to provide a selected current through the electrolyte, resulting in an electrochemical reaction known as "oxidation-reduction." In the electrolyte solution, the substrate becomes the cathode, while the source metal becomes the anode. Thus, atoms of the source metal are plated onto the substrate (Van Vlack 1977; ASMI 1994).

Stylus electroplating is simply a modification of bath electroplating in which the coating to be deposited is wiped or brushed onto the substrate, with the substrate biased at a negative polarity (thus, it becomes the cathode). The electroplating tool (i.e., the stylus) from which the coating is brushed is biased with a positive polarity; thus, the anode is composed of the electroplating tool and the solution that wets the cloth pad of the electroplating tool. As in bath electroplating, metal is removed from the anode to the cathode. In stylus electroplating, however, the source metal to be plated onto the substrate is actually predissolved in the electrolyte. Stylus electroplating is useful for plating parts that cannot be conveniently immersed into electroplating baths (Byrne 1993; ASMI 1994).

Unfortunately, the electroplating tool itself is easily degraded in this process when it is positively biased, because material is removed from the anode during the electrochemical reaction. When this happens, the electroplating tool becomes a source of contamination for the electrolyte solution, which ultimately results in the deposition of inferior coatings. In fact, any contamination on the electroplating tool (e.g., contamination from dried electroplated solutions trapped in the electroplating tool) can easily cause degradation. For this reason, electroplating tools must be thoroughly cleaned immediately after each plating session and eventually replaced. The recommended platinum-clad or stainless steel electroplating tools do not degrade as easily as graphite electroplating tools (ASMI 1994).

During the "Etch Step" in the stylus electroplating process, the substrate is positively biased and the electroplating tool is negatively biased. The purpose of reversing polarities is to remove oxides and other contaminants from the surface of the substrate prior to electroplating with the desired metals, as explained in ***Electroplating***

Procedure (p 6). Unless correct polarity is maintained for every step, undesirable results will occur.

Stylus electroplating solution and equipment vendors suggest that nickel be preplated onto the aluminum alloy substrates in order to provide a relatively "hard" surface prior to electroplating tin onto the relatively soft aluminum alloy substrate. In certain circumstances, however, copper preplates can also be used as underlayers, as discussed in Chapters 3 and 4.

Stylus electroplating expertise resides mainly with those vendors who provide the necessary stylus electroplating solutions and equipment, and those who are routinely engaged in the practice. As with many procedures of this type, stylus electroplating is "half science and half art." It is generally agreed that the quality of the resulting coatings can be significantly affected by the instincts and the skill level of the operator conducting the plating process.

Mode of Technology Transfer

It is suggested that the information presented in this report be incorporated into standing procedures for depot level maintenance or field maintenance of EMP/EMI gasket surfaces. It is further suggested that sections of this report, especially the sections subtitled "Optimum Stylus Electroplating Procedure" and "Mitigation of Blisters, Burning, Flaking, Scarring, and Poor Adhesion of Coatings" be published as a separate supplement to MIL-STD-865C (USAF) "Selective (Brush Plating), Electro-deposition" (DOD, 1 November 1988).

Metric Conversion Factors

This report uses U.S. standard units of measure throughout. When not provided in text, the table below provides the most frequently used metric conversion factors.

1 in.	=	25.4 mm
1 lb	=	0.453 kg
1 psi	=	6.89 kPa
1 μm	=	1×10^{-3} mm
°F	=	(°C $\times$ 1.8) +32
1 mil	=	0.001 in.

1 Phase I — Procedures and Initial Test Results

Equipment and Substrates

The equipment used in this research included:

- Electroplating equipment consisting of a Hewlett Packard Model 6274B DC* power supply and selected styli, pads, handles, and solutions (see Figures 1.1a,b**)
- Custom-designed USACERL Gasket Cycler Test System (Figure 1.2)
- Q-FOG SF/MP450 Salt Fog Testing Chamber*
- Sebastian I Adherence Testing Device (Figure 1.3)
- Olympus Model SZH zoom stereo optical microscope with a Model PM-10ADS automatic photomicrographic system*
- AMRAY Scanning Electron Microscope (SEM)* outfitted with an Energy Dispersive X-ray (EDX) Analysis unit* for elemental identification
- Physical Electronics Model 660 Scanning Auger Multiprobe*
- Leco M-400A Microhardness Tester* (University of Illinois Materials Research Laboratory).

The substrate samples are 6061-T6 aluminum alloy 4 in. (10.16 cm) long × 1.5 in. (3.81 cm) wide, with a knife-edge contact surface 0.375 in. (9.5 mm) high, with a 0.03 in. (0.76 mm) radius of curvature (see Figures 1.4a,b).

---

* Hewlett Packard, Inc., 211 Prospect Road, Bloomington, IL 61701; Q-Panel Co., 26200 First Street, Cleveland, OH 44145; Olympus Corp., SAN-E I Building 22-2, Nishishinjuku, 1-Chrome Shinjuku-ku, Tokyo, Japan; AMRAY Inc., 160 Middlesex Turnpike, Bedford, MA 01730-1491; EDAX Corp., 91 McKee Drive, Mahway, NJ 07430; Physical Electronics, 6509 Flying Cloud Drive, Eden Prairie, MN 55344; LECO Corp., 3000 Lakeview Avenue, St. Joseph, MI 49085-2396.

** Figures and tables are grouped at the end of each chapter.

Test Procedures

Adherence Test Procedure

The adherence strengths of sample coatings were determined (prior to being salt fog tested) using the Sebastian I Adherence Test. Test samples were obtained by cutting coupons measuring 0.25 in. × 0.25 in. (0.635 cm × 0.635 cm) from each of the electroplated substrates. Krazy Glue®* was used to adhere an aluminum stud to the electroplated side of the test coupon. With the coupon held in place, the bonded stud was loaded in tension, as shown in Figure 1.5 using the Sebastian I Adherence Device until failure of the coating or the adhesive occurred. The limit of this test is 10 thousand pounds per square inch (ksi), which is the nominal failure strength of the heat-cured adhesive precoated on the stud.

In some of the earlier adherence tests, a different stud-bonding procedure was used. High-temperature curing epoxy precoated aluminum studs were mounted and secured on the test coupon using a mounting clip. The samples were then placed in a small annealing furnace heated to 130 °C for 2.5 hr, in order to cure the epoxy and establish suitable bonding. After allowing an adequate time for the stud-mounted coupon to cool, the adherence test was conducted.

During the latter stages of this research, the high temperature curing may have caused exaggerated blisters in the coatings (perhaps because gases trapped during the coating process escaped during curing) resulting in poor adherence of the stud to the coating and causing the coating to "pop" and "crack" in some places. A 5-min curing time at 130 °C would also suffice to produce adequate stud-bonding; however, because these temperatures are not generally typical of thermal environments in which actual service coatings would be applied and exposed, use of the high-temperature curing adhesive was abandoned in favor of the room-temperature curing Krazy Glue®. Unfortunately, the bonding strength of Krazy Glue® (~3 to 6 ksi) was found to be considerably less than the bonding strength of the heat-cured adhesive (~7 to 10 ksi) on the precoated studs.

In cases where the adhesive failed, the coating adherence strength was taken to be equal to the tensile stress at which the adhesive failed. (In reality, the coating adherence strength is equal to *or larger than* the adhesive strength in such cases. If this were not the case, the coating would have been pulled off.)

---

*Krazy Glue® is a registered trademark of the Borden Corp., 180 E. Broad Street, Columbus, OH 43215.

Salt Fog Testing Procedure

Salt fog tests were performed on knife-edge samples in accordance with American Society of Testing and Materials (ASTM) Standard B-117-90. The salt fog chamber used was a Q-FOG™ Corrosion Chamber model SF/MP450. The reagent solution used was a simulated sea salt (Formula "D")[*] that complied with ASTM Standard D1141-52 produced by Lake Products, Inc. The solution contained 41.95 grams per liter (0.350 pounds per gallon) of the following dissolved solids:

Sodium chloride (NaCl) 58.490%

Magnesium chloride (hydrated) ($MgCl_2$-$6H_2O$) 26.460%

Sodium sulfate (Na_2SO_4) 9.750%

Calcium chloride ($CaCl_2$) 2.765%

Potassium chloride (KCl) 1.645%

Sodium bicarbonate ($NaHCO_3$) 0.477%

Potassium bromide (KBr) 0.238%

Boric acid (H_3BO_3) 0.071%

Strontium chloride (hydrated) ($SrCl_2$-$6H_2O$) 0.095%

Sodium fluoride (NaF) 0.007%

This sea salt solution was preferred over a pure sodium chloride solution because it provides a more rigorous test for the electroplated substrates, and it more closely simulates an ocean salt environment.

The salt fog tests took place over nonstop 72-hr periods. The corrosion chamber temperature was set at 95 °F (35 °C) and the humidifier temperature was set at 120 °F (49 °C). The humidifier was used to create a saturated salt fog between 95 percent and 98 percent humidity (Q-Fog, April 1991). The air pressure was 18 psi (124 kPa), and the humidifier temperature was kept at 120 °F (49 °C). A salt spray flow rate of 0.4 liters (0.423 qt) per hour was maintained. Upon completion of the salt fog test, a 3-min rinse protocol using deionized water was used to remove any "free" salt that might solidify on the surface as the specimens dried.

Gasket Cycling Tests

Lower contact resistance materials will provide better EMI shielding. Thus, the contact resistance was used as a first-order gauge of the comparative degree of shielding that any given EMI gasket would provide. The USACERL Gasket Cycler Test System was used for this task.

---

[*] Sea Salt (Formula "D") is manufactured by Lake Products, 71 Progress Parkway, Maryland Hts, MO 63043.

The Gasket Cycler Test System (Figure 1.2) measures four-wire contact resistance of gasketed assemblies as a function of "make-and-break" contact cycles. This device simulates the normal mechanical wear that a mesh gasket might encounter during day-to-day opening/closing of an EMI/EMP door, or assemble/disassemble cycles for tactical shelter components, such as the U.S. Air Force's DSMDPS bars. Knife-edge contact components typical of those in EMI shielding doors were premounted onto plexiglass retainer plates, which were, in turn, installed between the main plate and the slide plate using hold-down bolts and stop-blocks. The pneumatically-driven slide plate, as the name suggests, slides up and down, allowing the knife-edge samples to make and break contact with their mating elastomer mesh gaskets. The mating tin-copper-steel mesh/elastomer gasket assemblies[*] were mounted on the static main plate.

The closure force delivered by the Gasket Cycler Test System is adjustable over a range of 0 to 15 lb/in. (0 to 26.25 Nt/cm). In the tests performed during this research effort, the closure force was about 12 lb/in. (21 Nt/cm); however, the "stop" blocks on the Gasket Cycler Test System's bottom plate prevented the knife edge test pieces from compressing the gaskets by more than 20 to 25 percent. According to the wire mesh gasket vendor, this compression would correspond to an effective closure force of 3 to 4 lb/in. (5.25 to 7 Nt/cm) (private communication, J. Keenan, Tech-Etch, 5 January 1995).

The samples in this study were cycled with dwell times (i.e., the interval during which the knife edges were in contact with their mating surfaces) over the range of 30 seconds to 30 minutes. In most tests, a 30-second dwell time was used. Regardless of the dwell time, the slide plate takes 3 seconds to complete its disconnect/reconnect process; therefore, the entire cycle takes a total of 33 seconds.

An average of five contact resistance readings is computed for each of the 10 knife-edge/mesh gasket assemblies during the dwell time for each cycle. The electrical connection is then broken and reestablished in the 3-second interval, and a new cycle begins. The average resistance data for each knife-edge specimen are plotted as Contact Resistance vs Number of Cycles.

Microhardness Tests

The microhardness values for the electroplated coatings were determined on a Leco M-400A Microhardness Tester at the University of Illinois. In this test, a selected indentor is loaded with a given weight via a system of levers and thereby forced to penetrate the surface to be tested for microhardness. The average width of the

---

[*]Manufactured by Tech-Etch, Inc., 45 Aldrin Road, Plymouth, MA 02360.

resulting diamond-shaped indentation (for the Knoop indentor[*] used in this case) is measured, and this measurement is converted to microhardness units. To avoid substrate effects and for the microhardness values to be valid, the indenter must not be allowed to penetrate more than 20 percent of the coating thickness. ASTM standards[**] recommend that the indentor not penetrate more than 10 percent of the coating.

Optimum Stylus Electroplating Procedure

The following stylus electroplating procedure has evolved through the experiments described in this report. Various options included in and modifications to this general procedure were used in this research. Only those options deemed likely to ameliorate the resulting coatings were retained. Some of these earlier versions of the stylus electroplating procedure were described in previous reports (USAFSTO, February 1994, May 1994, and August 1994).

Equipment

The equipment and solutions used for these stylus electroplating experiments are listed below:

* stylus with carbon (or stainless steel) electrode and insulated handle
* cloth pads
* current electric power supply (capable of delivering at least 20 amperes at 20 volts)
* electroplating solutions
  — Etch solution
  — Desmut solution
  — Preplate layer solution (e.g., nickel or copper)
  — final layer solution(s) (e.g., tin or tin/lead alloy)

Generally, 1 gallon (3.784 liters) of electroplating solution provides 500 sq in. (3226 cm^2) of 2-mil (50.8 µm) thick coatings (i.e., a total coating volume of 1 cu in. (16.39 cm^3). *Note: Safety glasses, lab coats or aprons, and latex or polyvinyl chloride (PVC) gloves should be worn while working with these solutions. Proper ventilation is also recommended for removal of fumes generated during the electroplating process. The user should be familiar with all information on the Material Safety Data Sheets*

---

[*] As explained in ASTM Standard E-384.
[**] ASTM Standards B-578 and E-384.

(MSDS), especially with regard to safety and disposal of the small amount of waste solutions generated.

Formulas

The conventional formula suggested for calculation of the thickness of stylus electroplated coatings is given by the "Amp-hr" formula:

$$It = 10FAT$$

where:

I = current (amps.)
t = electroplating time (hr)
F = amp-hr factor (amp-hr/mil-sq in. or amp-hr/cm^2)
A = total area (sq in. or cm^2)
T= thickness (mils or μm)

The amp-hr factor (F) should be provided by the manufacturer of the electroplating solution; however, the "amp-hr" factor should be derated by 50 percent (i.e., the actual thicknesses using the electroplating procedure described here were usually found to be half that predicted by the formula).

For this electroplating procedure, the suggested current densities are in the range of 3 to 5 amp/sq in. (0.465 to 0.775 amp/cm^2). It should be noted that, while the total area to be coated is used in the "amp-hr" formula, the current density must be calculated using the contact area (A_c) (i.e., the area over which the electroplating pad makes contact with the substrate). The current density formula is:

$$\text{current density } (\delta) = I/A_c \text{ (amp/sq in. or amp/cm}^2)$$

Electroplating Procedure

Before specifying the procedure, it should be noted that "positive" or "forward" polarity means that the electroplating tool is electrically connected to the "positive" terminal of the DC power supply and the substrate is electrically connected to the "negative" terminal of the DC power supply. "Negative" (or "reverse") polarity means that the electroplating tool is electrically connected to the "negative" terminal of the DC power supply, and the substrate is electrically connected to the "positive" terminal of the DC power supply. In all but the Etch step, positive (forward) polarity will be observed. *Note: In all cases, the electroplating tool should be electrically grounded.*

Below is the general procedure for preparing and electroplating 6061-T6 aluminum substrates with tin alloy coatings.

1. Preclean parts by degreasing the substrate with gray Scotch-Brite™* No. 7448 and acetone. *Note: This degreaser may be replaced with other light alcohols or ketones, etc.* Degrease to remove any aluminum oxides until surface is shiny (free of dull luster). *Note: Proper preparation of the substrate before electroplating enhances adhesion of the coating. Conversely, improper substrate preparation can lead to poor coating adhesion.*

2. If required, mask the substrate using Microstop** (or some other lacquer that is soluble in acetone or methylethylketone). *Note: The unmasked area is the total area to be electroplated.* The procedure that follows is for an aluminum alloy substrate with a 6 sq in. (38.7 cm^2) total area.

3. Rinse thoroughly with water. *(IMPORTANT: Rinse thoroughly with water between all steps. If the residue left by the solution used in each coating step is not removed, a contaminating and nonconductive gel will form on top of the freshly coated layer.)*

4a. (Optional) Connect the "negative" clamp to the substrate and the "positive" clamp to the electroplating tool to obtain positive (forward) polarity. Electroclean with LDC-01 solution*** at 10-15 V for 30 sec per 6 sq in. (38.7 cm^2) of area. *Note: This step will be necessary only when the precleaning step (step 1) was not sufficient to remove contamination from the substrate.*

4b. Deactivate power supply. Rinse substrate thoroughly with water.

5a. Connect the positive clamp to the substrate and the negative clamp to the electroplating tool to obtain negative polarity. Etch with 10 percent HCl (LDC-02) with negative polarity at 12 to 15 V until the surface is a uniform black.

5b. Deactivate power supply. Rinse substrate thoroughly with water.

6a. Reverse electrical connections to obtain positive polarity. For this step and all following steps, positive polarity is observed. (A cleaning step between the Etch step and the De-smut test has been implemented, which consists of scrubbing substrate surfaces thoroughly with Scotch-Brite™ No. 7448. This renders the De-smut step, also known as the "Chromium/Sulfuric Acid Activator Step," optional).

6b. (Optional) De-smut with hard chrome activator/20%H_2SO_4 Solution (LDC-06) at 12 to 15 V (positive polarity) until the surface is a light color.

7a. Deactivate power supply. Scrub the substrate thoroughly with Scotch-Brite™ No. 7448 until a bright shiny surface is obtained.

7b. Rinse substrate thoroughly with water. Gently dry with clean lint free cloth or paper towel. Avoid scratching the surface.

8a. (Steps 8a,b may be omitted if steps 9a,b are to be performed.) Prewet surface with Formic Acid/Ni (LDC-2801) with *no* current (i.e., deactivate the power supply). Immediately preplate with Formic acid/Ni (LDC-2801) with a forward (positive) polarity at 18 V until uniform nickel color is obtained.

8b. Rinse substrate thoroughly with water. Gently dry with clean, lint-free cloth or paper towel. Avoid scratching the surface.

9a. (Steps 9a,b may be omitted if steps 8a,b have been performed.) Preplate with copper solution (LDC-2902) with a forward (positive) polarity at selected current densities (usually 3 to 5 amp/sq in. or 0.465 to 0.775 amp/cm^2) until the coating has acquired the desired thickness.

9b. Deactivate power supply. Rinse substrate thoroughly with water. Gently dry with clean, lint-free cloth or paper towel. Avoid scratching the surface.

10a. (Optional) Immediately plate with 60%Sn-40%Pb (LDC-5082A) forward polarity at selected current densities (usually 3 to 5 amp/sq in. or 0.465 to 0.775 amp/cm^2) until the coating has acquired the desired thickness.

10b. Deactivate the power supply. Rinse substrate thoroughly with water. Gently dry with clean, lint-free cloth or paper towel. Avoid scratching the surface.

11a. Immediately plate with 95%Sn-5%Pb (LDC-5082B) or with 100 percent Sn solution (LDC-5082) forward polarity at selected current densities (usually 3 to 5 amp/sq in. or 0.465 to 0.775 amp/cm^2) until the coating has acquired the desired thickness.

11b. Deactivate power supply. Rinse thoroughly with water. (As previously noted, it is important to remove the residue left by the coating solution used in each coating step, *including the final step*; otherwise, a contaminating and nonconductive gel will form over the freshly coated layer.) Gently dry with clean lint free cloth or paper towel. Avoid scratching the surface.

WARNING: Do not dry final coating with acetone. Acetone may cool the coating too quickly and exacerbate undesirable volume changes that may cause blistering.

Phase I Investigation: Survey of Effects of Basic Processing Parameters

From 1 October through 31 December 1993, the Phase I investigation surveyed the effects of various basic processing stylus electroplating parameters to establish basic trends with regard to the following factors:

1. Variations of the coating application conditions/process parameters and the efficacy of the resulting coating

2.   The ability of a stylus-electroplated coating to cover a flaw in the substrate surface

3.   Adherence strengths of these coatings

4.   Behavior of the test sample/electroplated coatings on the top "KE" surface in the USACERL Gasket Cycler Test System. (Only the "KE" surfaces were coated in Phase I.)

The main thrust of this work was to evaluate the process associated with the electro-plating of shelter surfaces for EMI/corrosion protection, with the final result address-ing the field maintenance approach to be used. Consequently, a portion of the testing addressed the resilience and performance of a field repair to the electroplated surface. A subset of all test samples were intentionally flawed through the introduction of a scratch, gouge, or chip on the surface.

Flaws in the form of scratches of controllable widths and depths were introduced into the aluminum alloy test samples by using an engraving device mounted on a fixture by which the force applied to the engraving apparatus was controlled. The scratches ranged from 0.45 mil (11.43 μm) deep × 5.62 mil (142.7 μm) wide to 6.75 mil (171.45 μm) deep × 9.75 mil (247.7 μm) wide across the width of the back sides of the test samples, and along the knife-edge contact surfaces.

Results of Phase I Electroplating Experiments

Table 1.2 provides a summary of the electroplating parameters in terms of sample numbers, electroplating current (amps), time (minutes), current density (amps per square inch), and the total coating layer thickness, as determined by optical micro-scopy. The contact areas of the broadface samples were 0.9375 sq in. (samples 9BF and 10BF) and 0.7031 sq in. (samples 11BF and 14BF); the contact area of the knife-edge samples was 0.059 sq in.

The estimated thicknesses for the 95%/5% Sn/Pb layer were obtained using the thickness formula "It = 10FAT." The reason for deviation between the observed and estimated values may be related in part to the degree of validity of the formula outside of the optimum current density range.

Note the higher current densities for the "KE" specimens; this is because of the much smaller contact area on the knife-edges that were coated.

When the flaws (i.e., scratches, gouges, chips) were coated according to the procedures outlined above, the coatings always followed the contours of the flaw, *up to 6.75 mil*

deep × *9.75 mil wide*, as shown in Figures 1.6 and 1.7. The coatings always follow the contours of the scratch, no matter how thick a coating is used, so a dip will always be present in the final coating layer (this dip takes the form of the original flaw). A method of filling in this dip before applying the final electroplating layer is discussed in Chapter 4.

Optical micrographs of the coated knife-edges are shown in Figure 1.8.

Adherence Test Results

Table 1.3 lists the adherence tests results. In this report period, the adherence tests samples were bonded to pull-studs using the high temperature curing epoxy. The samples with the studs attached were subjected to a curing temperature of 130 °C for 1 hour. Comments are also provided on the appearance of the adherence-tested area and the coating in general. It was believed that some of the "cooked" appearance of some coatings and exacerbation of some of the blisters may have resulted from exposure to the high curing temperature. As mentioned earlier, a 5 minute, 130 °C exposure is satisfactory to bond the studs to the coating; however, because these temperatures are not generally typical of thermal environments in which actual service coatings would be applied and exposed, use of the high-temperature curing adhesive was abandoned in favor of room-temperature curing with Krazy Glue®.

Gasket Cycling Tests

The samples in this study were cycled in the USACERL Gasket Cycler Test System at two cycles per minute, with a 30-second dwell time (i.e., the interval during which the knife-edges were in contact with their mating surfaces). For the first part of this research, only the knife-edge of the contact resistance test samples was electroplated because that part is the most degraded by contamination and mechanical wear during opening/closing cycles of an EMI door.

During this report period, some of the test samples tended to have higher contact resistances as a function of the test positions in which they were placed on the plexiglass mounting blocks (due, in part to the configuration of the steel wire mesh/ elastomer chosen for the mating surface of the knife-edge test samples on the bottom of the gasketed assemblies). To remove this position-factor bias inherent in the testing procedure, each of the test knife-samples were tested in several different positions and the resulting contact resistances were measured and compared. In this way, certain trends in contact resistance as a function of the knife-edge test samples (regardless of their test positions in the gasket cycling device) could be ascertained. A total of seven tests of 3,000 cycles each were conducted, according to the following test schedule:

The first test of 3,000 cycles was conducted on the set of knife-edge test samples in the as-received condition. The next 3,000-cycle test was conducted after the same set of knife-edge test samples was scrubbed with Scotch-Brite™. In the remaining five tests, the unplated knife-edge samples were scrubbed with Scotch-Brite™ as in the second test; however, the samples were moved to different positions on the Gasket Cycler Test System before each test.

Observations

Some contact-resistance trends have been observed; however, the nature of the testing process discussed above confounds the results and does not allow easy isolation of multiple factors inherent in the testing process that influences the contact-resistance measurement. However, these trends were observed:

1. The contact resistances for all knife-edge samples generally increase with the number of cycles, as seen in Figures 1.9a and 1.9b.

2. Over a 1000-cycle period, contact resistances for *uncoated* samples tend to exhibit more erratic measurements than those of *coated* samples, as seen by comparing Figures 1.9a and 1.9b. A similar observation has been made by Prof. Bruce L. Cain (private communication, Mechanical Engineering Dept., Mississippi State Univ., 1 November 1994).

3. Over a 1,000-cycle period, contact resistances for *uncoated* samples tend to increase at a faster rate than do contact resistances of *coated* samples, as shown in Figure 1.9b.

4. "Biting" of mesh into knife-edge—periodic marks (typically a rectangular 8 mils × 20 mils [0.20 × 0.51 mm] and typically 0.12 to 0.16 in. [3.05 to 4.1 mm] apart) were observed after gasket cycling tests. As the mesh gasket makes contact with the knife-edge samples, the wire mesh bites into the surface metal (coating or substrate) making discernable marks that seem to exhibit a degree of periodicity. These marks were observed after 9,000 cycles for the coated knife-edges, and 15,000 cycles for the uncoated knife-edges (Figures 1.10a,b). These bite marks seem to correlate to the periodic nature of the contact mesh weave; the spacing between each strand of the wire mesh was approximately 0.12 in. (3.05 mm).

The following trends pertaining to the Gasket Cycler Test System were also observed:

1. **Position effect**—Some test positions seem to provide lower contact resistance regardless of the preparation of the test samples. Some positions provide better electrical contact as seen from the first two cycling tests (of 3,000 cycles each) where only uncoated knife-edge samples were tested. Samples mounted in

positions 1 through 5 exhibited a lower resistance than samples in positions 6 through 10.

2. **Elastomer relaxation effect**—If the Gasket Cycler Test System is left overnight with the slide plate parked in the "down" position (with the knife-edge test samples making contact with the mesh gasket mating surfaces), contact resistances will initially be lower when the device is started again the next morning, compared to the contact resistances measured if the slide plate was parked in the "up" position overnight.

3. **Dwell time**—Contact-resistant value obtained also depends on the dwell time. For example, if a longer dwell time is chosen (2 minutes rather than 30 seconds), lower resistances are obtained.

4. **Squeeze effect**—By briefly and gently squeezing the ends of the mesh gasket, the contact-resistance measurements decreased drastically for the next 50 cycles, and then the contact resistances usually recover their "pre-squeeze" values. Actually, the effects described in 2, 3, and 4 are all apparently related to the general phenomenon of elastomer relaxation (Figure 1.11).

5. **Creasing**—The wire mesh elastomer deforms over a period of cycles; it acquires a permanent crease where the sample knife-edge has been connecting and disconnecting. If such a gasket is then inverted, the contact resistance on the non-creased side will be generally lower than the resistance of the creased side.

6. **Terminal fatigue**—Fatiguing of the electrical terminals that connect the cables on the test samples was observed. This fatiguing occurs as the electrical contacts are pressed against the flat back sides of the knife-edge test sample in cyclic loading. Eventually, the terminals bend and start to break.

7. **Consistency**—Consistency in installing test samples is always the goal, but is not always easily achieved.

8. **Effect of mating gaskets**—Obviously, the choice of mating gasket influences the value of the resistance measurement. (Alternative mating surfaces for the test knife-edge samples [e.g., fingerstock, phosphor-bronze mesh] are suggested for future research.)

9. **Other impediments**—One of the remaining impediments to establishing if these contact- resistance measurements represent the norm are small perturbations in the position of the bottom mesh gasket. For example, if the wire mesh gasket mating surfaces wiggle out of the firm contact configuration, the measured contact resistance may increase. This increase will tend to confound the measurements for the knife-edge test samples. One must then be aware of the idiosyncrasies inherent in the gasket cycling contact resistance measurement process, especially with regard to the elastomer-relaxation effects in mesh gasket mating surfaces. In real-world applications, this effect is directly related to how frequently an EMI door is left closed before it is again opened.

Discussion of Phase I Results

Table 1.4 summarizes the observations of coated samples and subsequent testing. The following general conclusions can be drawn:

1. All the coated samples showed periodic contact marks referred to as "bite marks," which seems to correlate to the periodic nature of the contact mesh weave.
2. The uncoated samples, at this point, did not show "bite marks," which is probably because of the hardness of the 6061-T6. However, after 9,000 cycles, the uncoated samples did exhibit bite marks similar to those observed on the post-cycled coated samples.
3. Generally, the mid- to high-range current densities do not leave blisters as do the low current densities.
4. Blisters produced at high-current densities tended to be smaller and form in "lines" compared with those produced at low-current densities, which were larger and randomly oriented. This indicates that (a) blisters produced at high-current densities are formed during the coating process and the blister lines parallel the direction of brush strokes and (b) blisters formed at low-current densities tend to be more randomly oriented and may form more slowly over a post-coating period of time.

Finally, the coated surface of the 6061-T6 aluminum alloy substrate can easily cover a flaw (in the form of a scratch ranging from 0.45 mil wide × 5.62 mil deep to 6.75 mil wide × 9.75 mil deep) by following the contours of the flaw.

Table 1.1. Factors affecting selection of various coatings.

	Electrical Resistivity of Coating ($\mu\Omega$-cm)	Electrical Resistivity of Oxide ($\mu\Omega$-cm)	Galvanic Potential of Coating (V)	AMP-HR FACTOR (amp-hr per sq in per mil)—related to ease of plating	Approx. Hardness Mohs[1] (Bulk) DPH[2] (Coating)
Tin (Sn)	11.0	3000 (SnO_2)	-0.14	0.05	Mohs: 2 DPH: 7
Copper (Cu)	1.67	N/A	+0.34	0.13	Mohs: 2.5 -3 DPH: 140 -210
Nickel (Ni)	6.84	N/A	-0.25	0.3	Mohs: 5 - 6 DPH: 280 -580
Aluminum (Al)	2.65	3×10^{19} (Al_2O_3)	-1.66	N/A	Mohs: 2 - 2.9 DPH: N/A

[1] Mohs hardness scale based on relative scratching capability.
[2] DPH = Diamond Pyramid Hardness values for stylus electroplated coatings.

(a)

(b)
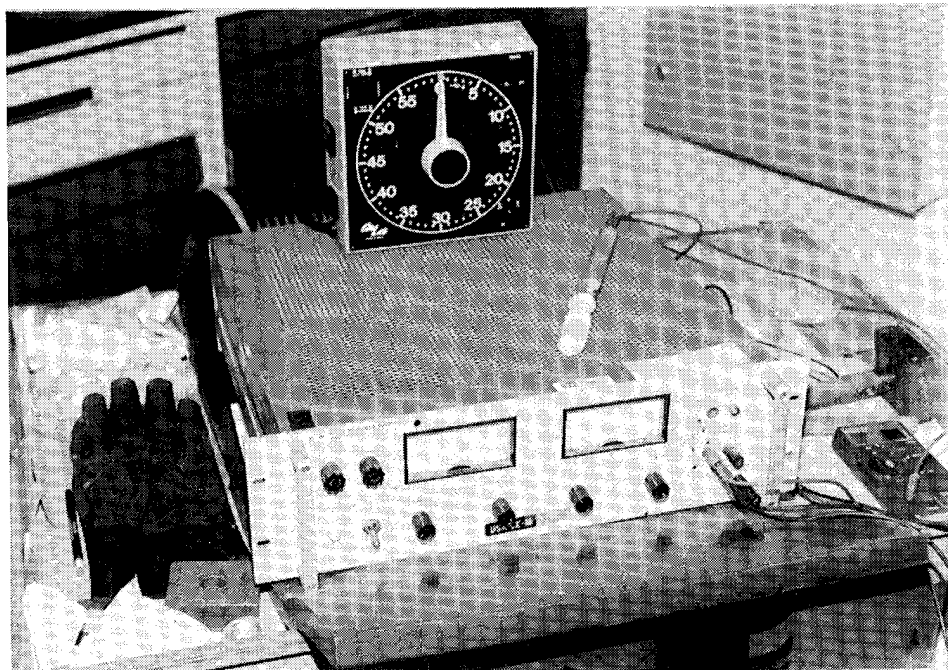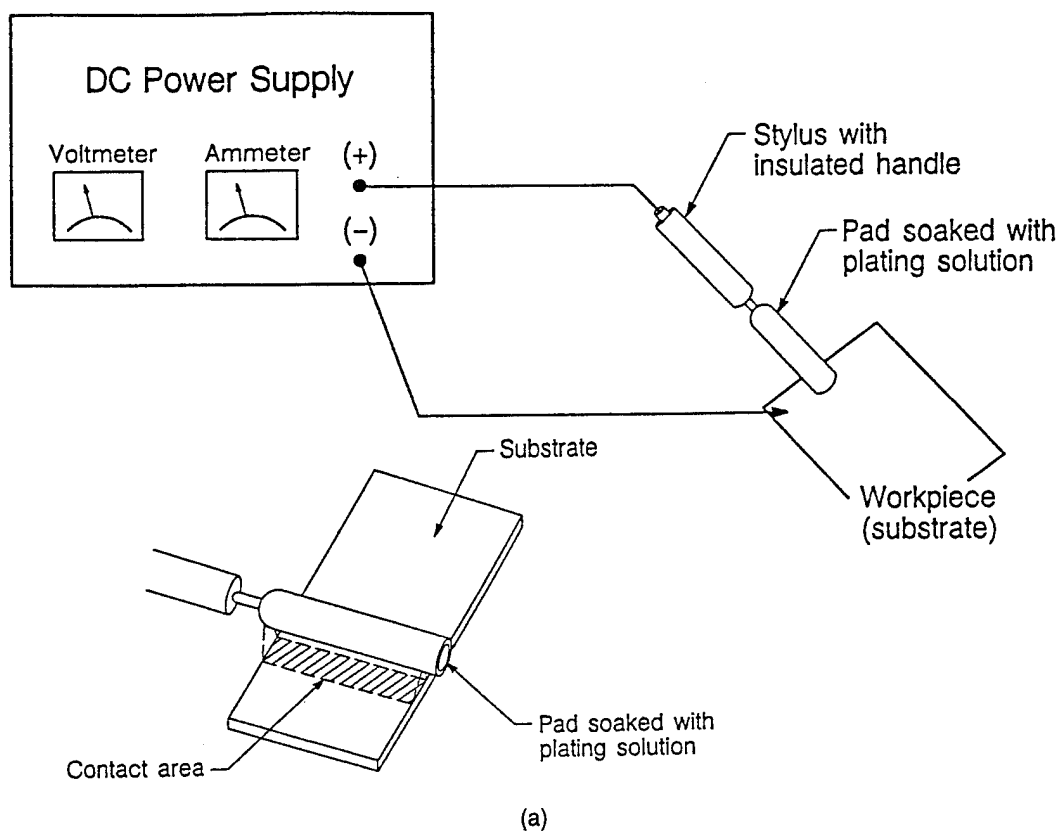
Figure 1.1. Stylus electroplating—(a)schematic diagram and (b) equipment: DC power supply, electroplating tool baton with Dacron® wrap, and timing clock.
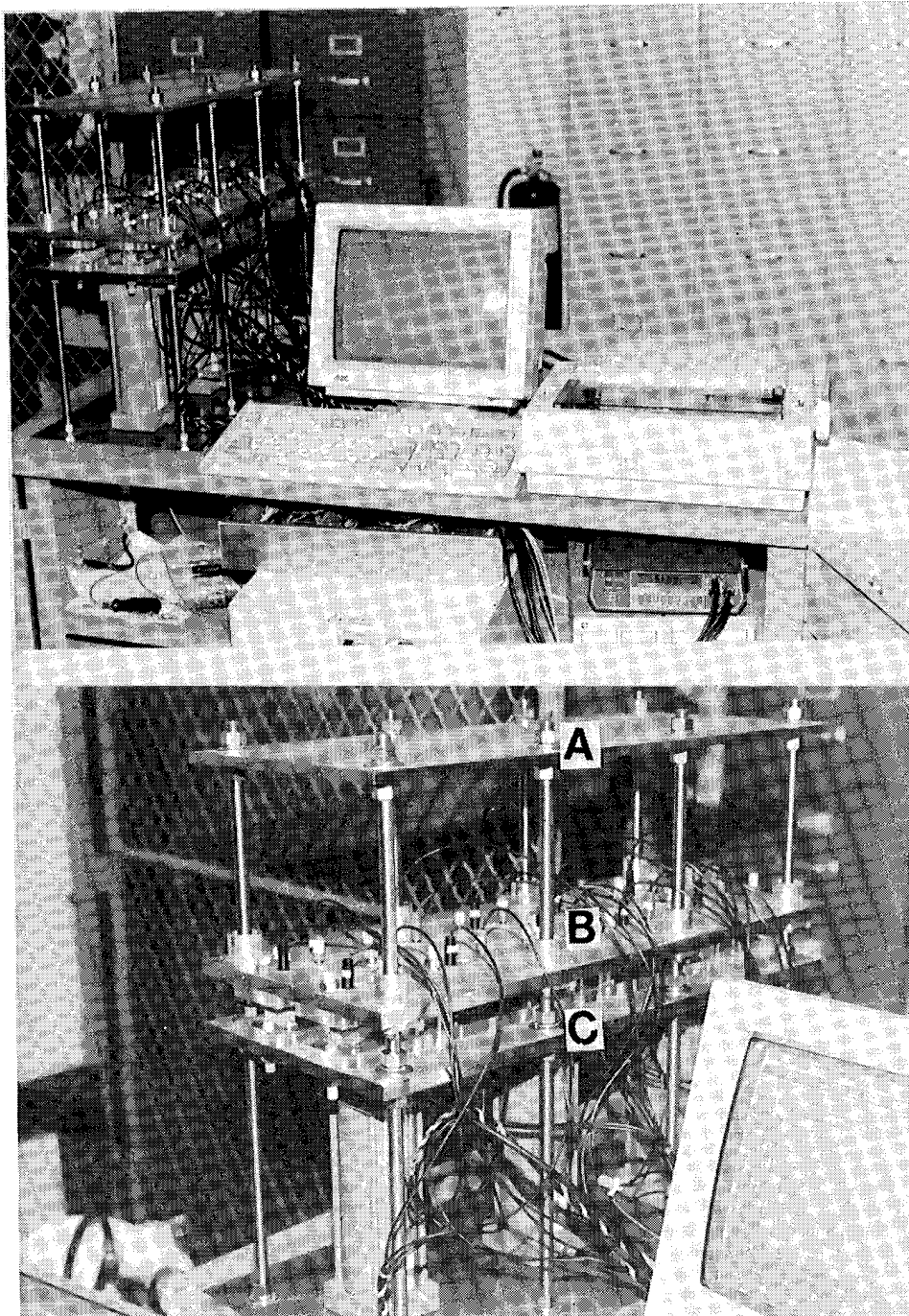
Figure 1.2. The USACERL Gasket Cycler Test System—(A) top plate, (B) slide plate, and (C) bottom plate.
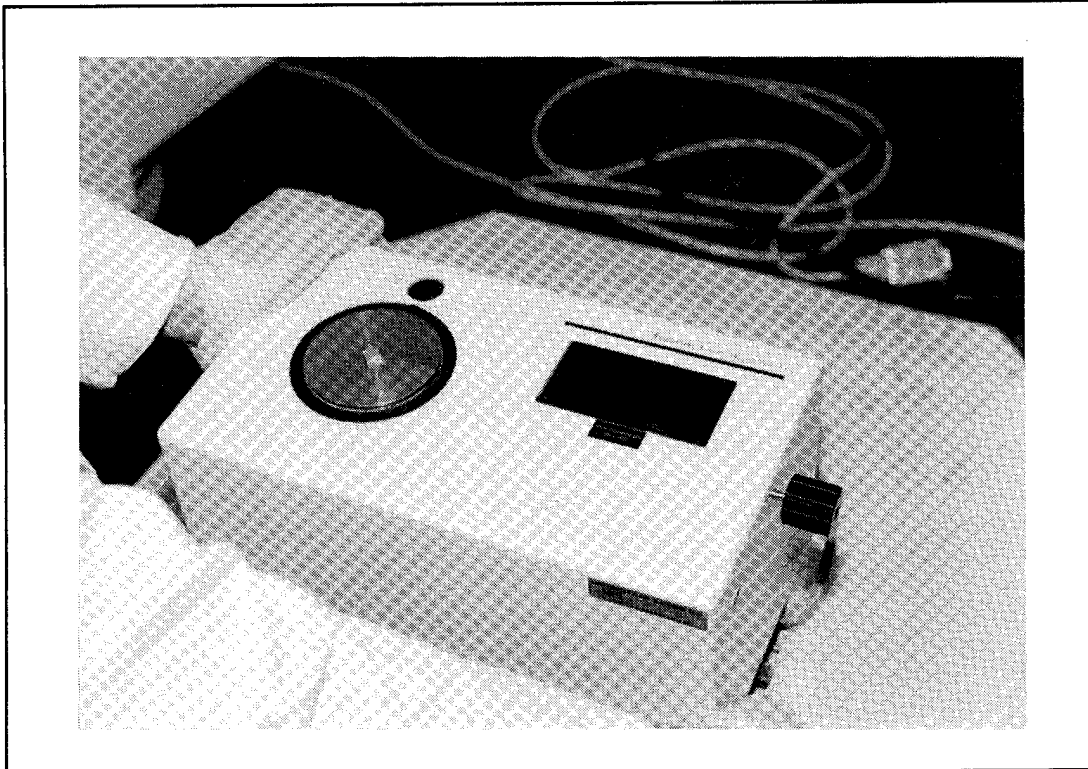
Figure 1.3. Sebastian Adherence Testing Device.

Knife-edge (KE)

Half-face (HF)   Half-face (HF)

Broad-face (BF)
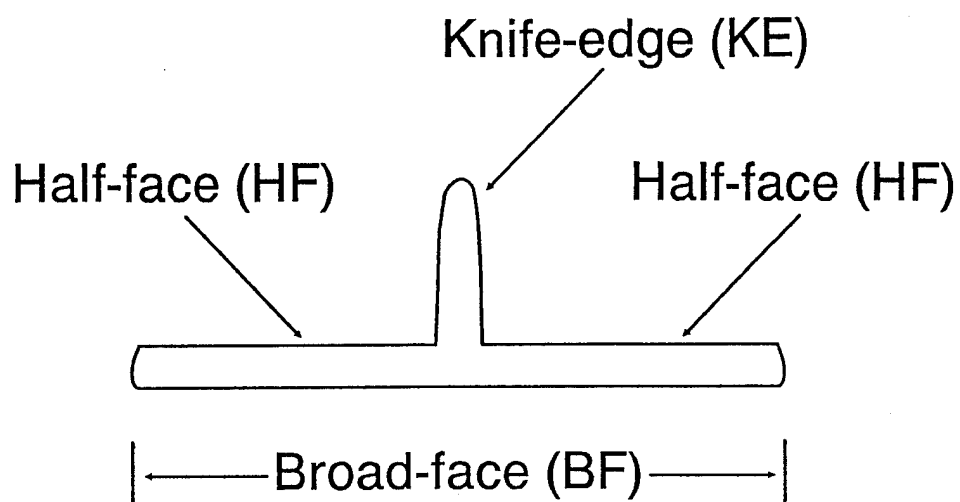
(a)
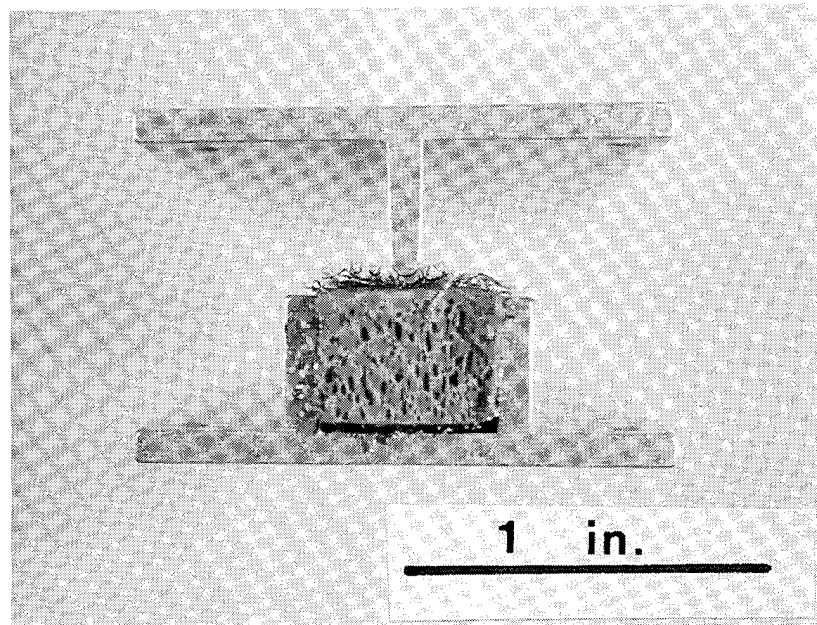
(b)

Note the knife-edge contact (typical of the pieces electroplated for this research) on top and its mating tin-nickel-iron wire-mesh covered elastomer core gasket mounted in the channel piece below. Knife-edges and channels were 6061-T6 aluminum alloy.

Figure 1.4. (a) Diagram of a cross-section of the knife-edge substrate showing the various surfaces of the knife-edge sections and (b) edge-on view of a typical EM Shielding Gasket Assembly.
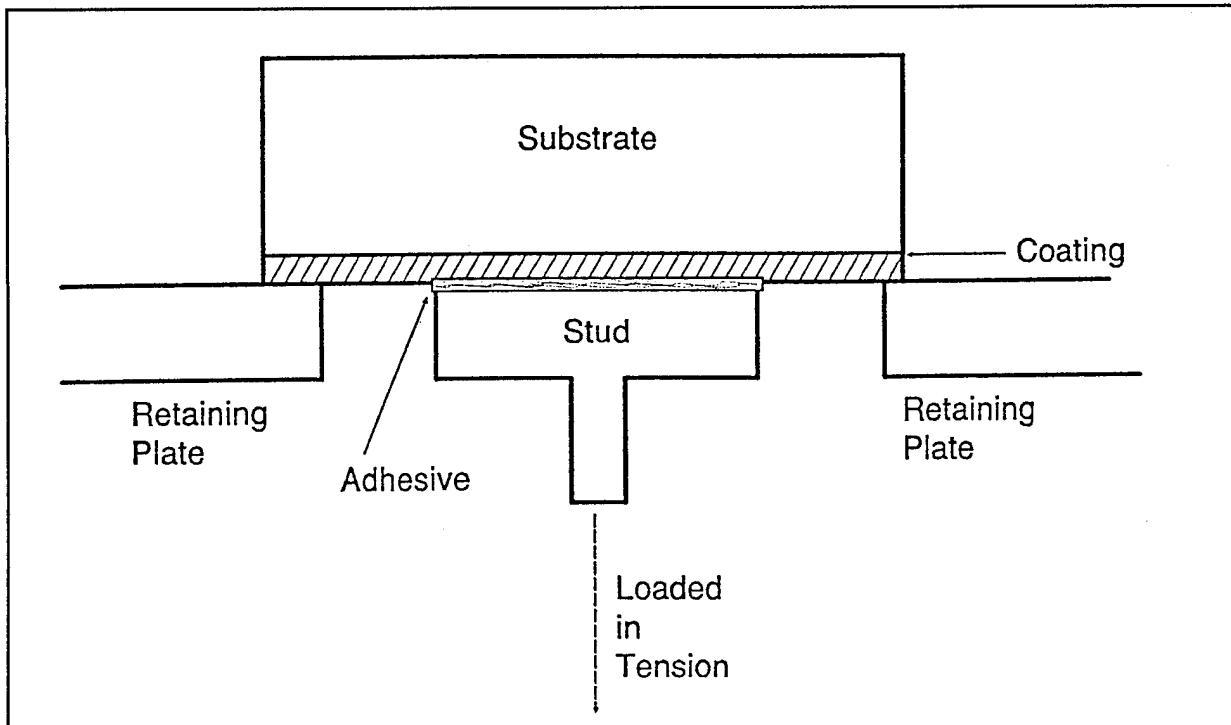
Figure 1.5. Adherence testing setup with the stud bonded with Krazy Glue® (or similar adhesive) to the coating to be tested.

Table 1.2. Stylus electroplating parameters for Samples 9BF – 14BF.

Sample#/Solution	Current (Amps)	Time (min)	Current Density (Amp/in.²)	Average Observed Thickness (mils)	Estimated Thickness (95/5) (mils)
#9BF)					
Ni	1.5	1.0	1.60		
60:40 Sn/Pb	1.8	1.0	1.92	0.90	0.89
95:5 Sn/Pb	2.0	6.0	2.13		
Coating exhibits uniform thickness.					
#10BF)					
Ni	3.5	2.5	3.73		
60:40 Sn/Pb	1.5	2.5	1.60	0.78	1.19
95: 5 Sn/Pb	4.0	4.0	4.27		
Coating exhibits uniform thickness.					
#11BF)					
Ni	3.5	2.5	4.98		
60:40 Sn/Pb	2.0	4.0	2.84	0.56	0.89
95:5 Sn/Pb	3.0	4.0	4.27		
Coating exhibits principally uniform thickness, with some variations.					
#12KE)					
Ni	0.8	1.0	13.6		
60:40 Sn/Pb	0.4	3.0	6.78	0.61	1.07
95:5 sn/Pb	0.4	3.0	6.78		
Coating exhibits uniform thickness.					
#13KE)					
Ni	0.7	2.0	11.9		
60:40 Sn/Pb	0.5	3.0	8.47	0.77	0.89
95:5 Sn/Pb	0.2	5.0	3.39		
Coating thicknesses are erratic; coating thicknesses range from 2.5 mils to 0.08 mils.					
#14BF)					
Ni	2.3	3.0	3.27		
60:40 Sn/Pb	2.8	5.0	3.98	0.77	1.48
95:5 Sn/Pb	2.0	10.0	2.84		
Coatings exhibit principally uniform thicknesses, but thicknesses vary in some regions; 60Sn/40Pb layer is easily distinguished (darker than 95Sn/5Pb), and accounts for approximately 30 percent of the entire coating thickness.					
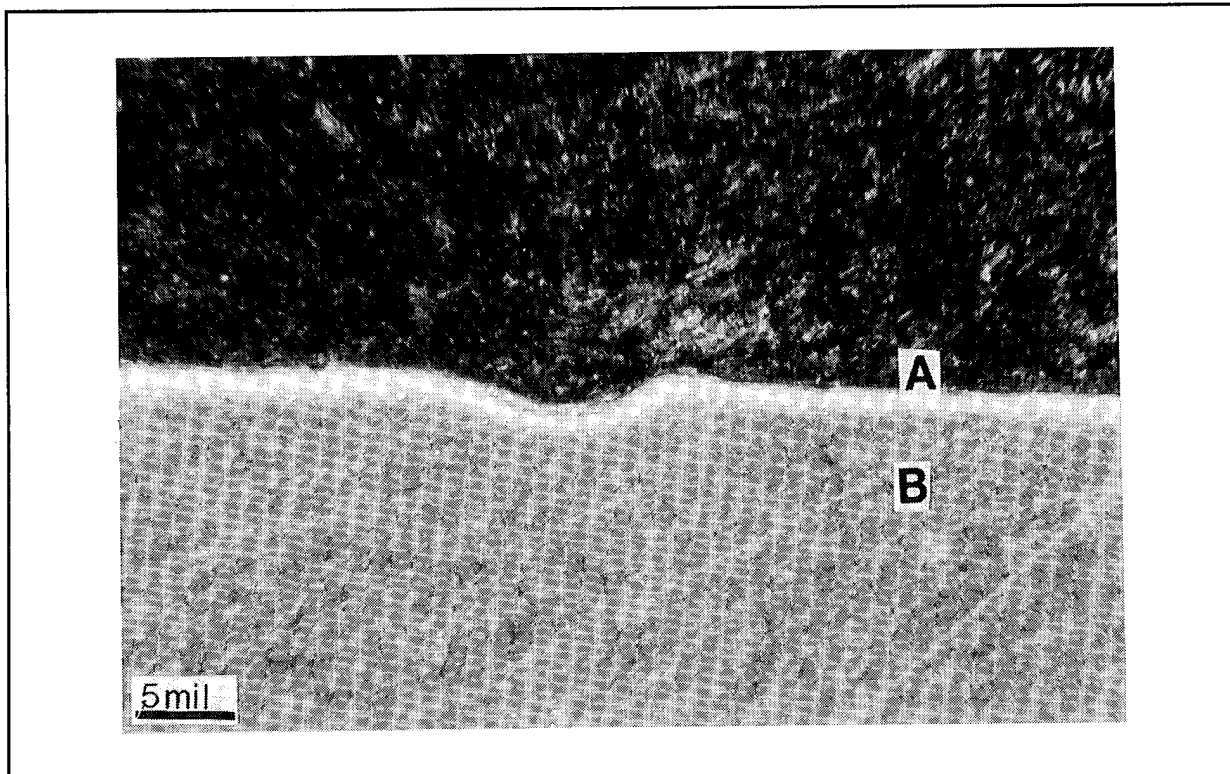
Figure 1.6. Optical micrograph of cross-sections of a 6061-T6 aluminum substrate scratched to a depth of 1.0 mil and then coated with 95%Sn/5%Pb over 60%Sn/40%Pb over Ni—(A) coating and (B) substrate of Sample 10 BF.

Arrow indicates approximate center of scratched area.
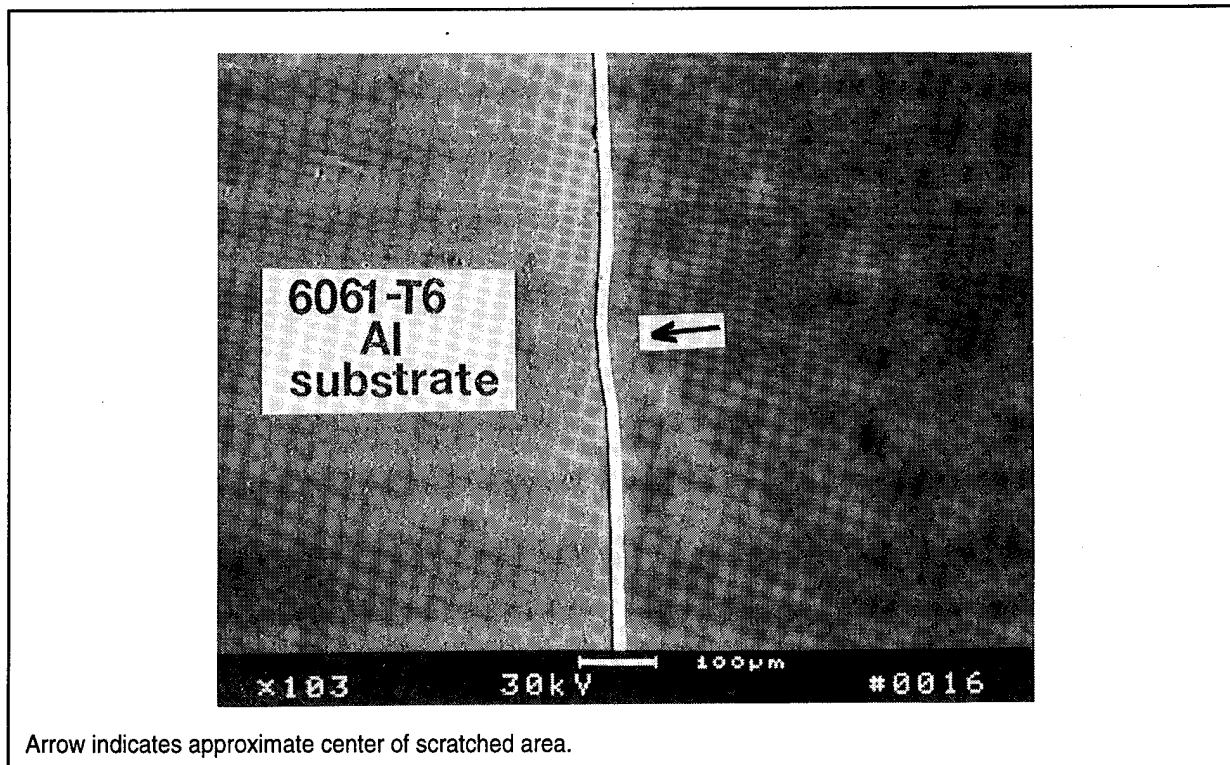
Figure 1.7. Scanning electron micrograph of cross-sectioned 6061-T6 aluminum substrate scratched to a depth of 0.5 mil and then coated with 95%Sn/5%Pb over 60%Sn/40%Pb over Ni.
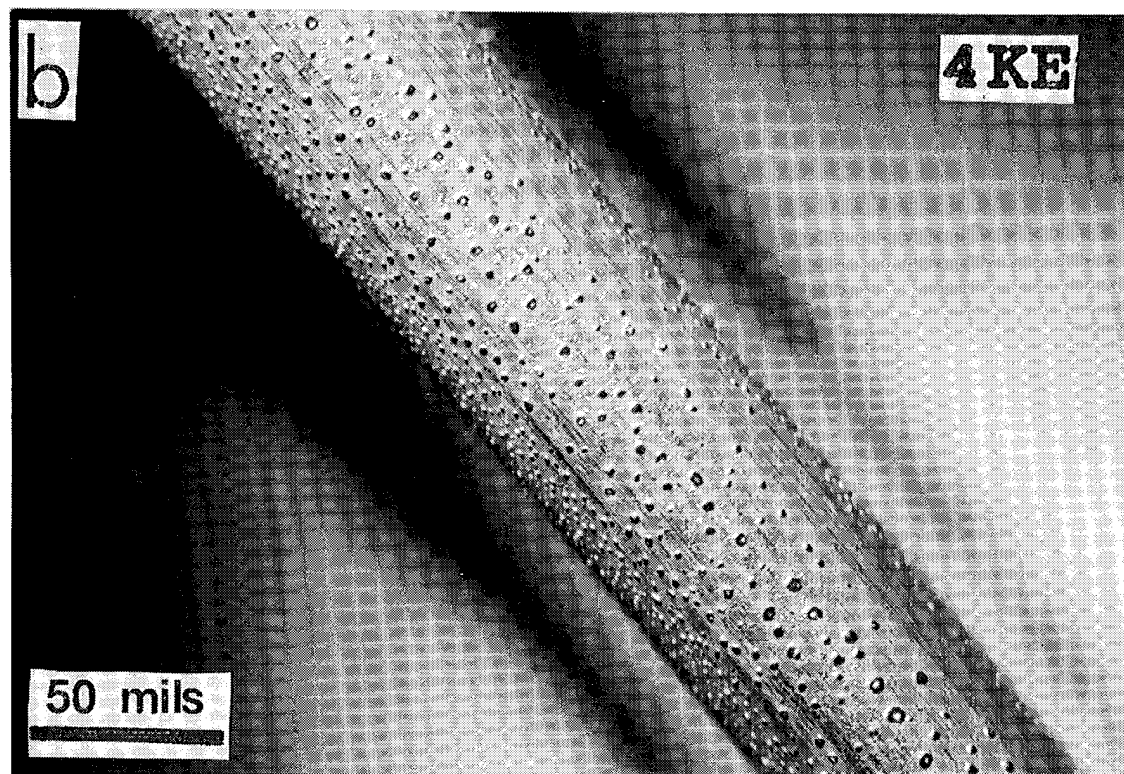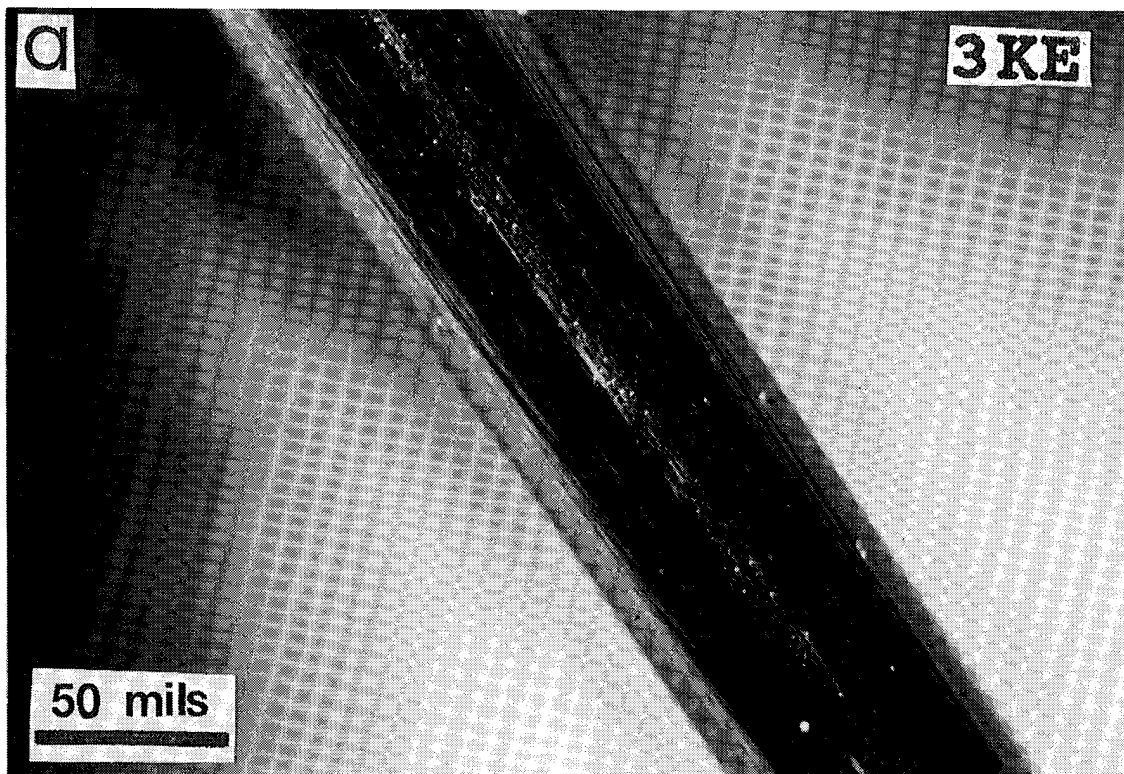
Figure 1.8. A series of optical micrographs, (a) through (f) show coated knife-edge specimens with numbers in upper-right hand corner correlating to processing parameters in Table 1.2.
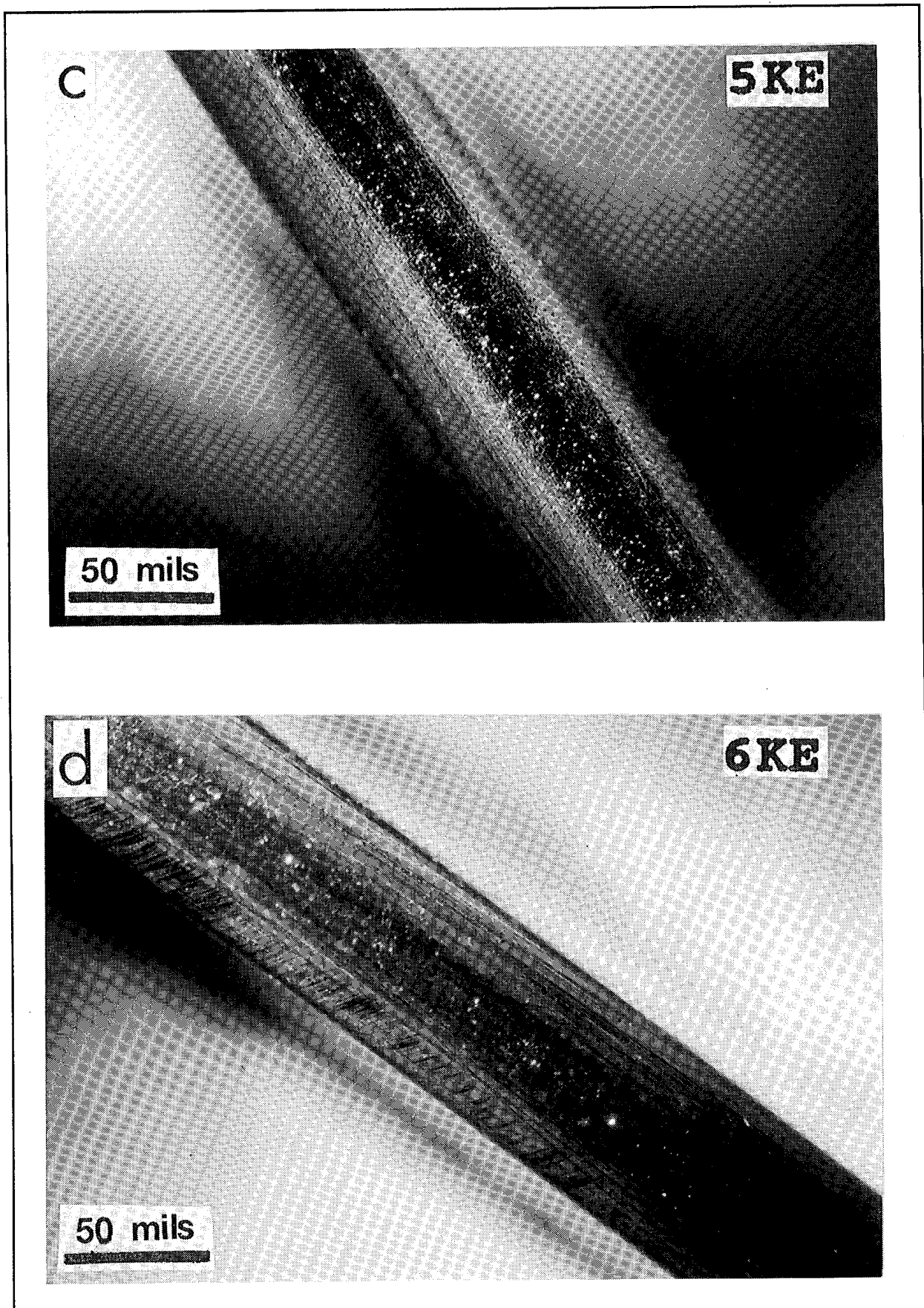
Figure 1.8. (Cont'd).
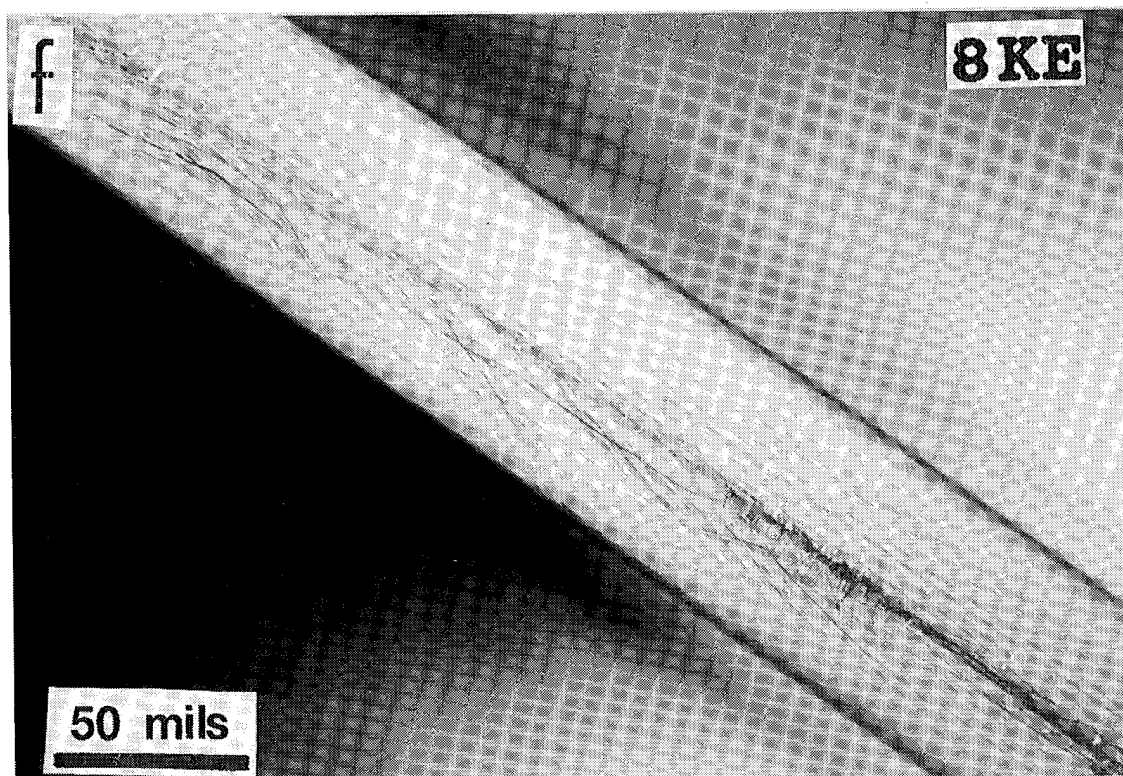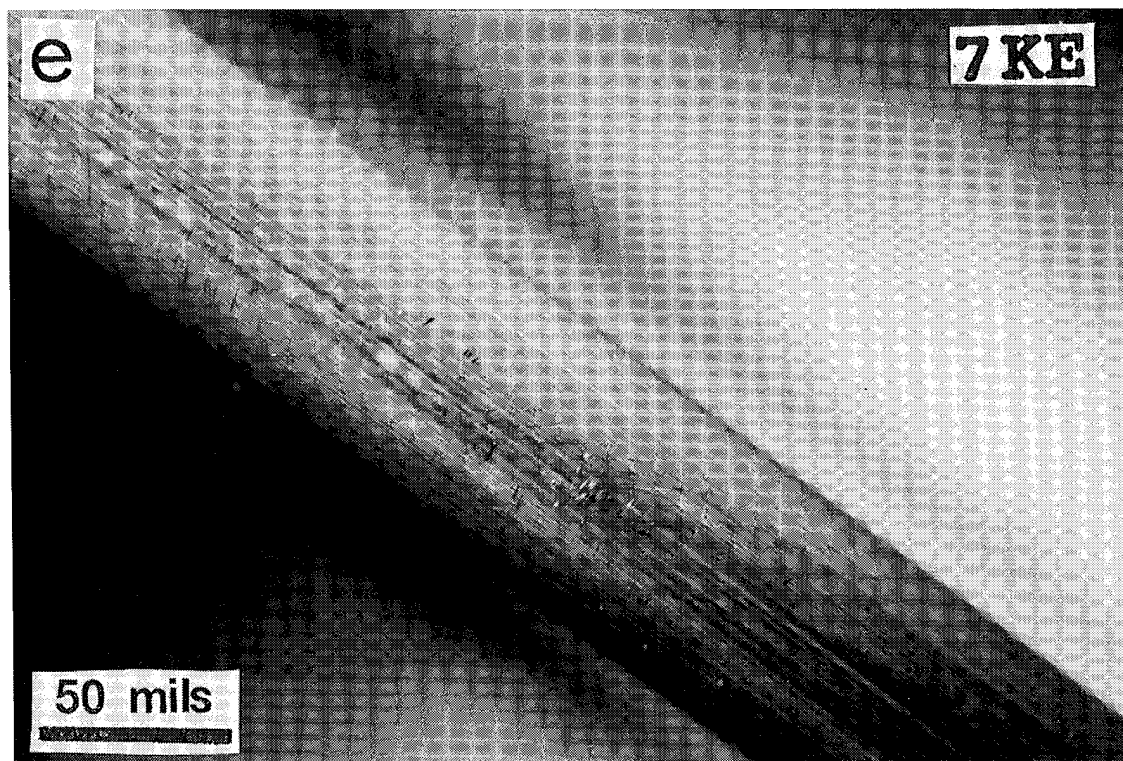
Figure 1.8. (Cont'd).

Table 1.3. Sebastian Adherence test results for Samples 9BF – 14BF.

Stress (psi)	Comments
Sample #9BF	
1.42	- 75% of the Sn/Pb coating was debonded down to the Ni layer - Surface looks "cooked" - Erratic blisters and pits - Area adjacent to contact stud "peeled off"
0.93	- 96% debond of the Sn/Pb layer - Cooked (as above) except higher and more exaggerated blisters - Pits - Area adjacent to stud contact area "peeled"
0.62	- 75% of the Sn/Pb coating was debonded down to the Ni layer - 100% Sn/Pb removed - "Cooked" - Peeled
Sample #10BF	
8.01	- Pits are big; blisters are small - Surface looks "cooked" - 92% of the "top" layer peeled off - 50% of the second layer (perhaps the 60/40 Sn/Pb) peeled off to expose Ni
2.12	- "Enormous" blisters on the surface - Occasional pitting - Appears to be cohesive failures within layers - 50% of the top layer remained
3.07	- 35% debond of the first layer - Appears to be cohesive failures within layers; also, debond of the coatings down to the Al substrate - Blisters found on center of intact contact area - Major blisters; few pits
Sample #11BF	
3.50	- Blisters, small - Some of the small blisters appear to be bounded by "lines", while others are more randomly distributed - Pits in surface down to second layer - 70% debond of Sn/Pb layer - 3% debond off of Ni
5.97	- 98% debond off of Sn/Pb layer - Stud was placed near the edge; the blisters were slight in this region - 10% Ni debonded (but still good substrate-Ni interface adhesion) - A few blisters around contact site
Sample #11BF	
1.12 (Different Batch)	- Bad adherence of epoxy - 30% debonded of top layer - 70% debonded, but not top first layer (NOTE: 95%Sn/5%Pb is the "top layer") - Slight blistering, nondirectional - Lines of blisters barely visible

Sample #14BF	
2.97	- Surface very badly blistered - Area immediately surrounding stud-to-sample contact showed increased blistering - There appear to be lines parallel to the brush strokes - The blisters appear to be bounded by lines - 95% of the Sn/Pb coating appears to have been completely debonded - It appears that 30% Ni was debonded, but not to substrate
0	- Stud easily debonded with zero measurement - 100% of the Sn/Pb appeared to have been debonded - 5% of the Ni was debonded, but not to substrate
7.01	- 97% top layer, difficult to determine if only topmost (95Sn/5Pb) layer debonded
	- 5% of the next lower surface was removed
	- Blisters not as prevalent, although present
	- Rather weak blister lines

NOTES:
1. It is difficult to determine the exact nature of the layers that were debonded. Generally, it appears that either the 95/5 Sn/Pb was the "top" debonded layer, or that both Sn/Pb layers debonded together. In most cases, however, the Ni layer appeared to remain intact.
2. Many of the specimens showed increased blistering at the area immediately adjacent to the contact stud.
3. Also, many of the post-tested adherence specimens exhibited a debonded area exposing a small amount of residual coating metal, either Sn/Pb or Ni, in the center (left behind as other parts of the coating debonded around it).

EMI Gasket Cycler
Knife-edge Sample 6 through 10

(a)

USACERL Gasket Cycler
Test 931221C; Sample# 7(Sn/Pb coated)
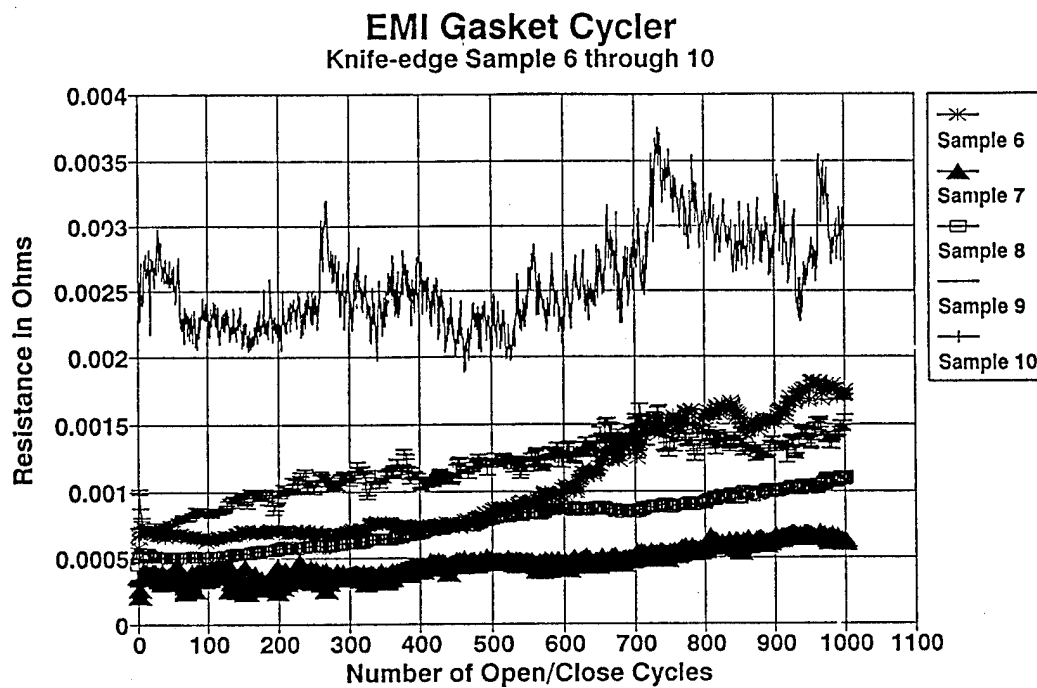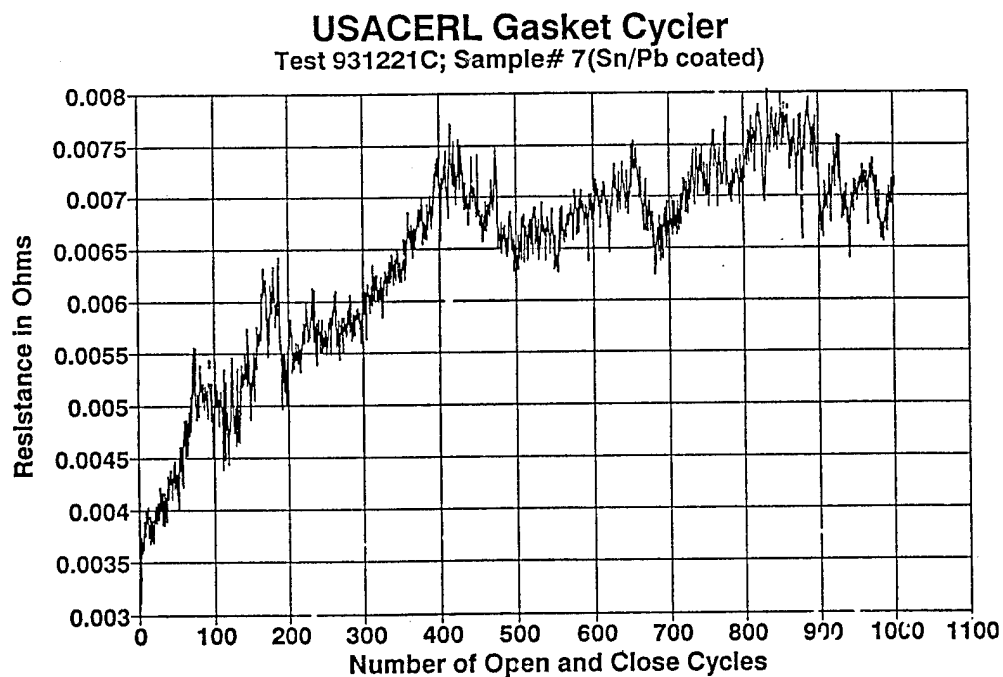
(b)

Figure 1.9. Resistance vs. Cycles for stylus electroplated coated knife-edge test samples (a) KE6, KE7, KE8, KE9, and KE10 and (b) KE7 before being coated with tin-lead over a nickel underlayer.
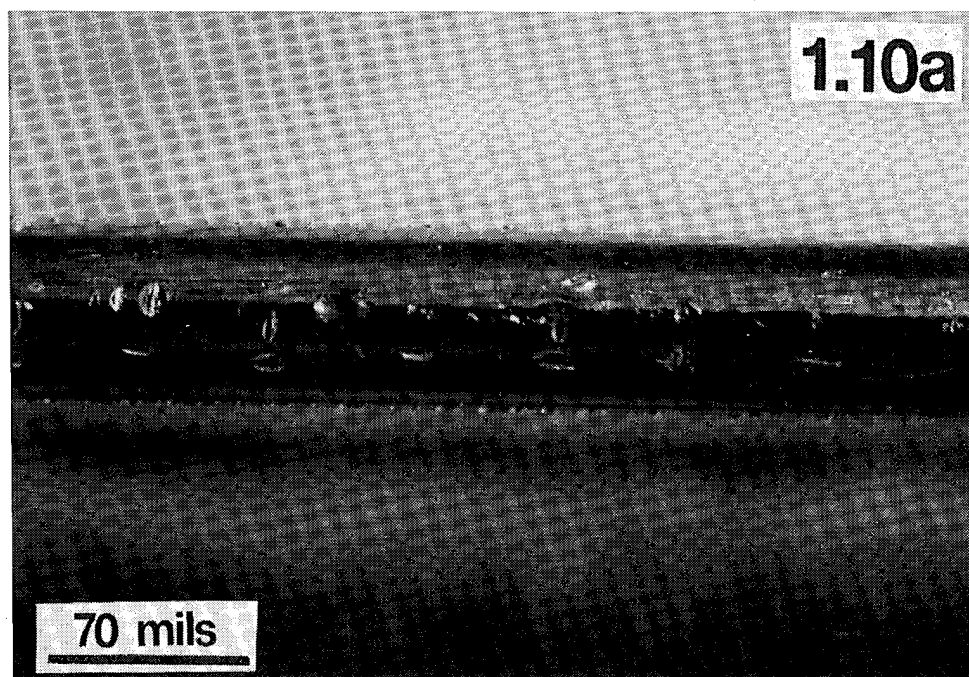
(a)
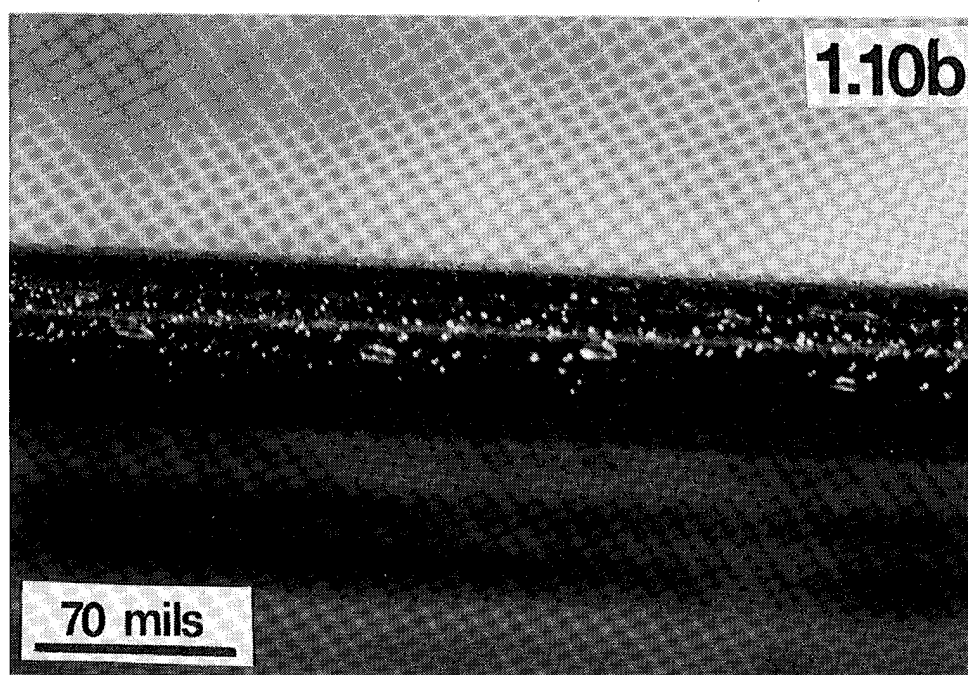
(b)

Figure 1.10. Optical micrographs of a Pb/Sn coated knife edge samples (a) 1KE and (b) 6KE, showing "bite marks" after 9,000 cycles on the USACERL Gasket Cycler Test System.

EMI Resistance vs. Cycles Plot
File 940112G; Position 10.

The elastomer was squeezed at point "S."
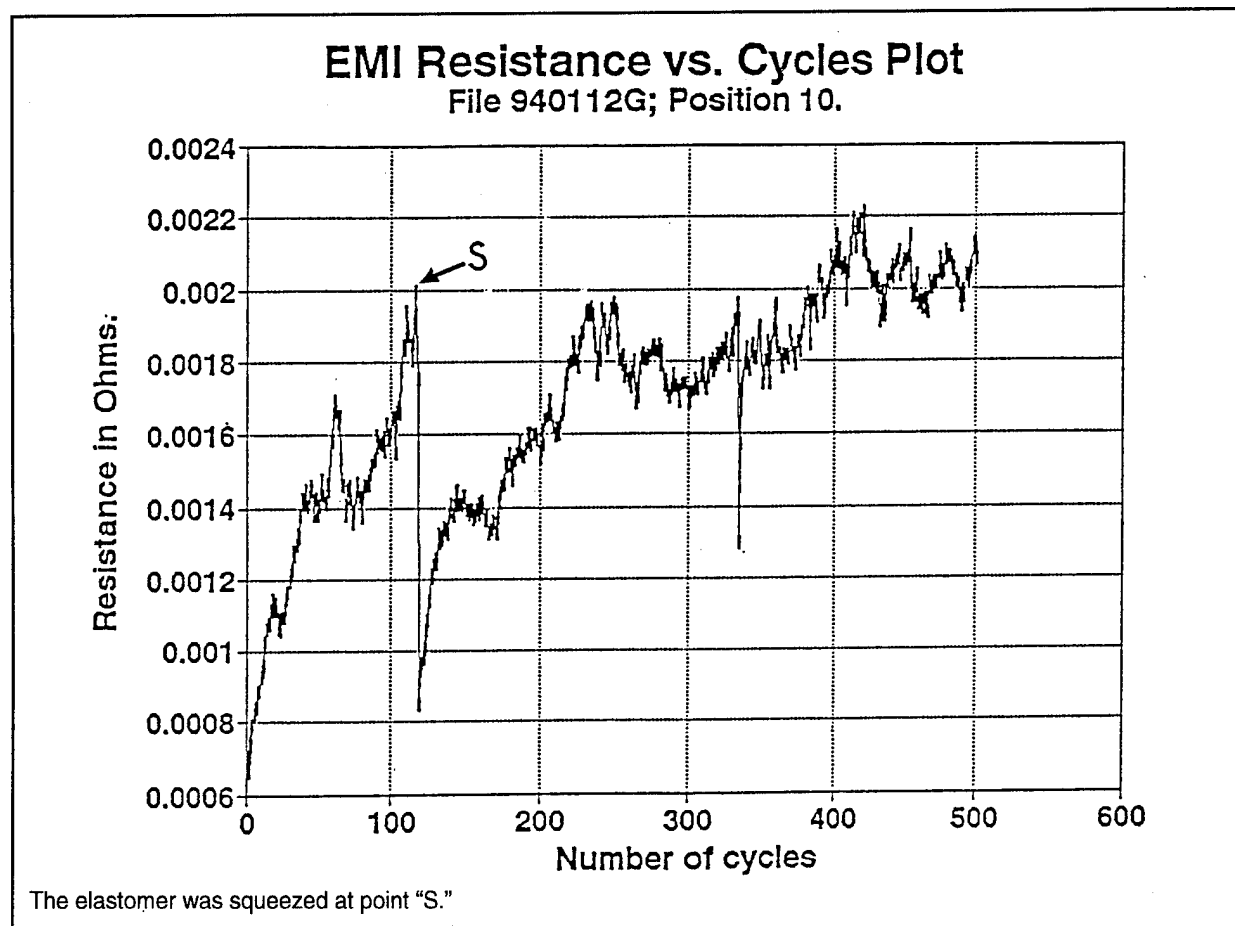
Figure 1.11. Resistance vs. Cycles of a cycled knife-edge test sample showing the "squeeze effect."

Table 1.4. Other observations from gasket cycling tests on knife-edge samples.

Test Specimen Summary
In this table, current densities are designated as "Low," "High," or "Mid-range." Also given here are the visual inspection results (with the aid of optical microscopy) after 9,000 and 15,000 cycles. The key is given below:

Current Density*
Low = < 3 amp/sq in.
Mid = 3 - 5 amp/sq in.
High = > 5 amp/sq in.

Sample number		
1KE (Low)	Blisters:	NO
	Bite marks:	YES
2KE (High)	Blisters:	NO
Ni only	Bite marks:	YES
3KE (High)	Blisters:	Very slight; they appear as lines.
	Bite marks:	YES
4KE (Low)	Blisters:	YES
	Bite marks:	YES
5KE (Low)	Blisters:	YES
	Bite marks:	YES
6KE (Low)	Blisters:	YES
	Bite marks:	YES
7KE (Mid)	Blisters:	NO
	Bite marks:	YES
8KE (Mid)	Blisters:	NO
	Bite marks:	YES
9KE	Blisters:	N/A
(uncoated)	Bite marks:	NO*
10KE	Blisters:	N/A
(uncoated)	Bite marks:	NO*

2 Phase II — Investigation of the Blistering Problem

During the second stage of this research (1 January through 15 April 1994), determining the causes of blisters and preventing them were top priority.

Test pieces of 6061-T6 knife-edge substrates were stylus electroplated with tin coatings, and were compared with pieces coated with a tin-lead coating during the first report period. Optical microscopy was used to observe the coating microstructures, especially blisters and ridges or the absence thereof.

Some new correlations between electroplating parameters and the resulting surface coating appearance, adherence, and contact resistance of knife-edge gaskets emerged, especially with respect to current densities and the production of less blistered and smoother coatings. New gasket cycling tests and data reduction strategies were implemented, using more cycles (up to 3,000) for short dwell times and longer dwell time (up to 30 min) for fewer cycles with longer cumulative running times. Normalized slopes for a linear approximation were compared to the Contact Resistance vs. Number of Cycles curves.

During this phase of the project the following tasks were conducted:

1. AISI/SAE[*] 304 stainless steel electrodes were substituted for the carbon electrodes in an attempt to produce cleaner coatings. Contamination of the plating solutions had been suspected as being the cause of blistering and substandard adherence.
2. Coatings of 100%Sn on nickel on aluminum were tested.
3. Salt fog testing on the 95%Sn/5%Pb and 60%Sn/40%Pb/Ni knife edges previously tested on the Gasket Cycler Test System commenced. Because these samples were coated on the knife-edge contact surface only, some portions of the uncoated surfaces were protected with a stop-off lacquer (Microstop). The remainder of the coating surfaces were left exposed to the salt fog for comparison purposes.
4. Complete knife-edge samples (front and back) were now electroplated. Previously, only the knife-edge contact surface was electroplated because it was the

[*]American Iron and Steel Institute/Society of Automotive Engineers.

only part that would make contact during the gasket cycling test. These same samples were subjected to the ASTM B-117 Salt Spray (Fog) Test, so the entire knife-edge sample was coated.

5. When new areas or sections of the sample were coated, the previously coated areas were protected from contamination (possibly arising from solution dripping or other similar mechanism) by applying Microstop to protect the parts of the sample already coated.

6. The cleaning step between the Etch step and the De-smut test was introduced, as described under the section "Optimum Stylus Electroplating Procedure," (p 5), which consists of scrubbing substrates surfaces thoroughly with Scotch-Brite™ No. 7448. This renders the Chromium/Sulfuric Acid Activator Step optional, so it was omitted in some of the coatings.

7. To produce thicker corrosion-resistant electrically conductive coatings, thicker coatings of nickel were attempted, because past experience indicates it is easier to apply nickel to greater thicknesses.

8. Krazy Glue® was used to bond the stud to the coating during adherence testing.

Electroplating Procedure

The following samples were plated for runs on the EMI gasket cycler. The electroplating procedure was essentially the same as used in Chapter 1 with a few notable exceptions. First, more consideration was given to controlling the voltage, instead of the current densities. Second, a Scotch-Brite™ step has been added after the Etch step to remove the aluminum oxide and to inhibit the possibility of trapped gases or solutions under the coating that otherwise might have been trapped in the scale. Third, the 60:40 tin/lead solution has been omitted for simplicity in all samples except full plate samples 28FPA and 28FPB.

Sample 26 was coated on the broadface side and then masked. When the masking was peeled off, massive coating failure occurred. For this reason, Sample 26 was not used in the EMI gasket cycler, nor was it duplicated.

Table 2.1 gives the electroplating parameters; constant voltages were maintained. The currents often fluctuated, so a current range was taken and an average found as cited in Table 2.1. The current densities were found using these average values with the corresponding contact areas. The contact areas were: 0.9375 sq in. for the broadface (BF); 0.4688 for the half face (HF); and 0.092 for the knife edge (KE). Current density equals the average current divided by the contact area.

The BF of samples 28A and 28B were plated under essentially the same conditions. As shown in Table 2.1, Sample 28 was unusual in that plating was initially conducted at low-current densities; then the current was increased. The purpose of this exercise was to evaluate whether an initial low current density was necessary in order to allow good adherence of the higher current density platings.

To compare the new plating procedure with the procedure previously used (in Phase I of this work), Sample 28A and 28B included a 60/40 tin/lead step between the nickel and pure tin steps.

Two samples (23CBF and 23CBF.ACT) were prepared for the Sebastian Adherence Test. These coatings were preformed on the broadfaces of "channel" assemblies, thus the acronym "CBF." The number "23" is used because the same current densities and voltages were used as for samples 23FPA and 23FPB. Both 23CBF and 23CBF.ACT (performed with the activator step) showed shiny, blister-free coatings.

Results of the Sebastian Adherence Tests

Sample 23CBF

1. No failure at 10.35 psi.
2. Failure at 7.24 psi.
3. Failure at 1.67 psi.
4. No failure at 10.42 psi.

Sample 23CBF.ACT

1. No failure at 10.34 psi.
2. Failure at 2.56 psi.
3. No failure at 10.35 psi.
4. Failure at 1.28 psi.

Gasket Cycling Tests

It was noted during the project review meeting on 29 March 1994 that uninterrupted runs with more cumulative cycles were desired in order to (1) help establish long-term Resistance vs Cycles trends and (2) determine if an asymptote is approached. Knife-edge test samples were subjected to more cumulative open/close cycles with the USACERL Gasket Cycler Test System.

Uninterrupted 25-hr gasket cycling runs of 3,000 cycles per run with 30 sec dwell times were implemented to make these tests more consistent with the real-world situations where doors typically experience at least that many open/close cycles annually. These 25-hr tests were conducted just after an overnight idle with an approximate 12-hr dwell time, which made comparison of the contact resistances possible immediately following a 12-hr dwell time (i.e., the overnight closed situation).

Also conducted were 6.25-hr gasket cycle run sets of 25 cycles with 15-min dwell times. In addition, an 80-cycle "no-air" test with a 15-min dwell time was implemented to test the resistance vs time trends with no cycling (with the exception of the one open/close cycle at the beginning of the test). The results reveal that, as expected, the contact resistance measurements are *almost* completely constant with respect to time; however, the contact resistance does tend to rise *slightly* over time.

Finally, a 72-hr gasket cycling test with dwell times of 30 min per cycle (for a total of 144 cycles) was conducted. Figure 2.1 shows the results of these tests. From the results of the gasket cycling tests, the following observations were made:

1.   Bite marks (caused by the mating gasket steel mesh biting into the test sample knife-edges) were observed after the samples were subjected to 3,000 cycles.

2.   Although some runs tended to show that resistances "level off" and approach an asymptote, the resistance generally tends to increase with respect to dwell time.

3.   Some runs (especially the 72-hr, 30-min dwell time) tended to exhibit a sinusoidal behavior for unknown reasons; however, they also showed a long-term trend toward an increasing contact resistance with respect to time.

4.   A linear approximation may be generated to the first order for each of the curves shown in Figure 2.1. The slopes of the line fits resulting from the data were then computed and normalized to cumulative running time (dwell time × the total number of cycles). The results shown in Table 2.2 indicate that longer dwell times may result in a lower rate of increase in contact resistance over time. Doors and interfaces are normally closed for 30 min or longer before reopening, so the gasket cycling runs with these dwell times may provide more typical indications in contact resistance. The one test sample where the contact resistance actually increased consistently with increasing test duration time (23FP-B) actually appeared to approach an asymptote at 0.15 mΩ in the 72-hr test.

Possible Origin of Blisters

Professor John Ableson of the Department of Materials Science and Engineering, University of Illinois, Urbana-Champaign (15 December 1993) offers the following hypothesis for the origin of the blisters:

> The *a priori* assumption is that the blisters are formed from trapped gases. At the low current density, there is sufficient time for the atoms to order, and they do so with a more dense microstructure than at the high current density. As the current density is increased, the time for deposition is reduced, and the microstructure is more porous. This porous microstructure allows gases to escape instead of trapping them as would the dense low current density microstructure. (This is consistent with the observations that as the current density is increased, the amount of blistering of the coating decreases.) Unfortunately, if the high current density coatings are porous enough to allow trapped gases to escape, then they might also be porous enough to allow moisture and corrosive gases in, which, of course, enhances the possibility of corrosion.

Also, as previously noted, blisters generally appear either in a random fashion, as shown by the optical micrograph in Figure 2.2a, or sometimes in "lines," which appear to follow the brush strokes (Figure 2.2b).

Observations of Coatings

Some new correlations between electroplating parameters and the resulting surface coating appearance, adherence, and contact resistance of knife-edge gaskets have been ascertained. The coatings that exhibited fewer blisters and smoother surfaces were applied at either low-current densities (less than 3 amp/sq in.) or high-current densities (greater than 4 amp/sq in.) while medium current densities (3 to 4 amp/sq in.) lead to larger blisters and more pronounced ridges.

A correlation between the electroplated surface microstructures and the stochastic contact resistance measurements has yet to evolve; however, it will be necessary to compare the results presented in this chapter with the results of the next round of gasket cycling tests, when these test samples are moved to new sample positions. The combined results of such testing may reveal new insights into the relationship, if any, between electroplating process parameters and the appearance of the resulting coatings. Table 2.3 summarizes the observations of the coatings discussed in this chapter.

Occasionally, a coating is produced similar to that presented in Figure 2.3. In these cases, some of the coating solution appears to solidify into fine particles when the pad

is touched to the substrate. These particles cling to the application pad and can scar additional coating material being deposited, preventing its adherence. So far, this phenomenon has only been observed for the KE and HF surfaces. The causes and prevention of this problem will be discussed in the Phase IV chapter.

Table 2.1. Stylus electroplating process parameters test matrix.

Sample #	Nickel Current Density (A/sq in.)	Tin Current Density (A/sq in.)		Plating Time (min) Nickel	Plating Time (min) Tin	Other Notes
23FP.BF-A 23FP HF 23FP KE	3.413 5.120 13.59	0.640 0.640 2.174		1.50 1.50 0.50	5.0 5.0 5.0	No Cr-H_2SO_4 Activator
24FP.BF-A 24FP HF 24FP KE	3.200 3.200 1.087	0.267 2.133 1.087		1.50 1.50 1.50	7.0 7.0 7.0	No Cr-H_2SO_4 Activator
25FP.BF-A 25FP HF 25FP KE	2.667 2.667 5.435	2.667 2.667 3.261		2.00 2.00 2.00	3.5 7.0 7.0	
27FP.BF-A 27FP HF 27FP KE	3.733 3.413 9.783	4.800 5.333 9.783		2.00 2.00 1.25	5.0 5.0 2.5	No Cr-H_2SO_4 Activator
28FP.BF-A 28FP HF 28FP KE	2.667 3.200 6.522	Sn-Pb 1.867 1.387 3.261	Sn 2.667 3.164 9.601	1.00 2.00 2.00	1.0 1.0 2.0 3.0 2.0 3.0	60/40 Sn-Pb plating performed before pure Sn step.
23CBF 23CBF.ACT CF.TEST.NEW PRO	3.840 3.627 2.667	0.640 0.427 0.800		1.50 1.50 2.00	5.0 5.0 5.0	See results of Sebastian Adherence Test.
23FP.BF-B 23FP HF 23FP KE	3.467 5.333 13.59	0.533 0.533 2.174		1.50 1.50 0.50	5.0 5.0 5.0	No Cr-H_2SO_4 Activator
24FP.BF-B 24FP HF 24FP KE	2.773 3.627 2.174	0.267 3.200 1.087		1.50 2.00 2.00	7.0 7.0 7.0	No Cr-H_2SO_4 Activator
25FP.BF-B 25FP HF 25FP KE	2.667 2.667 4.891	2.667 1.920 3.478		2.00 2.00 2.00	3.5 7.0 7.0	
27FP.BF-B 27FP HF 27FP KE	3.467 4.907 8.152	2.667 5.333 9.783		2.00 2.00 1.25	5.0 5.0 2.5	No Cr-H_2SO_4 Activator
28FP.BF-B 28FP HF 28FP KE	2.667 2.987 6.522	Sn-Pb 1.867 0.960 3.261	Sn 2.667 2.773 8.514	1.00 2.00 2.00	1.00 1.00 2.00 3.00 2.00 3.00	60/40 Sn-Pb plating per-formed before pure Sn step.
26FP.BF (A)	3.200	1.067		2.00	5.0	Very poor ad-herence; coating failed when unmasked.
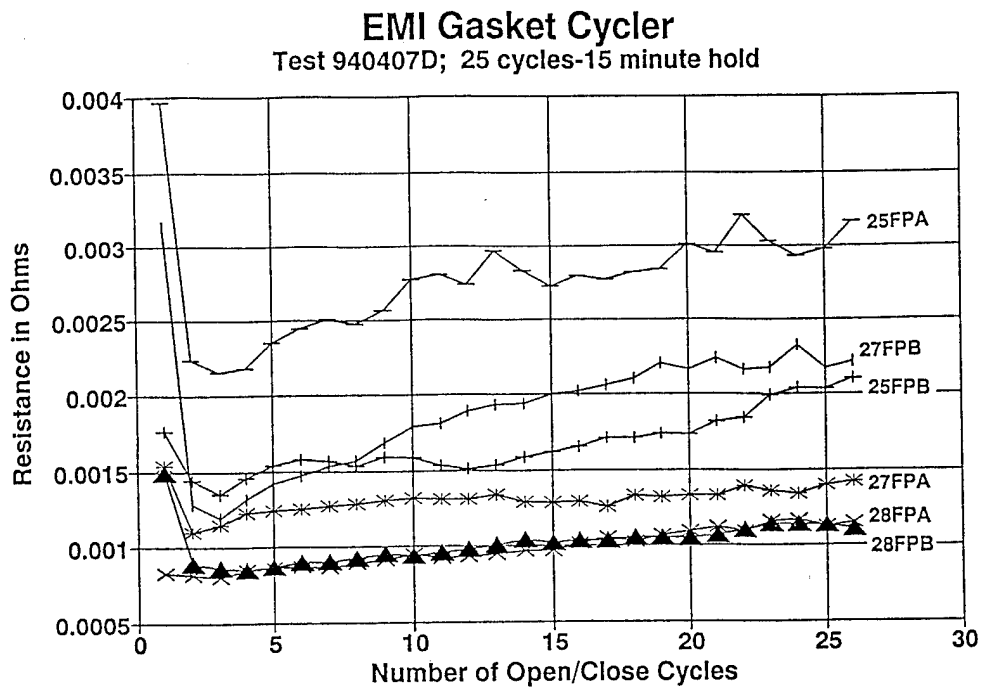
(a)
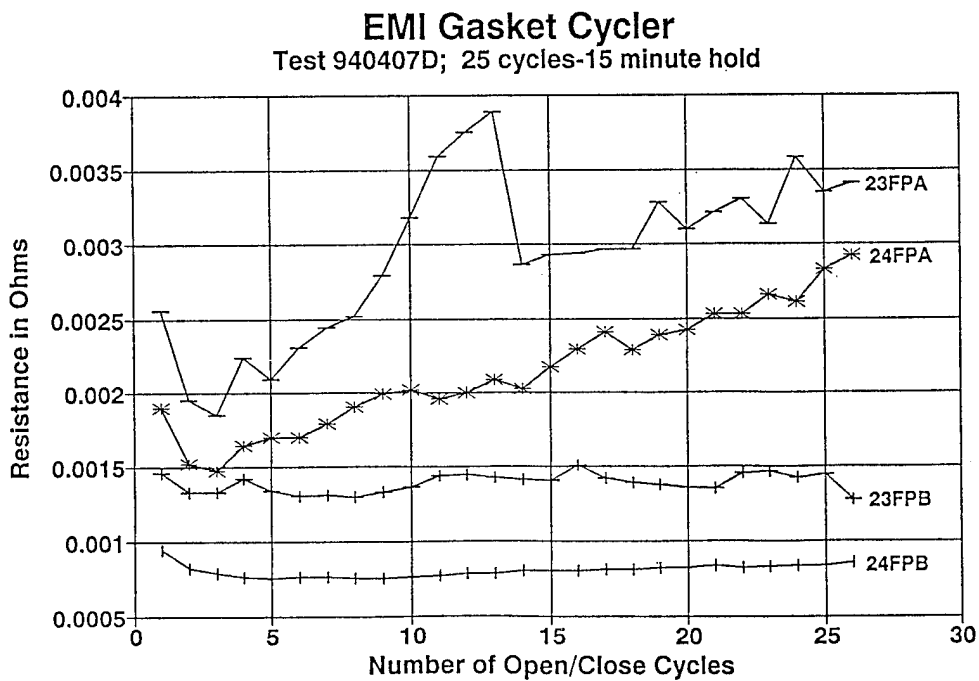
(b)

Figure 2.1. Resistance (ohms) vs number of cycles for (a) and (b) 25 cycles at 15-min dwell time.

EMI Gasket Cycler
Test 940405C; 3000 Cycles-30s hold

(c)

EMI Gasket Cycler
Test: 940405C; 3000 Cycles-30s hold

(d)
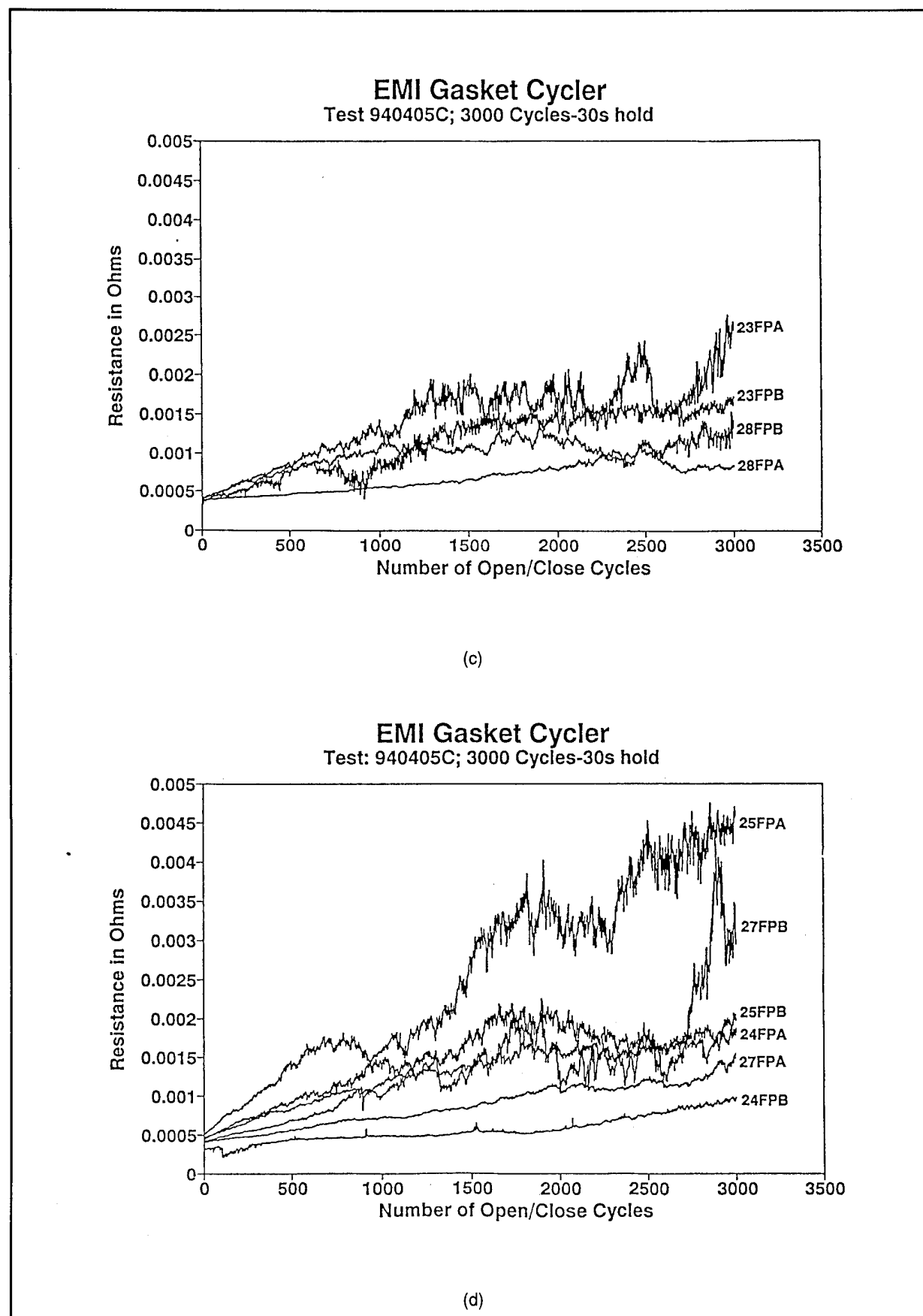
Figure 2.1. (Cont'd). Resistance (ohms) vs number of cycles for (c) and (d) 3,000 cycles at 0.5-min dwell time.
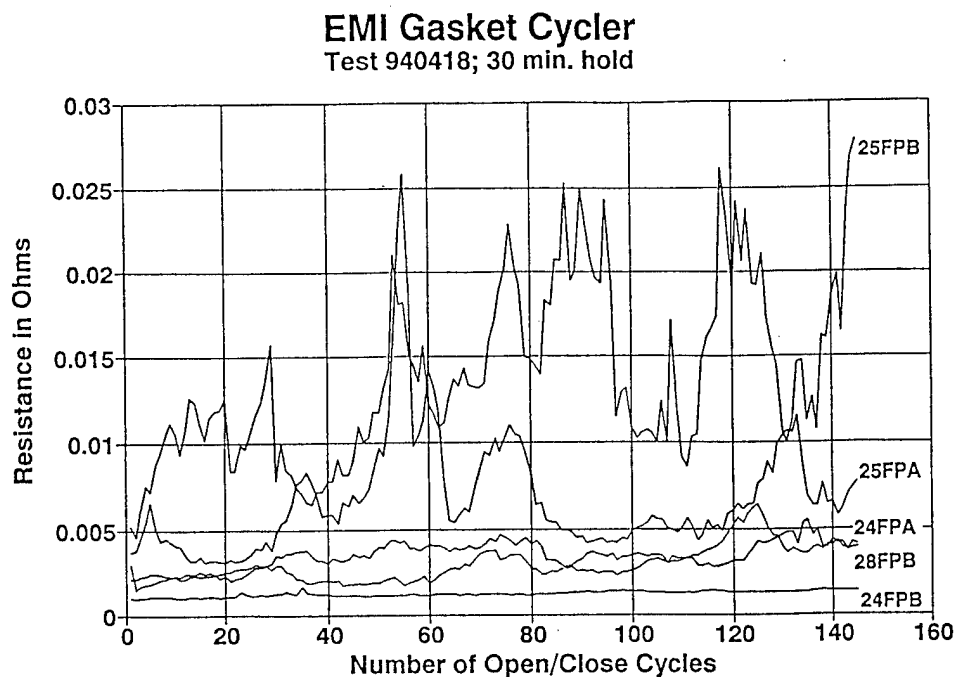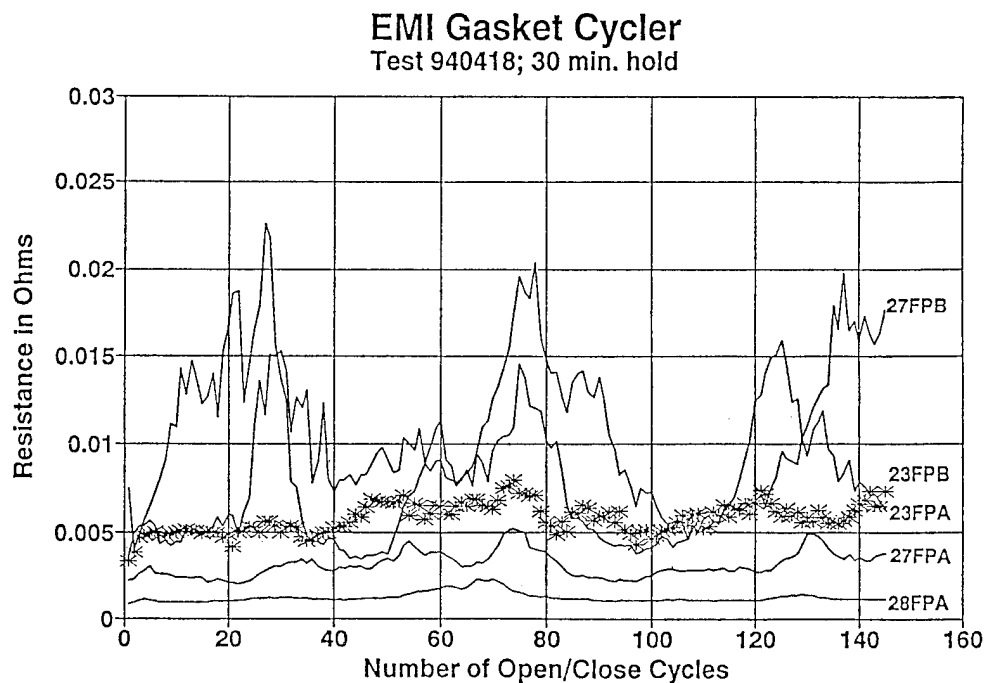
Figure 2.1. (Cont'd). Resistance (ohms) vs number of cycles for (e) and (f) 144 cycles at 30-min dwell time.

Table 2.2. Normalized slopes from gasket cycling tests.

Sample #	SLOPE (mΩ/hr) 25 cycles @ 15 min dwell time per cycle (6.25 hr run)	SLOPE (mΩ/hr) 3000 cycles @ 0.5 min dwell time per cycle (25 hr run)	SLOPE (mΩ/hr) 144 cycles @ 30 min dwell time per cycle (72 hr run)
23FP A	0.22	0.083	0.042
23FP B	0.016	0.040	0.069
24FP A	0.19	0.048	0.035
24FP B	0.016	0.16	0.0070
25FP A	0.12	0.16	0.055
25FP B	0.11	0.056	0.017
27FP A	0.064	0.036	0.014
27FP B	0.16	0.100	0.097
28FP A	0.032	0.020	0.014
28FP B	0.032	0.035	0.028
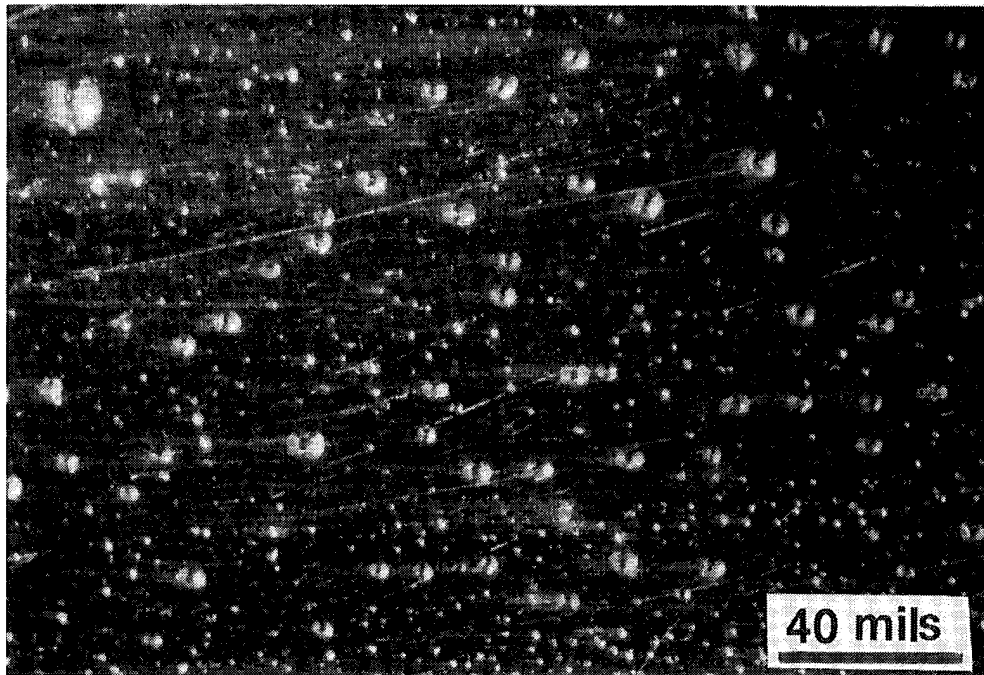
(a)
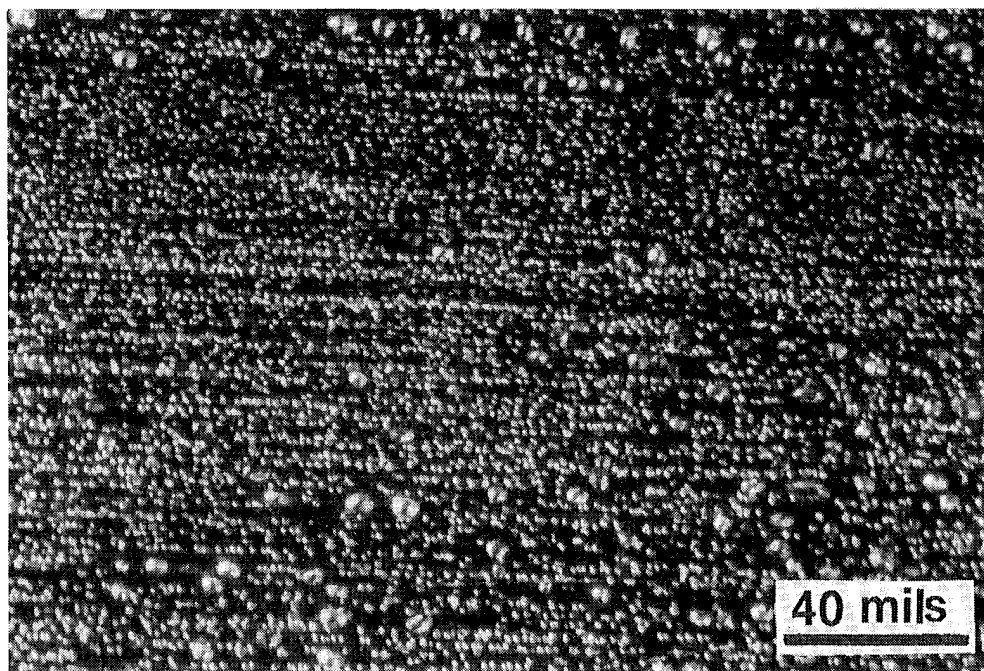
(b)

Figure 2.2. Optical micrograph showing a broadface view of a 6061-T6 aluminum substrate coated with 95%Sn/5%Pb (a) with randomly oriented blisters and (b) with lines of small blisters that appear to follow the brush strokes.

Table 2.3. Observations of coatings for Samples 23 – 28 before B-117 Salt Spray (Fog) tests.

23FPA
- No blisters at all

23FPB
- Very slight, sparse blisters on BF
- No blisters on HFs
- Blisters on KE

24FPA
- No blisters on KE
- One HF, very shiny with no blisters
- Other HF, discontinues such as "valleys"
- BF was shiny

24FPB
- Shiny BF
- One HF: part shiny, part blisters
- Other HF: slight blisters, part shiny
- Blisters and ridges on KE
- Adherence problems in some areas on KE

25FPA
- KE: Slight ridges or lines along the brush axis
- KE: Very slight blisters
- One HF: slight blisters
- Other HF: slight "valleys"
- BF: dark, yet shiny, very sparse slight blisters

25FPB
- No blisters on BF
- Slight blisters on one HF, but none on the other
- Large blisters on KE

27FPA
- Small blisters and slight ridges on KE
- One HF: shiny with no blisters
- Other HF: very bad discontinuities
- BF: shiny, yet some dull spots

27FPB
- BF: shiny, yet some dull spots
- One HF, shiny with only a few blisters
- Other HF, exaggerated blisters
- HF blisters often found around KE
- Very slight blisters at 30X

28FPA
- No blisters on BF
- One HF: shiny but slightly duller toward KE
- Other HF, small blisters leading into large blisters
- KE: shiny with no blisters

28FPB
- One HF: can see the milling through the coating
- Other HF: Non-spherical blisters (slight)
- KE: small blisters
- Shiny, blister free BF

23CF and 23CFACT
- Both had shiny, blister-free surfaces

Figure 2.3. Optical micrograph showing a broadface view of a poorly adhering tin coating deposit, probably caused by contamination of the electroplating solutions or the application pads.

3 Phase III — Gasket Cycling Tests, Coating With Copper Underlayers, and Salt Spray Testing

During Phase III (16 April through 15 August 1994), samples were tested both before and after salt fog testing. In each case, coated knife-edge samples were tested at 30 sec dwell times for up to five sets of 10,000 or more cycles. The causes and prevention of blistering, burning, scarring, and poor adhesion were identified, and the electroplating procedure was modified to greatly reduce their occurrence. Also, it was determined that carbon electrodes are not necessarily causes of contamination of the plating solutions if they are properly cleaned after use. AISI/SAE 304 stainless steel electrodes are also acceptable for plating; however, they also must be properly cleaned after use.

Finally, some samples were fabricated with copper, rather than nickel, underlayers, and the relative performances of the coated samples was determined.

Table 3.1 summarizes the coating thicknesses for the coated knife-edge samples tested in this phase. (The micrographs used in making these measurements are shown in Figure 3.3.) The table lists a "low," "high," and "average" thickness reading for each sample.

Gasket Cycling Test Results for Samples Coated in Phase II

Salt fog testing data were obtained on the 95%Sn-5%Pb and 60%Sn-40%Pb/Ni knife-edges previously tested on the USACERL Gasket Cycler Test System. These samples were coated on the knife-edge contact surface only, so some portions of the uncoated surfaces are protected with a stop-off lacquer (Microstop). The remainder of the coating surfaces were left exposed to the salt fog for comparison purposes. Also, salt-fog testing data have been obtained on a set of 100 percent tin coatings with nickel or copper as the intermediate layer (or "undercoat").

These samples were subjected to the gasket cycling test, both before and after salt fog exposure. Table 3.2 summarizes the post-salt fog observations.

Thicker coatings of 100 percent tin using nickel or copper as an intermediate layer have been produced, and up to five sets of gasket cycling tests with 10,000 Resistance vs Cycles per set were run to determine the long-term effects of open/close cycles on the electroplated knife-edge mating surfaces (equivalent to approximately 2 years of open/close cycles for an actual EMI shielding door, based on 20 open/close cycles per day). The gasket cycling tests were run both before and after the samples were subjected to the ASTM B-117-90 Salt Spray (Fog) Test. Figure 3.1 shows the Resistance vs Number of Cycles plots for pre-salt fog gasket cycling data, and Figure 3.2 shows the post-salt fog gasket cycling data.

Attempts have been made to fit equations to the curves obtained from the data. Although higher order approximations have been explored, the most reasonable curve fits are linear with random oscillations about statistically fitted lines, as indicated by Table 3.3, which gives pre-salt fog gasketing cycling data, and Table 3.4, which gives post-salt fog test data. The data indicate occasionally drastic departures from quasi-linearity at certain points along the line. These stochastic variations are the reason for most of the low linear correlation coefficient values (r) listed in Tables 3.3 and 3.4.

In some cases, the Resistance vs Number of Cycles data indicate that asymptotes may have been reached. In those cases, the linear correlation coefficients will be low, and an exponential curve fit may provide a more meaningful interpretation of the data. In cases where the data appear to follow a linear trend, the slopes ranged from 2.925018×10^{-9} ohms/cycle (for Sample 25A) to 1.131949×10^{-7} ohms/cycle (for Sample 28A) for the pre-salt fog exposure cycling data. The slopes ranged from 2.778205×10^{-8} ohms/cycle (for Sample 23B) to 3.986752×10^{-7} ohms/cycle (for Sample 25B) for the post-salt fog exposure cycling data. In the best cases, the asymptotes are 0.0057 ohms for Sample 24A, 0.0044 ohms for Sample 25A, and 0.0032 ohms for Sample 27B. This near-asymptotic behavior has only been observed so far for these three samples exposed to the salt fog test. In a few uncertain cases, ascertaining any trend is difficult because of the erratic nature of the data. The one trend that has finally emerged from these tests is the tendency for the slopes of the linear fit to the post-salt fog resistance vs number of cycles curves to be about one order of magnitude larger than the pre-salt fog linear fit slopes. In some cases, several extremely large deviations in the curve from quasi-linearity were observed. These deviations were usually manifested as decreases in contact resistance (e.g., at around 7,500 cycles for Sample 24B in Figure 3.1c). The discontinuities most likely originate from relaxation effects caused by the elastomer underneath the wire mesh during the brief rest periods between 2,500-cycle runs when the samples were in contact with the wire mesh gaskets. These rest periods were necessary in order to download data and to prepare for the next run. Although researchers attempted to minimize the rest periods, it normally took about 15 to 30 min to perform the necessary functions between each run. Thus, it is not unusual to

see a discontinuity of this sort every 2,500 cycles. In most cases, however, the discontinuities were not as large as the example used here.

The mesh gasket elastomer apparently requires a finite time to undergo relaxation effects. In fact, in related work, the contact resistance decreased exponentially when 6 to 8 minute dwell times were used and contact resistance measurements were taken every 20 seconds during the closed cycle (personal communication, Prof. Cain, 1 November 1994). This is analogous to leaving an EMI door in the closed position for a long time, which is much more typical than the situation modeled in this study with the gaskets being cycled every 30 seconds to simulate worst-case estimates of the physical degradation of the gasket interface system.

The *uncoated* knife-edge gaskets generally exhibited larger and more erratic fluctuations in resistance values over time, consistent with findings in previous gasket cycling tests. This effect has also been verified in other independent testing by Prof. B.L. Cain, who has noted very high standard deviations of the five resistance readings per cycle (which are averaged to give the resistance readings used in the resistance vs cycles plots) for uncoated aluminum substrates. This erratic behavior is most likely due to the cyclic action of oxides forming on the knife-edge contact surface, then breaking, being torn off, and reforming again. These observations are consistent with the theory that the tin-alloy coatings help to prevent surface oxides from forming.

Note: The uncoated aluminum samples generally exhibited the larger final resistances and larger resistance vs cycles slopes, as shown in Tables 3.3 and 3.4.

Intermediate Coating Layer (Copper vs Nickel)

The following samples were plated to examine the validity of using copper (rather than nickel) as an intermediate layer (undercoat) over which tin and tin/lead alloys are plated. ASTM B-117-90 Salt Spray (Fog) and Sebastian adherence tests were also performed. These "copper-undercoat" coatings showed the best resistance to the sea salt corrosion test.

Using the copper strike as opposed to the nickel preplate has a few notable advantages:

1. The nickel is more difficult to see than the copper as it is being applied.
2. Copper has a much higher microthrowing power than nickel. This means that copper has a much greater ability to fill in surface defects and smooth them over

than does nickel, which only follows the contours of the defect and does not "smooth" the surface.

3.   Most important, copper is cathodic with respect to tin. These phenomena are discussed in more detail in Chapters 4 and 5.

Table 3.5 indicates electroplating parameters used in the deposition of these coatings. The samples are designated 23CF, 23CF-ACT, and 31CF through 40CF. Note that:

1.   Constant voltages were easily maintained during any given step. Currents tended to be a bit more erratic; therefore, a range (or average) was used. [As previously noted, the electroplating tool pad, which is polarized so that it becomes the "anode" during metal deposition, needs to be dipped into the solutions at given intervals. Where "D" (dry anode) and "W" (wet anode) values are indicated, separate current averages were computed immediately before and immediately after the anode was dipped into the solutions, respectively.]

2.   The effective contact area for electroplating the substrates was 0.9375 sq in. (6.048 cm^2).

3.   Solution 1 is the electroclean solution, which has been omitted in many of these platings because it is primarily used when substrates contain heavy oils or particles that cannot be easily removed with solvents. Solution 2 is the Etching solution. "60/40" refers to a solution of 60%Sn-40%Pb. "95/5" refers to a solution 95%Sn/5%Pb. Sn, Ni, and Cu refer to solutions of 100 percent tin, 100 percent nickel, and 100 percent copper, respectively. "ACT" refers to the hard chrome activator, also known as De-smut.

Adherence Test Results

The adherence test results, given in Table 3.6, revealed coating failures ranging from 3.29 ksi (22.69 MPa) to 6.14 ksi (42.34 MPa). The highest coating strengths were obtained for the samples 23CF-ACT, 31, 32, 33, and 35 with adherence strengths above 5 ksi (34.48 MPa). Samples 23CF, and 36, 37, 38, 39, and 40 had adherence strengths lower than 5 ksi (34.48 MPa). The sample standard deviations (STD) ranged from 0.888 to 2.000 ksi (6.12 to 13.79 MPa). A statistical analysis using Duncan's Multiple Range Analysis indicated that no significant difference existed in the adherence values.

With the exception of Sample 35, those coatings exhibiting the best adhesion strengths had intermediate layers of copper sandwiched between the final layer and the substrate. The omission of the activator (de-smut) step did not appear to have any effect on the adherence of the coatings, although the solution manufacturer suggested that

the sulfuric acid in the activator helps to clean the surface. Otherwise, no obvious correlations exist between the processing parameters and the resulting adherence tests.

Results of the Salt Fog Tests

Samples 23CF, 23CF-ACT, and 31CF through 40CF were exposed to the ASTM B-117-90 Salt Spray (Fog) Test. Optical microscopy cross-sections were prepared from post-salt fog samples to determine the thicknesses of the coatings, as presented in Table 3.1, and to determine the efficacy of the coating in preventing damage to the substrate during salt fog testing. These micrographs are shown in Figure 3.3a-t. Table 3.7 shows results of a qualitative visual inspection of the post salt fog coatings.

Because it was difficult to ascertain visually whether the residue found on the specimens was in fact corrosion or salt solution that had solidified on the surface of the specimens, scanning electron microscopy/energy dispersive x-ray spectroscopy (SEM/EDX) analysis was performed. Figure 3.4a is a plot of the SEM/EDX analysis. The atomic percentages of the elements in the sample were:

| 45.7% Cl | 19.3% Na | 18.6% Al | 8.0% Mg | 5.4% S | 2.6% K | < 1.0% Ca |

The EDX analysis has an accuracy of 1 atomic percent. These percentages indicate an elemental composition primarily of salt-forming elements that were observed to accumulate on the sample surfaces, along with a significant quantity of aluminum, ostensibly from a corrosion product.

These tin-composite coatings appear to protect the aluminum alloy substrate except in those areas where holidays (or "breaks") occur in the protective coatings. Samples with scratches intentionally cut through their coatings to expose their substrates tended to show corrosion only near, or in, the cut (Figure 3.4b). Other defects, such as blisters, sometimes proved to be corrosion sites (Figure 3.4c). It is presumed that localized low thicknesses, coupled with porosity, may be another origin for corrosion. In these cases, the corrosion actually pits under the coating and, as the corrosion product is formed, flakes the coating away (Figures 3.4d and 3.4e). Blisters formed either from trapped gases or escaping solution or from volume changes that often accompany post-electroplated deposits, may exacerbate the porosity and give rise to sites for corrosion. Using electroplated Sn over other electroplated Cu, Ni, and even Sn-Pb alloys for protection against oceanic environments is easily seen as valid in this test. Copper is considered to be "highly resistant to corrosion by air and salt water" (Hornbostel 1978); however, copper quickly discolors in an ocean salt ambient, possibly because of the sulfur introduced from the sodium sulfate found in the sea salt solution,

as in the case of Sample 33, which had been coated only with copper. Nickel top layer coatings also exhibited poor corrosion resistance (as in samples #39 and #40) relative to tin, most likely because of the presence of chloride ions. Although little difference was seen between the Sn and the Sn/Pb alloy coatings overall, the differences that were observed seemed to indicate that the pure Sn coating was preferable. During "normal" environmental exposure (i.e., in ambient nonaggressive environments), both the Cu and Ni coatings became discolored significantly more than the Sn and Sn/Pb alloys and are much more susceptible to water spots.

The tin/lead coating system was chosen as potentially useful because it was suggested that alloy coatings may yield better corrosion resistance (Bunshsah 1982), and provide better resistance to the formation of the brittle alpha-tin ("tin pest") powder on the surface of the aluminum alloy substrate (ASMI 1994). However, in this case, the introduction of relatively large lead atoms into the predominately tin coating may cause unwanted porosity. Furthermore, the use of lead as an electrolyte constituent is problematic due to its identification as an environmentally hazardous heavy metal subject to Resource Conservation and Recovery Act (RCRA) Subtitle C regulations [40 CFR 268.43(a)].

Because of the galvanic coupling of the metals and their exchange current densities, accelerated corrosion would not occur if a surface defect such as porosity or a scratch penetrated the tin layer and exposed the copper. Instead, the corrosion would be "spread out" over the large anodic tin area, avoiding a localized attack at the exposed copper site. In another case where a nickel strike was used, the nickel undercoat is anodic with respect to the coating, the corrosion would be localized and accelerated, resulting in the type of pitting corrosion shown in Figure 3.4f. Eventually, the corrosion transcends the nickel layer and begins to degrade the aluminum alloy substrate. Pitting corrosion is especially problematic in corners, or recessed areas (Figure 3.4g). In any case, if a flaw exposes the aluminum alloy substrate, the importance of the undercoat becomes negligible. At this point, the large difference in the galvanic potentials of the cathodic tin top coating and the highly active anodic aluminum alloy substrate would determine corrosivity, as would the type of environment involved.

Figure 3.5 illustrates the relative corrosion resistance of the various coatings in a salt environment. The figure shows the five broadface electroplated 6061-T6 aluminum substrate samples that were subjected to the ASTM B-117 Salt Spray (Fog) Test. The samples were: (a) coated with tin, (b) uncoated, (c) coated with tin, (d) coated with nickel, and (e) coated with copper. Note that only the tin coatings were relatively unaffected by the salt spray, while the uncoated aluminum was discolored, and the copper and nickel coatings both show evidence of being attacked by sulfide and chloride anions in the salt spray.

Table 3.1. Summary of coating thicknesses of stylus electroplated 6061 aluminum samples placed on the USACERL Gasket Cycler Test System and then in the B-117 Salt Spray (Fog) Test Chamber.

Sample Number	Thickness of KE (mils)		Thickness of BF (mils)		Thickness of HF (mils)		Thickness Side of KE (mils)	
23 FPA	LOW HIGH AVG.	0.13 2.26 1.40	LOW HIGH AVG.	0.11 0.68 0.18	LOW HIGH AVG.	0.23 0.93 0.58	LOW HIGH AVG.	0.23 0.75 0.49
23 FPB	LOW HIGH AVG.	0.68 2.60 1.64	LOW HIGH AVG.	0.27 0.45 0.32	LOW HIGH AVG.	0.16 0.68 0.42	LOW HIGH AVG.	0.59 0.68 0.67
24 FPA	LOW HIGH AVG.	0.18 2.51 1.35	LOW HIGH AVG.	0.00 0.14 0.07	LOW HIGH AVG.	1.22 1.27 1.24	LOW HIGH AVG.	0.67 0.77 0.72
24 FPB	LOW HIGH AVG.	0.68 1.18 0.93	LOW HIGH AVG.	0.20 0.72 0.27	LOW HIGH AVG.	0.88 1.24 1.06	LOW HIGH AVG.	0.43 0.45 0.44
25 FPA	LOW HIGH AVG.	1.56 2.00 1.78	LOW HIGH AVG.	0.59 1.00 0.84	LOW HIGH AVG.	0.50 1.02 1.02	LOW HIGH AVG.	0.79 2.67 2.26
25 FPB	LOW HIGH AVG.	0.77 1.40 1.09	LOW HIGH AVG.	* 1.13 1.13	LOW HIGH AVG.	1.02 1.13 1.07	LOW HIGH AVG.	0.50 0.59 0.55
27 FPA	LOW HIGH AVG.	0.00 * *	LOW HIGH AVG.	2.04 2.17 2.10	LOW HIGH AVG.	* 2.69 1.29	LOW HIGH AVG.	0.45 0.57 0.57
27 FPB	LOW HIGH AVG.	* 2.06 1.31	LOW HIGH AVG.	0.93 1.09 0.98	LOW HIGH AVG.	* 2.76 *	LOW HIGH AVG.	1.04 1.47 1.26
28 FPA	LOW HIGH AVG.	0.81 2.15 1.49	LOW HIGH AVG.	* 0.18 *	LOW HIGH AVG.	0.70 1.31 1.09	LOW HIGH AVG.	0.27 1.00 0.68
28 FPB	LOW HIGH AVG.	0.27 2.10 1.19	LOW HIGH AVG.	0.11 0.50 0.31	LOW HIGH AVG.	0.91 4.98 4.98	LOW HIGH AVG.	0.38 1.24 0.81

* Unable to obtain good data to determine thickness values due to defects induced by salt exposure.

Table 3.2. Results of the Gasket Cycler Test System post B-117 Salt Spray (Fog) Test on stylus electroplated 6061 aluminum samples.

Sample #	Coating thicknesses of knife edges	Coating thicknesses of broadface	Coating thicknesses of half faces (Note: 2HFs on each)
23 FPA	Erratic, no "good" average. No KE pitting corrosion.	Uniform, but very thin. No pitting corrosion.	Smooth, varying from low to mid-thickness. Both sides alike. No pitting corrosion.
23 FPB	Somewhat wavy; good coverage and average. no pitting corrosion.	Thin, but smoothly covering surface. No pitting corrosion.	Both HFs same. Low thickness, but good averages. No pitting corrosion.
24 FPA	Coating appears to have not covered all the KE. No pitting corrosion.	Thin, inadequate coating. Large pits in surface.	Both HFs same. Mid-thickness, smooth and uniform. No pitting corrosion.
24 FPB	A thin but uniform cover of the surface Smooth; no pitting corrosion.	Thin and rough, but covering surface. No pitting corrosion.	Both HF's same. Mid-thickness, smooth and uniform. No pitting corrosion.
25 FPA	Excellent coating; smooth and thick. No pitting corrosion.	Mid-thickness, good average. No pitting corrosion.	Both HF's same. Mid-thickness, good average but rough surface. No pitting corrosion.
25 FPB	Mid-thickness. A bit rough on the surface but good avg; no pitting corrosion.	Midthickness coating w/ good average, but pitting corrosion is present.	Smooth, uniform coating. No pitting corrosion. Both Half-faces same.
27 FPA	Poor, hardly any coat on KE. Slight pitting corrosion.	Excellent coat: high thickness, smooth, uniform. No pitting corrosion.	Erratic in spots. Low to mid-thickness. Pitting corrosion.
27 FPB	Mid-thick. uniform until top of KE; coat is rough - pits.	Good average, mid-thickness, but pitting corrosion due to porosity.	Ranging for mid to high thickness, uniform to blistered. pitting corrosion present.
28 FPA	Smooth, thick coat. Only one low spot. No pitting corrosion.	Very thin coat, but pitting corrosion. Low thickness on each.	Corrosion flaked away coating and pitted Al.
28 FPB	Rougher w/ no good average. No pitting corrosion.	Thin, discontinuous coat w/rough surface no pitting corrosion.	Uniform, low to mid-thickness. Smooth w/ no sign of pitting corrosion.

EMI Gasket Cycler — Resistance vs. Cycles
Compilation of four tests (10,000 cycles): 940608, 09, 13, and 14.

(a)
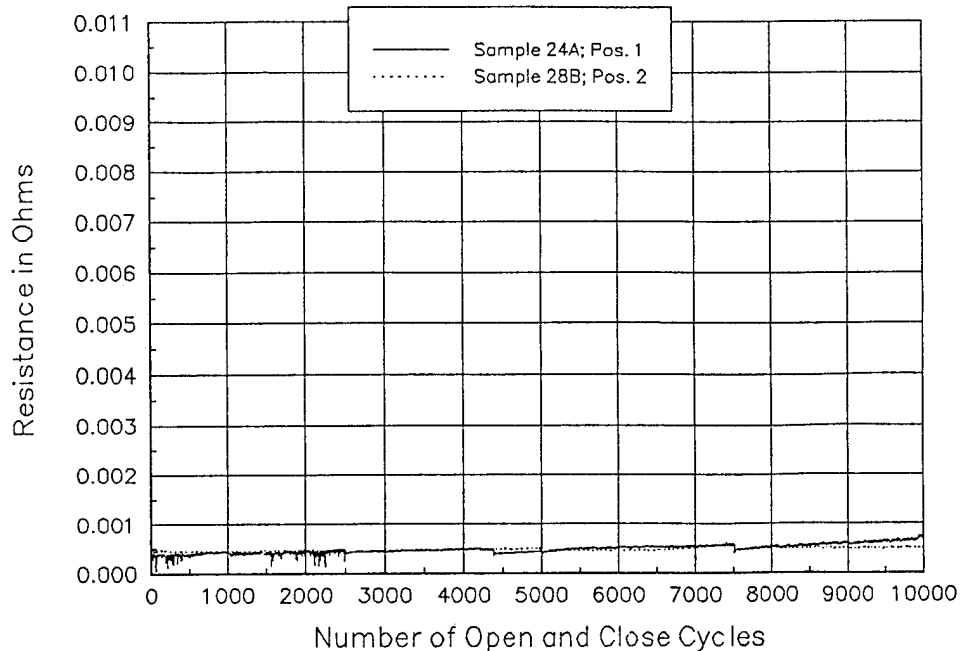
EMI Gasket Cycler — Resistance vs. Cycles
Linear Fit of Resistance per 100 Cycles (Tests 940608, 09, 13, and 14.)
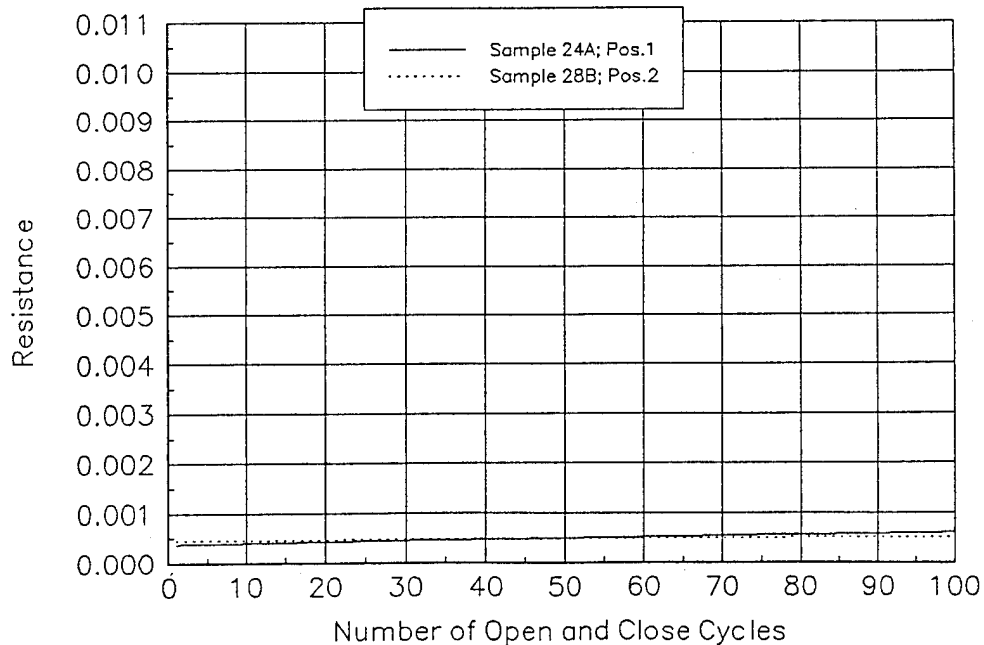
(b)

Figure 3.1. (a) Resistance vs cycles and (b) linear regression plots for 10,000 cycles pre-salt fog test for Samples 24A and 28B.

EMI Gasket Cycler — Resistance vs. Cycles
Compilation of four tests (10,000 cycles): 940608, 09, 13, and 14.

(c)

EMI Gasket Cycler — Resistance vs. Cycles
Linear Fit of Resistance per 100 Cycles (Tests 940608, 09, 13, and 14.)

(d)

Figure 3.1. (Cont'd). (c) Resistance vs cycles and (d) linear regression plots for 10,000 cycles pre-salt fog test for Samples 24B and 25B.

EMI Gasket Cycler — Resistance vs. Cycles
Compilation of four tests (10,000 cycles): 940608, 09, 13, and 14.

(Sample 23A; Pos. 5 / Sample 28A; Pos. 6)

(e)

EMI Gasket Cycler — Resistance vs. Cycles
Linear Fit of Resistance per 100 Cycles (Tests 940608, 09, 13, and 14.)

(Sample 23A; Pos.5 / Sample 28A; Pos.6)

(f)

Figure 3.1. (Cont'd). (e) Resistance vs cycles and (f) linear regression plots for 10,000 cycles pre-salt fog test for Samples 23A and 28A.

EMI Gasket Cycler — Resistance vs. Cycles
Compilation of four tests (10,000 cycles): 940608, 09, 13, and 14.

(g)

EMI Gasket Cycler — Resistance vs. Cycles
Linear Fit of Resistance per 100 Cycles (Tests 940608, 09, 13, and 14.)

(h)

Figure 3.1. (Cont'd). (g) Resistance vs cycles and (h) linear regression plots for 10,000 cycles pre-salt fog test for Samples 27A and 27B.

EMI Gasket Cycler — Resistance vs. Cycles
Compilation of four tests(10,000 cycles): 940608, 09, 13. and 14.

Sample 23B; Pos.9
Sample 25A; Pos.10

Number of Open and Close Cycles

(i)

EMI Gasket Cycler — Resistance vs. Cycles
Linear Regression Plots (940608 — 14)

Sample 23B; Pos. 9
Sample 25A; Pos.10

Number of Open and Close Cycles

(j)

Figure 3.1. (Cont'd). (i) Resistance vs cycles and (j) linear regression plots for 10,000 cycles pre-salt fog test for Samples 23B and 25A.

Figure 3.2. (a) Resistance vs cycles and (b) linear regression plots for 10,000 cycles post-salt fog test for Samples 25A and 27A.

EMI Gasket Cycler — Resistance vs. Cycles
Compilation of four tests (10,000 cycles): 940723, 25, 26, and 27.

(c)

EMI Gasket Cycler — Resistance vs. Cycles
Linear Regression Plots (940723 — 27)
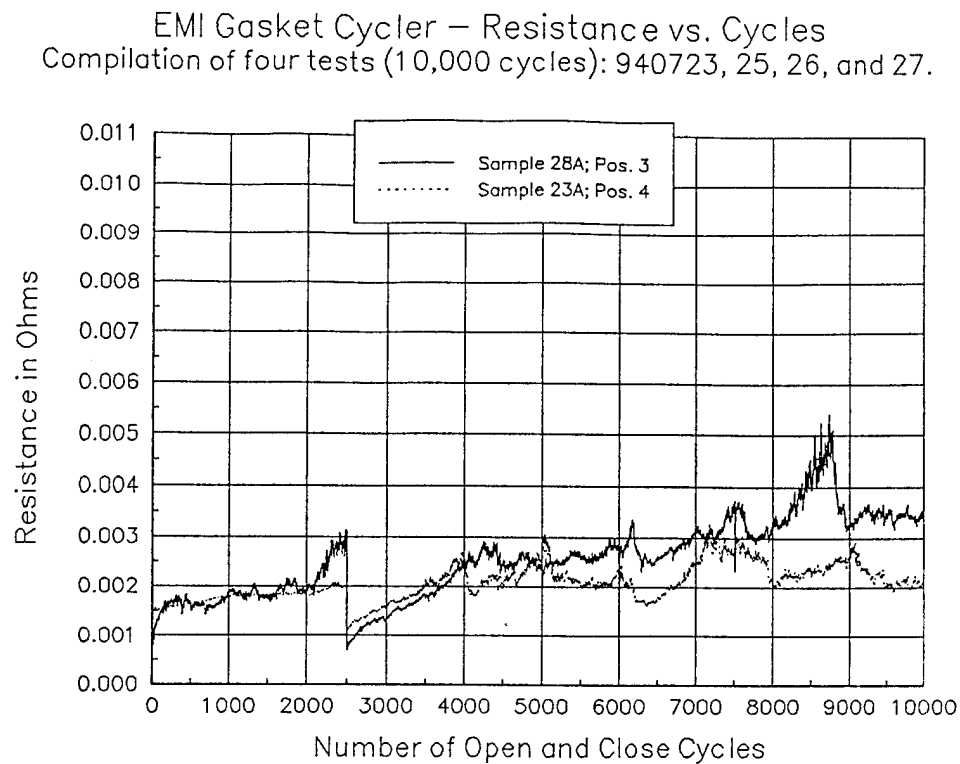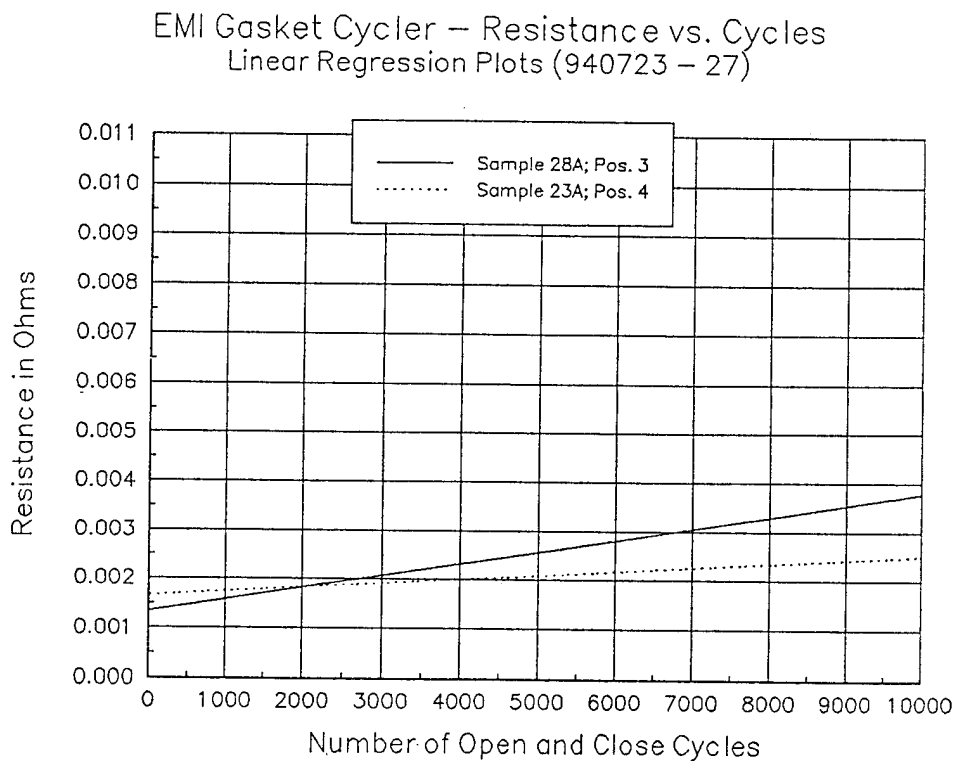
(d)

Figure 3.2. (Cont'd). (c) Resistance vs cycles and (d) linear regression plots for 10,000 cycles post-salt fog test for Samples 28A and 23A.
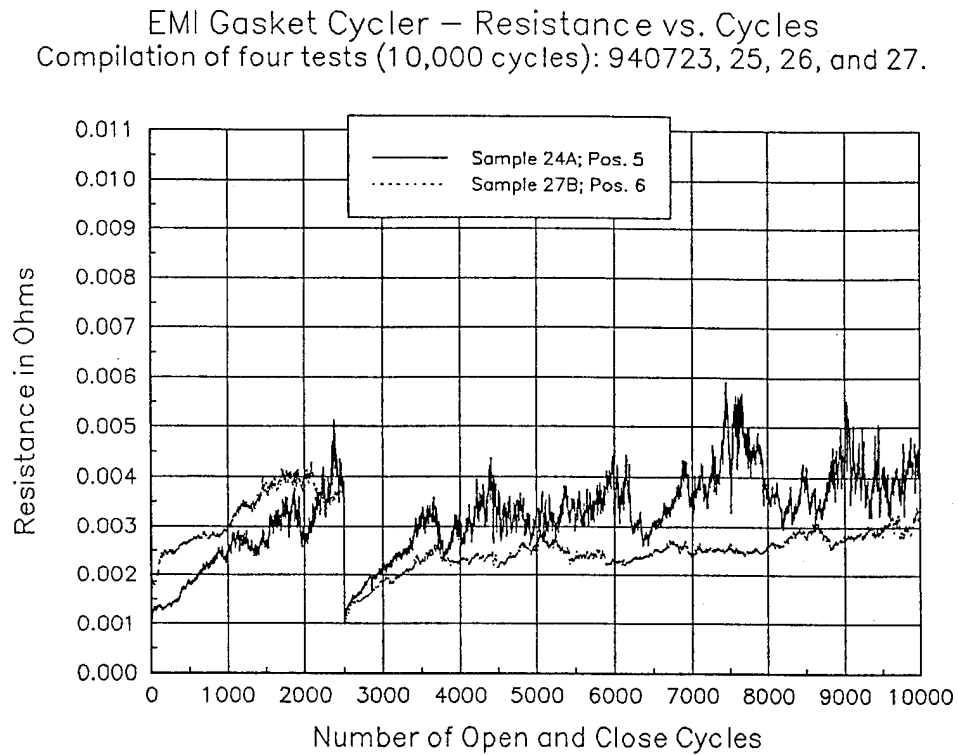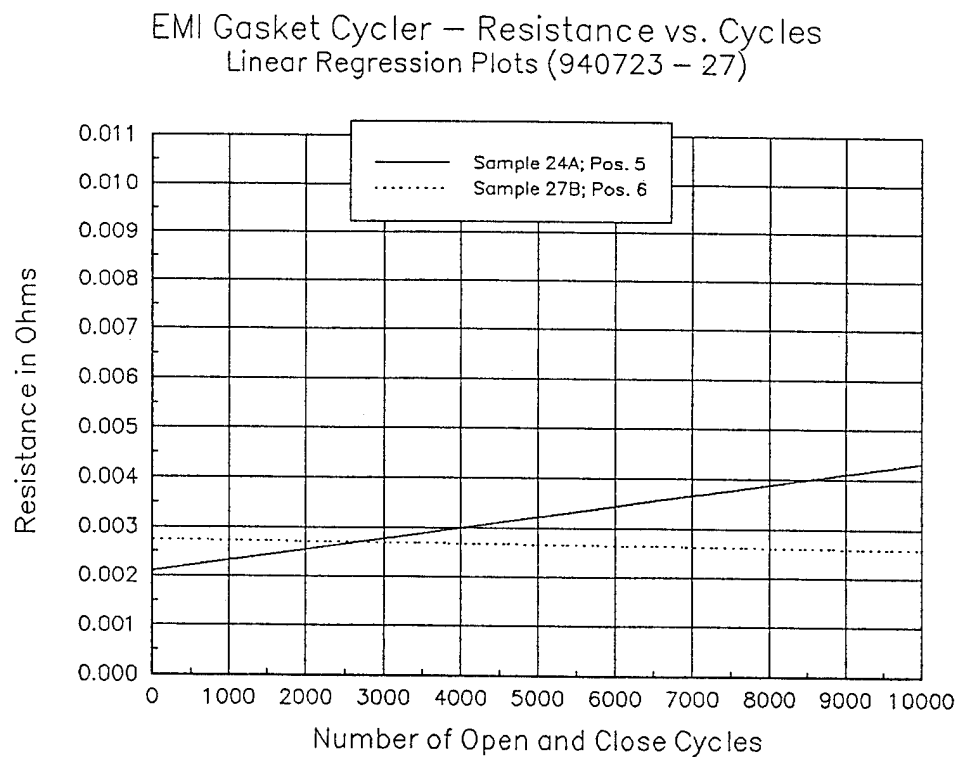
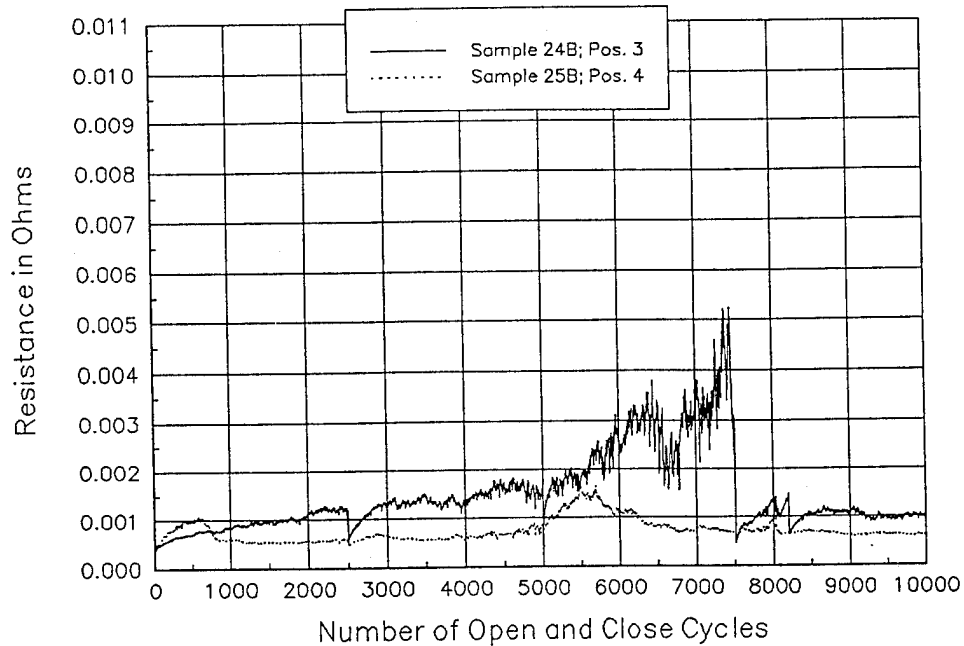Figure 3.2. (Cont'd). (e) Resistance vs cycles and (f) linear regression plots for 10,000 cycles post-salt fog test for Samples 24A and 27B.
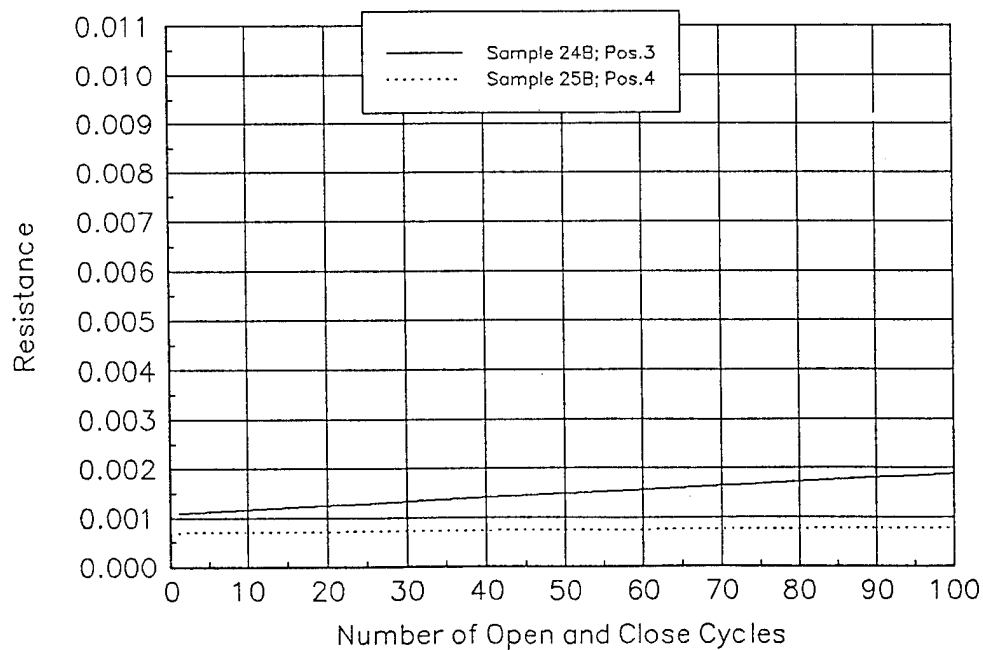
EMI Gasket Cycler — Resistance vs. Cycles
Compilation of four tests (10,000 cycles): 940723, 25, 26, and 27.
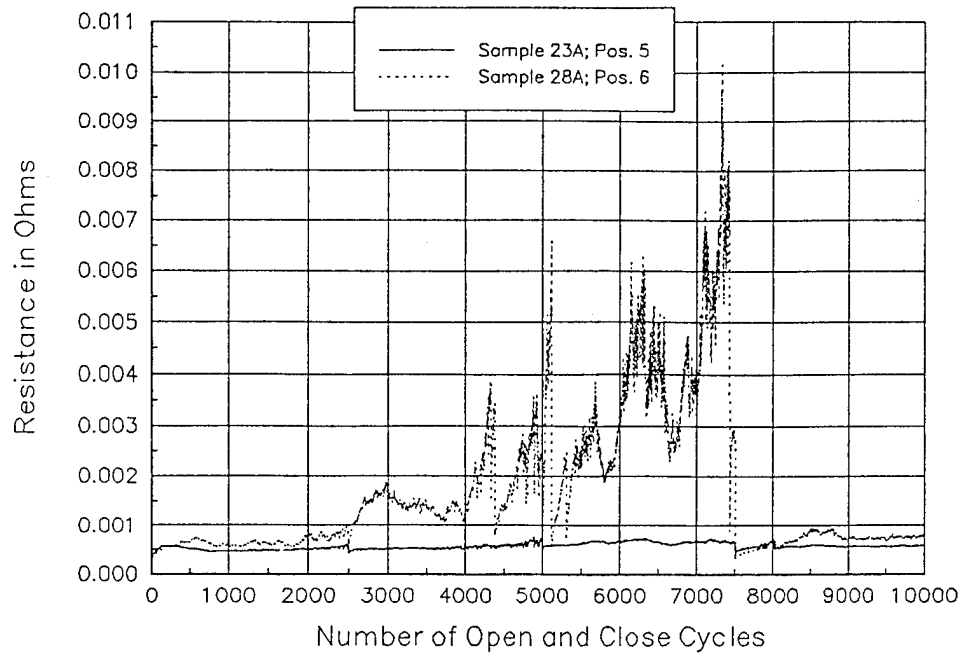
(g)

EMI Gasket Cycler — Resistance vs. Cycles
Linear Regression Plots (940723 — 27)
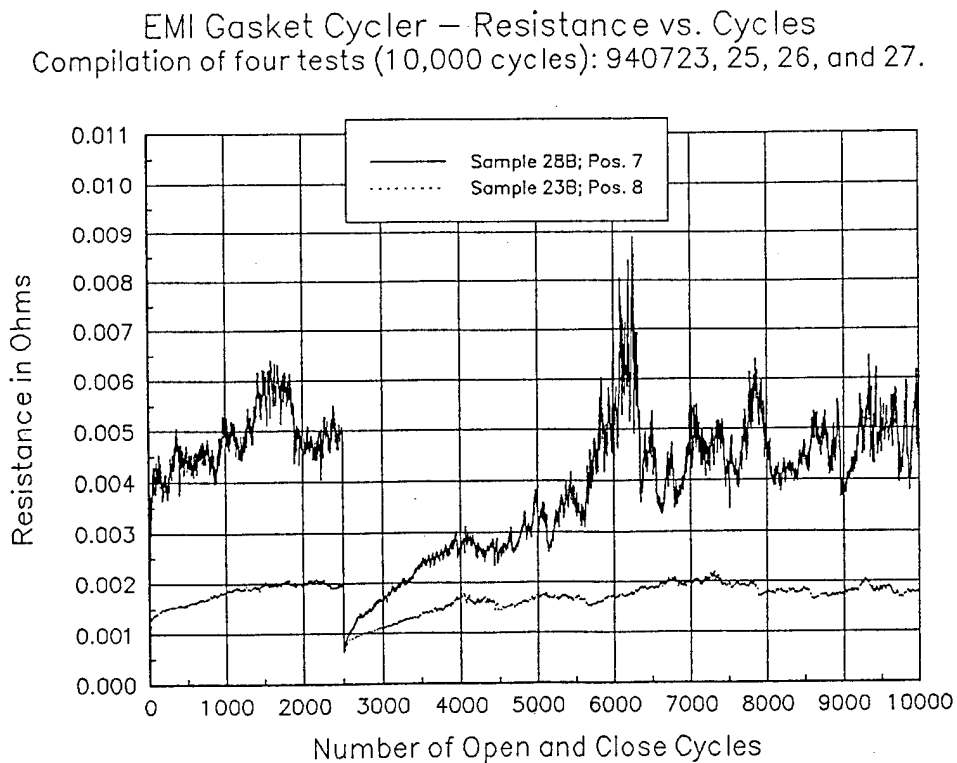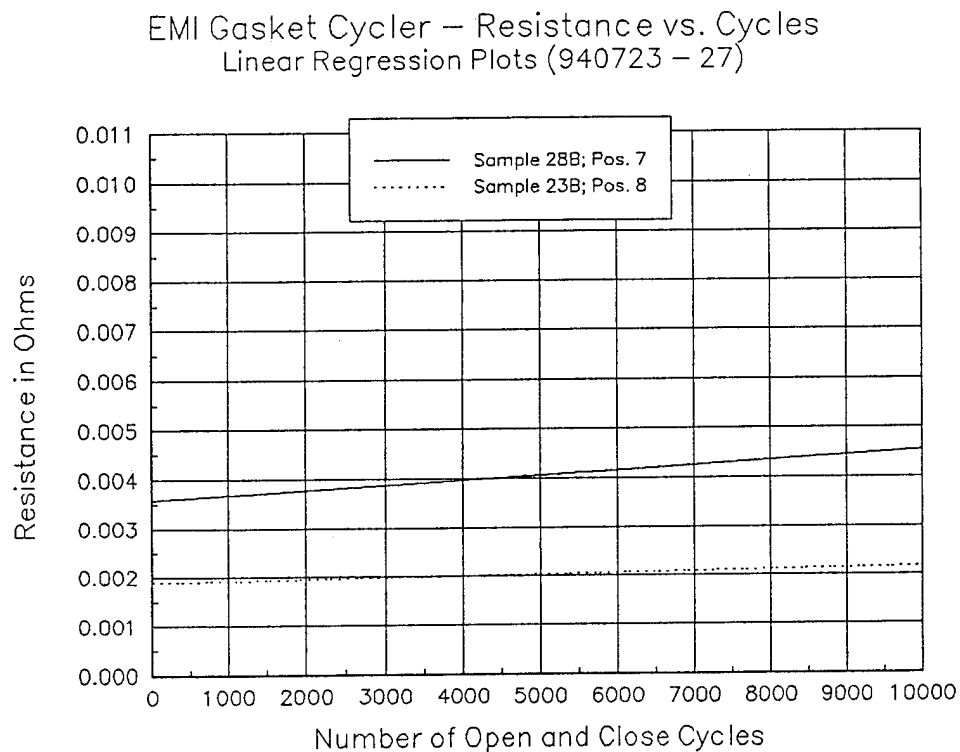
(h)

Figure 3.2. (Cont'd). (g) Resistance vs cycles and (h) linear regression plots for 10,000 cycles post-salt fog test for Samples 28B and 23B.

EMI Gasket Cycler — Resistance vs. Cycles
Compilation of four tests (10,000 cycles): 940723, 25, 26, and 27.

(i)
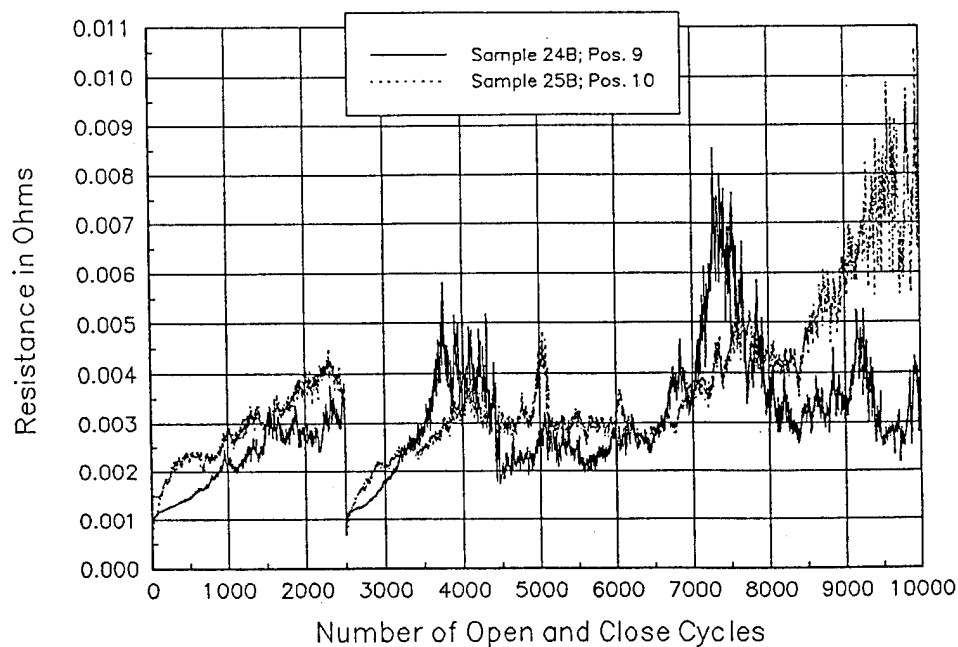
EMI Gasket Cycler — Resistance vs. Cycles
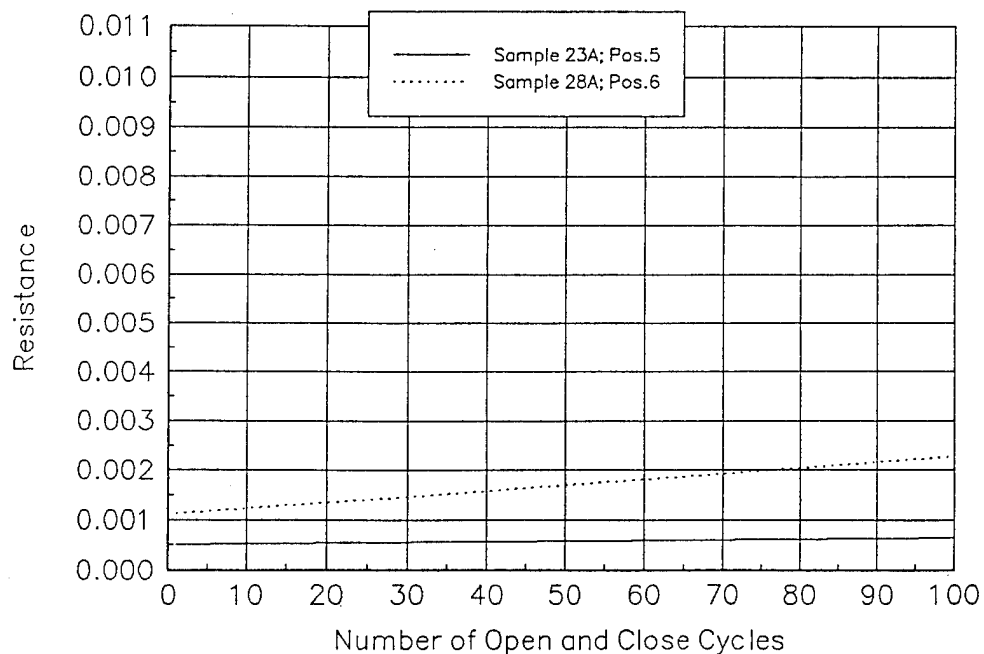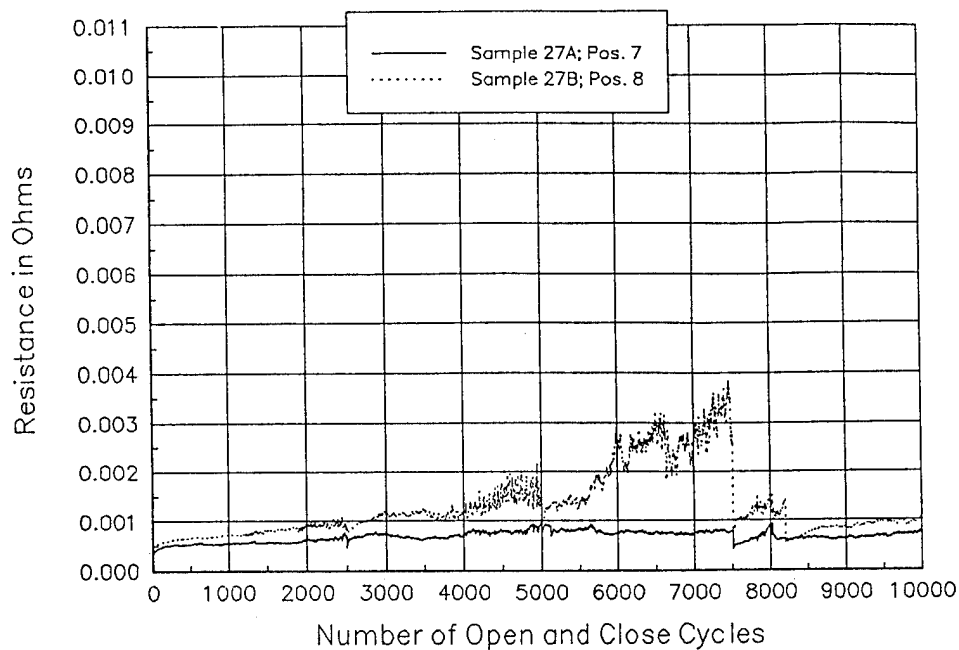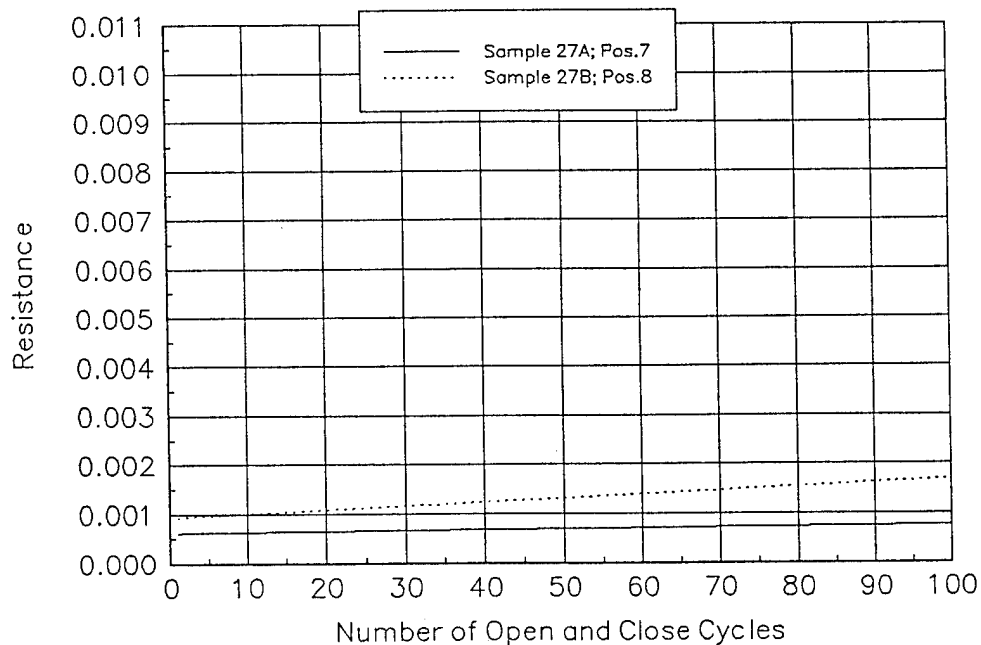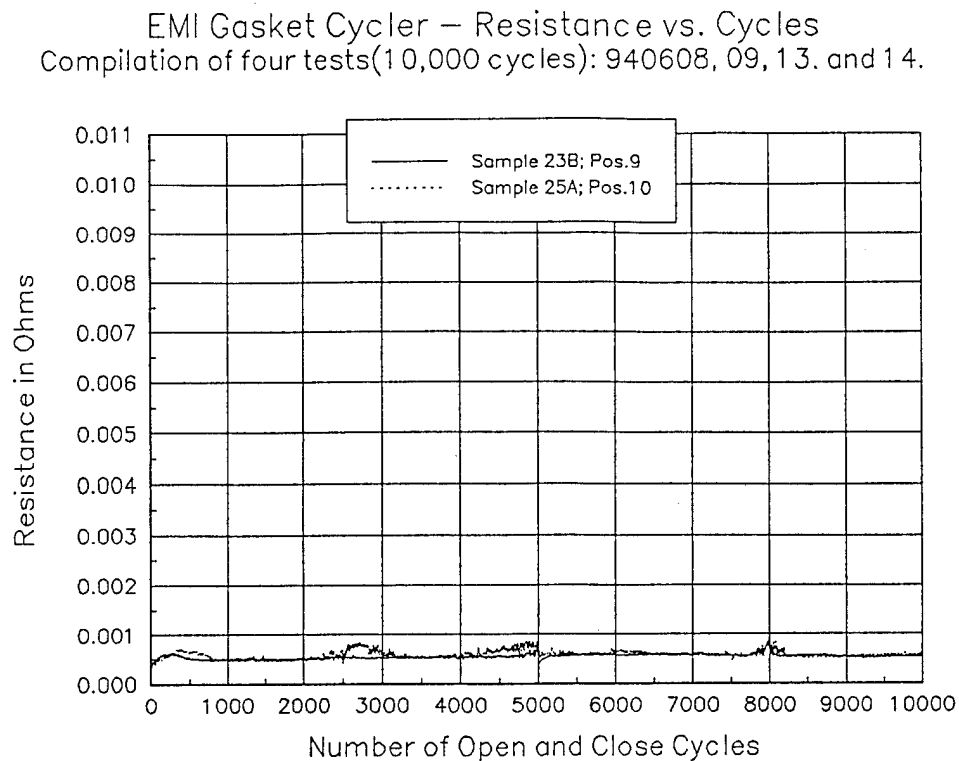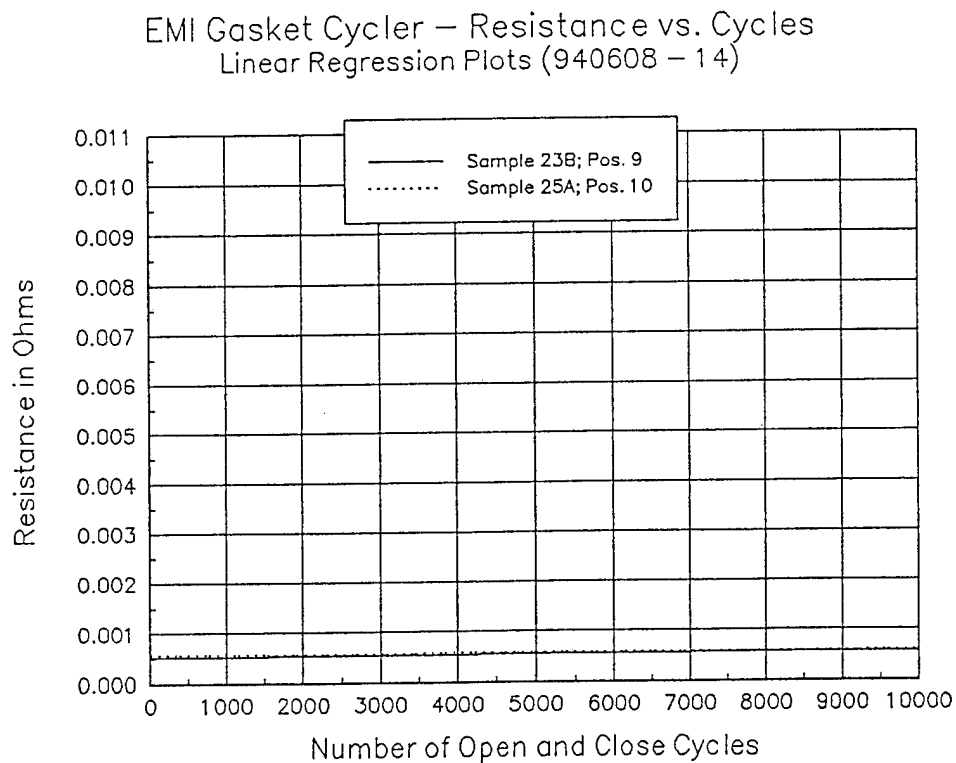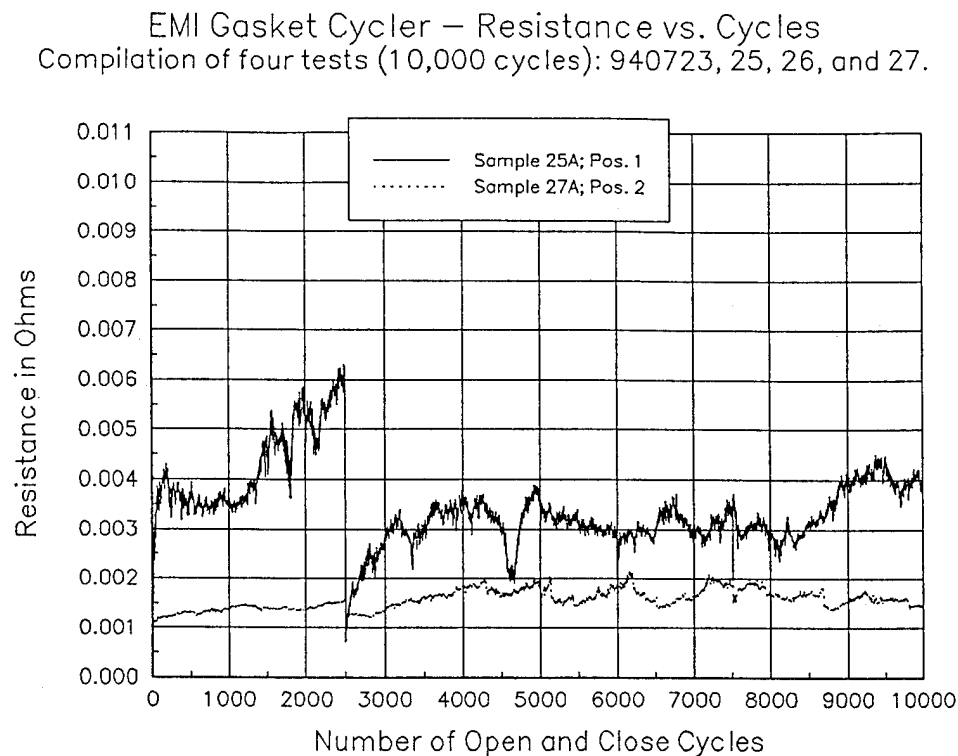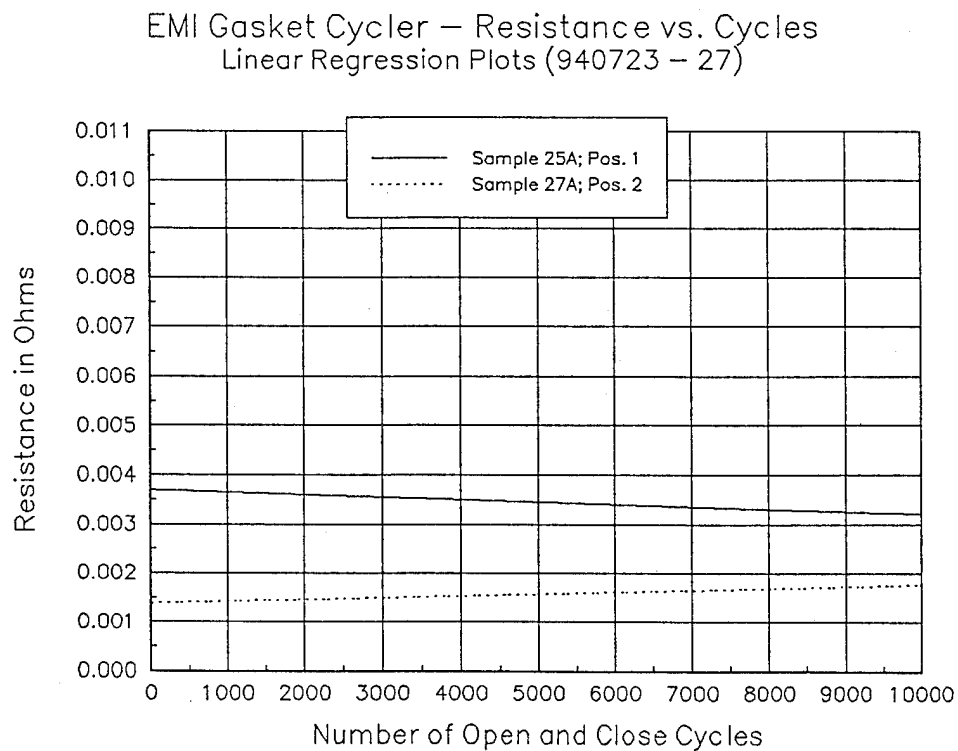### Linear Regression Plots (940723 — 27)
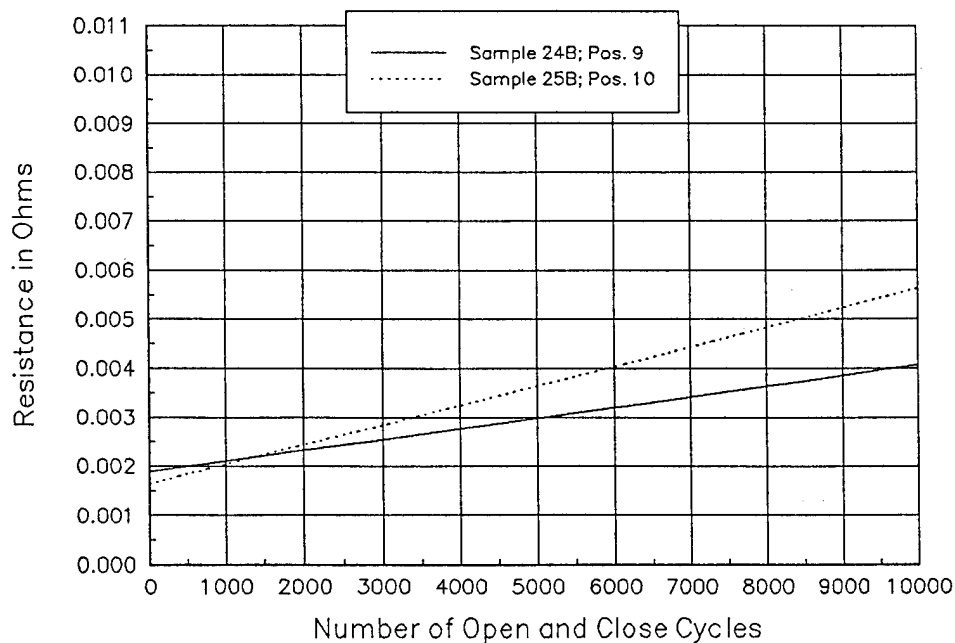
(j)

Figure 3.2. (Cont'd). (i) Resistance vs cycles and (j) linear regression plots for 10,000 cycles post-salt fog test for Samples 24B and 25B.

Table 3.3. Results of the pre-salt fog gasket cycling tests—resistance vs number of cycles.

Sample #	Slope (μΩ/cycle)	Initial Resistance (ohms)	Final Resistance (ohms)	r-Values of line fit
23FPA; Pos.5	0.0136511	0.0003686	0.0005834	0.57
23FPB; Pos.9	0.00607311	0.000359	0.0005548	0.42
24FPA; Pos.1	0.0236054	0.0003568	0.0007332	0.88
24FPB; Pos.3	0.0830322	0.0003734	0.0010704	0.30
25FPA; Pos.10	0.002925018	0.0003596	0.0006952	0.11
25FPB; Pos.4	0.00927006	0.0003638	0.0006132	0.12
27FPA; Pos.7	0.01454738	0.0003216	0.0007706	0.42
27FPB; Pos.8	0.07748994	0.000419	0.0010866	0.33
28FPA; Pos.6	0.1131949	0.0003218	0.0007708	0.22
28FPB; Pos.2	0.005905022	0.0003556	0.0005166	0.59

Note: μΩ/cycle = 1 X 10^{-6} ohms/cycle
Tests: 940608, 09, 13, and 14. Each test was 10,000 cycles at 30-sec dwell time for 72 hr.

Table 3.4. Results of the post-salt fog gasket cycling tests—resistance vs number of cycles.

Sample #	Slope (μΩ/cycle)	Initial Resistance (ohms)	Final Resistance (ohms)	r-Values of Line Fit	Comments
23FPA; Pos.4	0.0840885	0.0015306	0.002092	0.65	
23FPB; Pos.8	0.0277820	0.00098	0.0018306	0.30	
24FPA; Pos.5	0.222403	0.0009636	0.0043446	0.75	asym.≈0.0057*
24FPB; Pos.9	0.217791	0.0008552	0.003842	0.54	
25FPA; Pos.1	0.135969	0.0009506	0.0038544	0.56	asym.≈0.0044*
25FPB; Pos.10	0.398675	0.0007792	0.0098232	0.76	
27FPA; Pos.2	0.0378458	0.0007796	0.0014578	0.55	
27FPB; Pos.6	0.141167	0.0012056	0.0032472	0.83	asym.≈0.0033*
28FPA; Pos.3	0.243974	0.000691	0.003507	0.87	
28FPB; Pos.7	0.967588	0.001569	0.0059178	0.22	

* Exponential curve fits to the data may be better descriptions in these cases. The approximate asymptotes have been computed and are labeled "asym." in the table.
Note: μΩ/cycle = 1 X 10^{-6} ohms/cycle.
Tests: 940723, 25, 26, and 27. Each test was 10,000 cycles at 30-sec dwell time for 72 hr.

Table 3.5. Stylus electroplating parameters for Samples 31 – 40.

Sample #	Solution	Voltage	Current	Duration
31	Sol 1 Sol 2 ACT Ni Cu Sn	10 V 12-14 V 8 V 16 V 10 V 8 V	0.6-1.5 A 15 A 3-6 A 4.5 A 2.5-3.5 A 0.45-0.65 A	1 min 30 sec 1 min 2 min 2 min 5 min
32	Sol 2 Cu Sn	10 V 10 V 8 V	12.4 A 2.5-3.5 A 0.5-0.7 A	45 sec 2 min 5 min
33	Sol 2 Ni Cu	10 V 16 V 8 V	8 A 5W;3D 2.2-2.6 A	1 min 2 min 5 min
34	Sol 2 Ni Sn	10 V 16 V 8 V	6.5-7.5 A 5W;3D 0.5-0.6 A	1 min 2 min 5 min
35	Sol 2 Ni 60/40 Sn	10 V 16 V 6 V 10 V	9 A 3-5 A 0.75-0.9 A 0.6-0.9 A	1 min 2 min 2 min 5 min
36	Sol 2 Ni 60/40	10 V 16 V 6 V	9-10.4 A 2.5-5.5 A 0.5-0.9 A	1 min 2 min 5 min
37	Sol 2 Ni 60/40 95/5	10 V 16 V 6 V 6 V	9 A 3D-5W A 0.5-0.7 A 0.5-0.7 A	1 min 2 min 2 min 5 min
38	Sol 2 Ni 95/5	10 V 16 V 8 V	9-10 A 3.5-5.5 A 0.7-1.0 A	1 min 2 min 5 min
39	Sol 2 Ni	10 V 14 V	9 A 3D-5W A	1 min 7 min
40	Sol 2 ACT Ni	10 V 8 V 14 V	9 A 6 A 3D-5W A	1 min 2 min 7 min

Table 3.6. Results of the Sebastian Adherence tests for broadface channel samples.

Sample #	Stress (ksi)	Percent of Area Failed	Other Comments
23 CF	3.04 6.80 3.74	10% adhesive failed 70%	AVE = 4.53 STD= 2.00
23CF-ACT	5.28 7.73 5.42	5% adhesive failed adhesive failed	AVE= 6.14 STD= 1.38
31	7.84 4.52 3.79	97% 100% 5%	AVE= 5.38 STD= 2.16
32	7.38 5.80 3.88	95% adhesive failed adhesive failed	AVE= 5.69 STD= 1.75
33	6.17 4.32 4.66	adhesive failed adhesive failed adhesive failed	AVE= 5.05 STD= 0.985
34	2.19 4.31 3.37	adhesive failed adhesive failed adhesive failed	AVE= 3.29 STD= 1.06
35	7.11 6.21 3.52	50% 50% 35%	AVE= 5.61 STD= 1.87
36	5.04 3.35 3.72	100% 90% 5%	AVE= 4.04 STD= 0.888
37	4.92 4.81 2.79	15% 45% 100%	AVE= 4.17 STD= 1.20
38	4.42 2.89 4.54	65% adhesive failed 25%	AVE= 3.95 STD= 0.920
39	3.18 5.76 2.77	adhesive failed adhesive failed 30%	AVE= 3.90 STD= 1.62
40	2.87 2.50 6.06	adhesive failed adhesive failed adhesive failed	AVE= 3.81 STD= 1.96

Notes: 1 ksi = 6.896551 MPa.
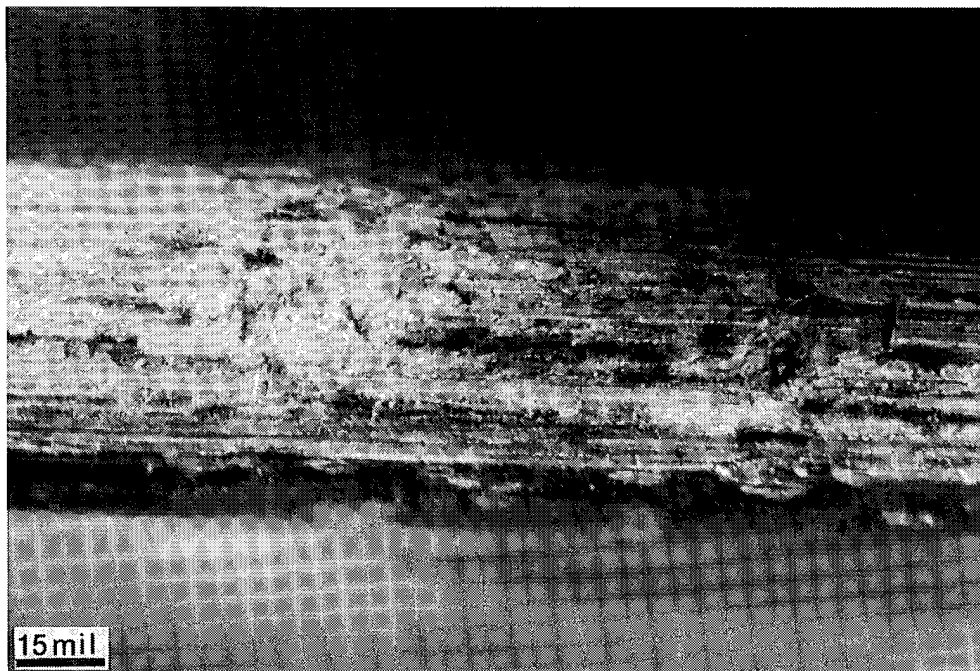
(a)
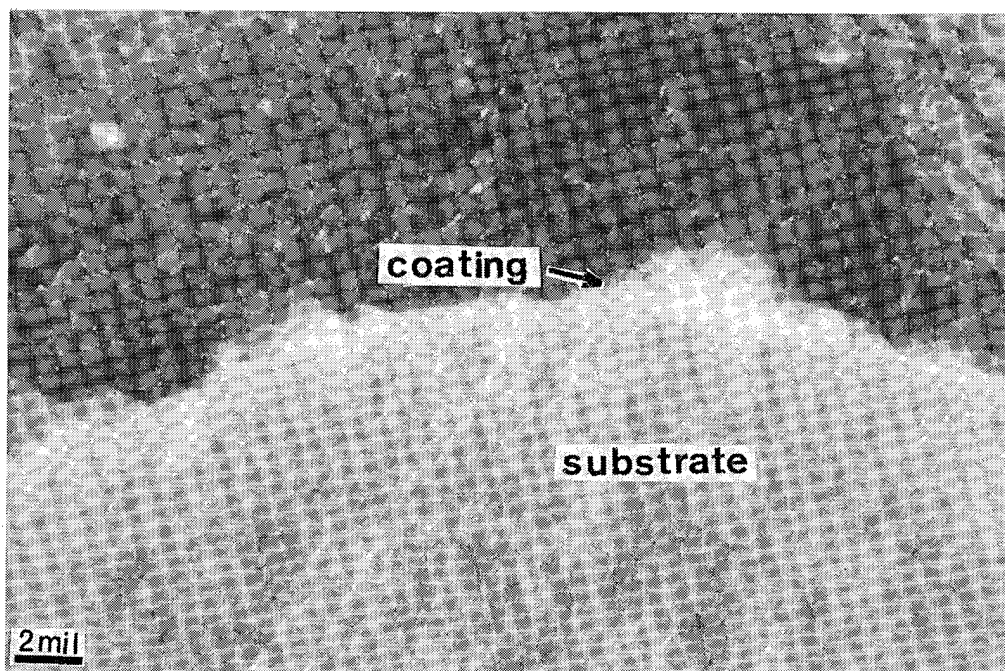
(b)

Figure 3.3. Optical micrograph of knife-edge (a) Sample 23FPA and (b) cross-section Sample 23FPA.

(c)

(d)

Figure 3.3. (Cont'd). Optical micrograph of knife-edge (c) Sample 23FPB and (d) cross-section Sample 23FPB.

(e)

(f)

Figure 3.3. (Cont'd). Optical micrograph of knife-edge (e) Sample 24FPA and (f) cross-section
Sample 24FPA.
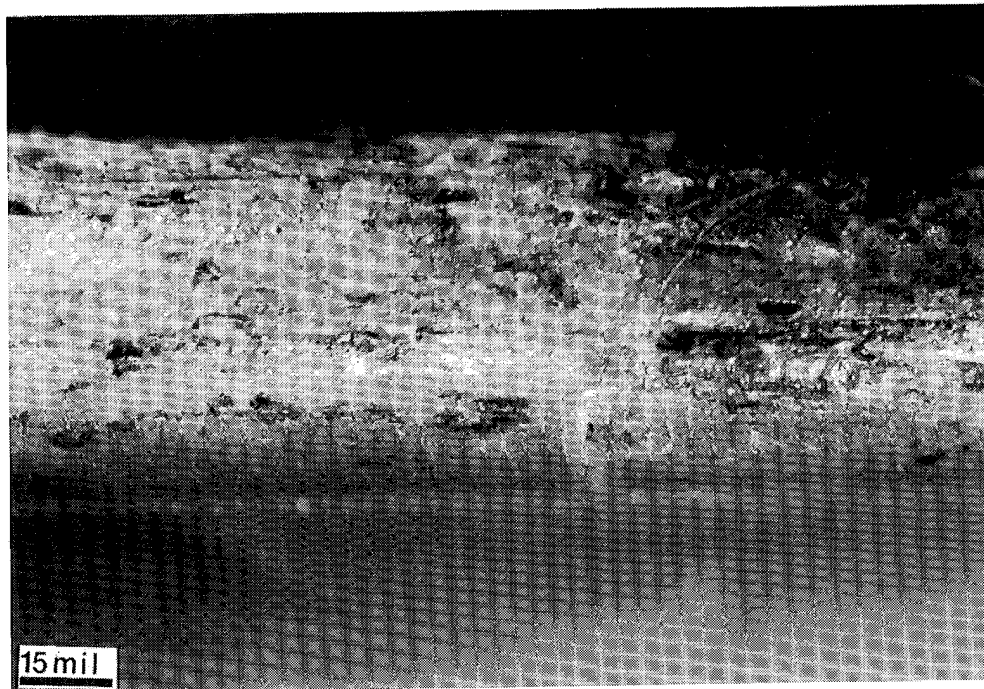
(g)
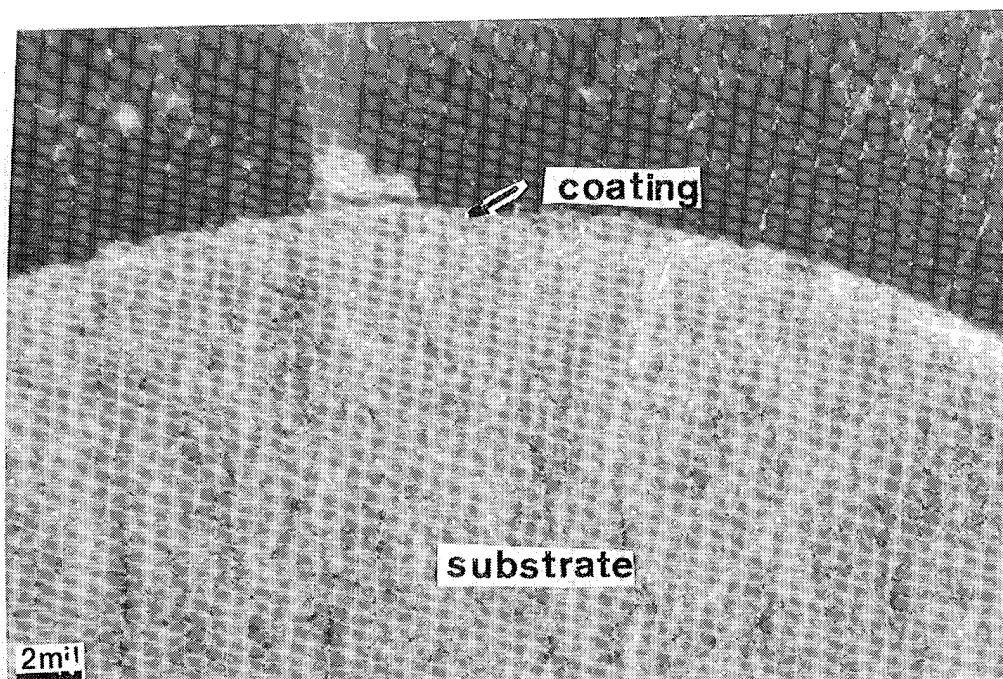
(h)

Figure 3.3. (Cont'd). Optical micrograph of knife-edge (g) Sample 24FPB and (h) cross-section Sample 24FPB.
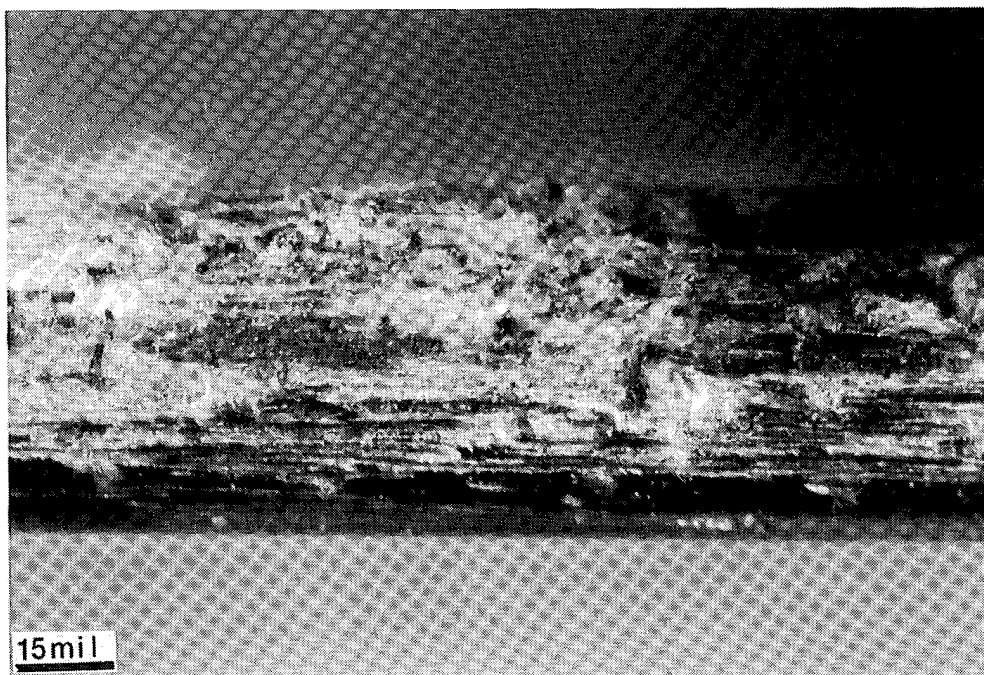
(i)
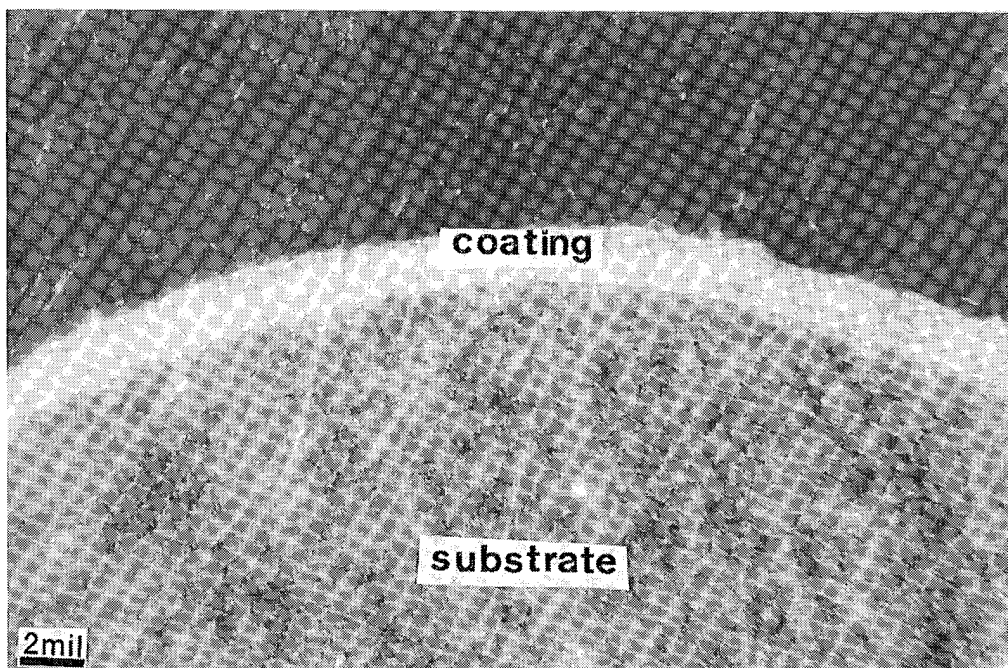
(j)

Figure 3.3. (Cont'd). Optical micrograph of knife-edge (i) Sample 25FPA and (j) cross-section Sample 25FPA.
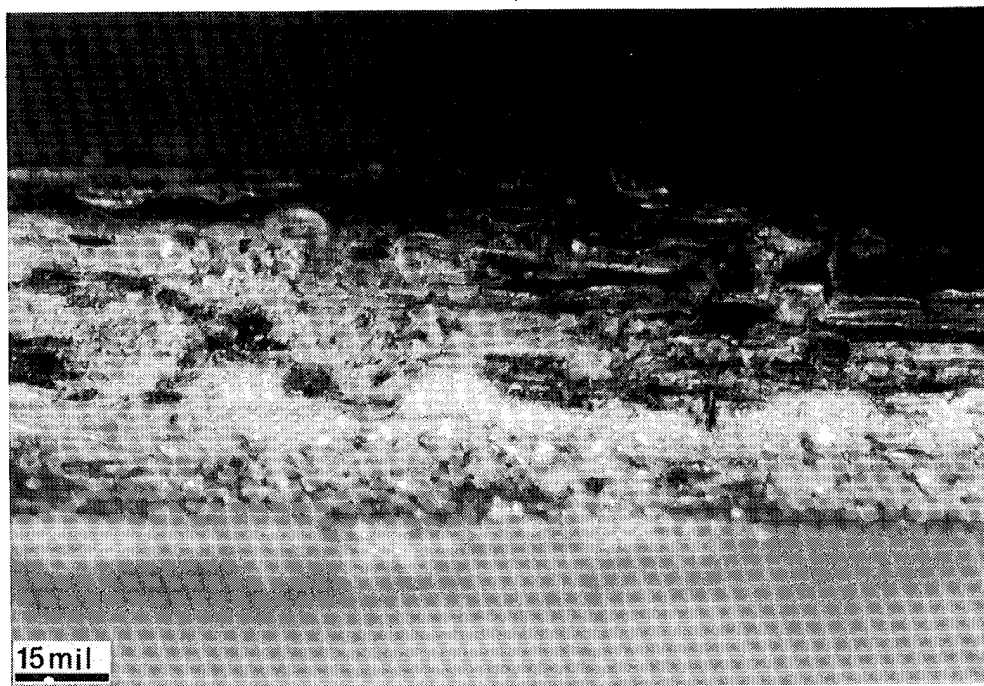
(k)
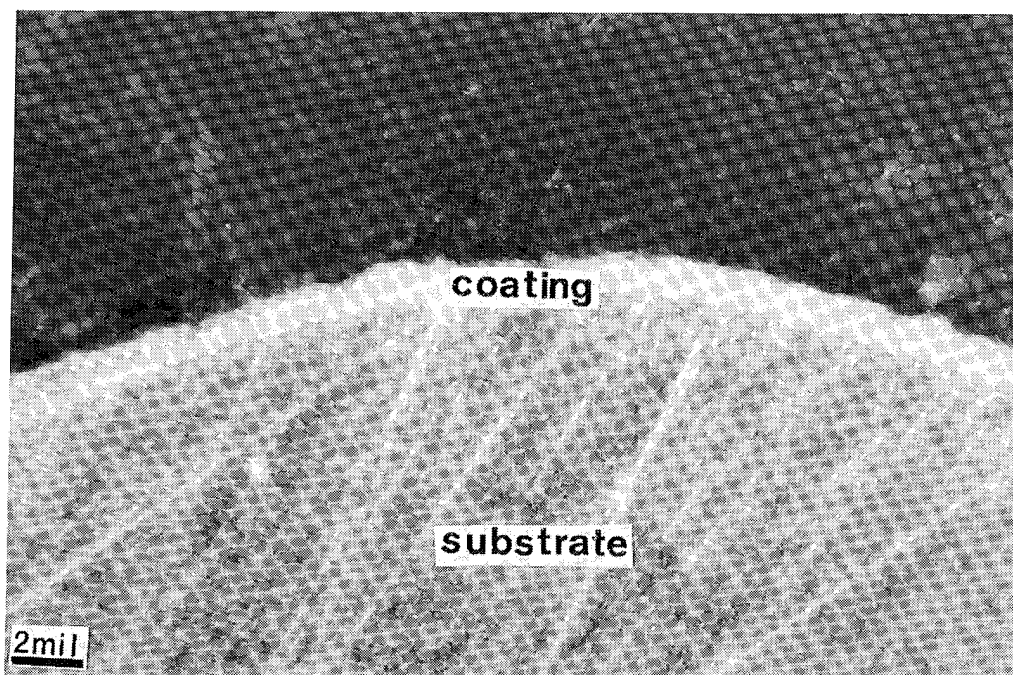
(l)

Figure 3.3. (Cont'd). Optical micrograph of knife-edge (k) Sample 25FPB and (l) cross-section Sample 25FPB.
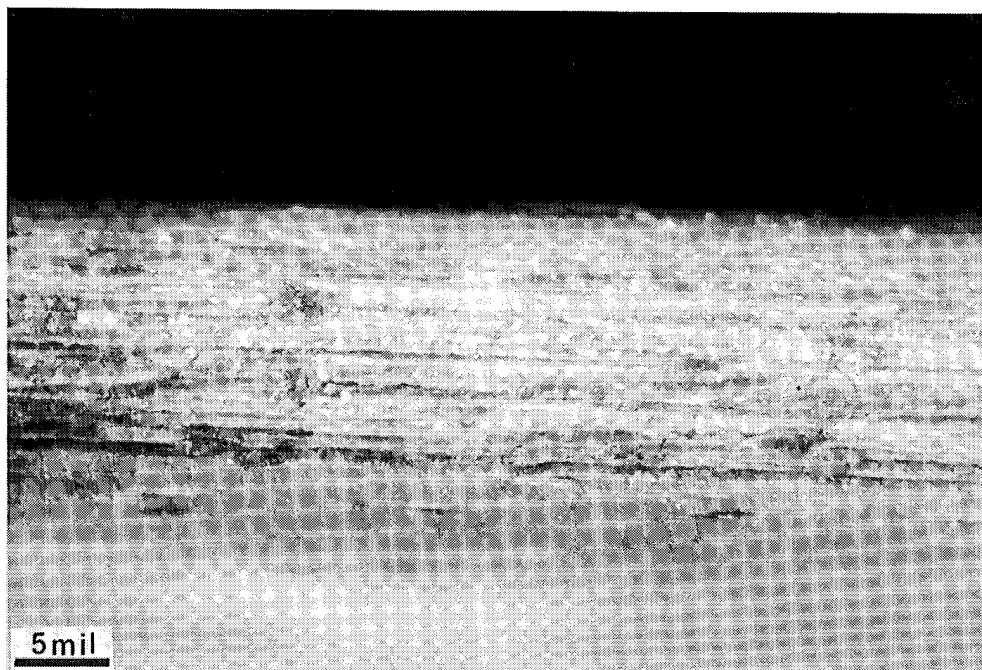
(m)
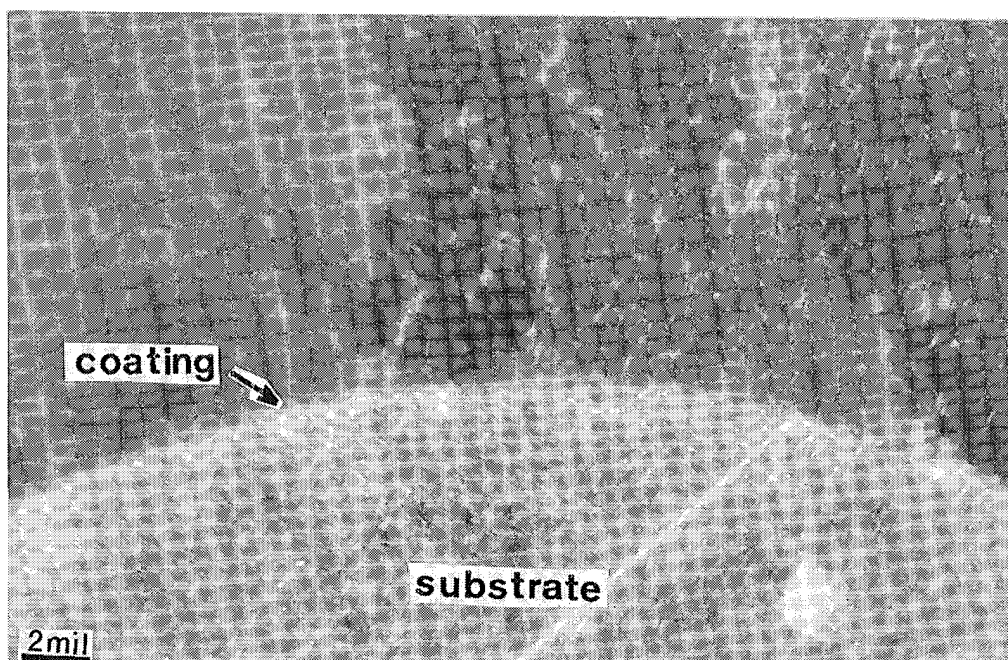
(n)

Figure 3.3. (Cont'd). Optical micrograph of knife-edge (m) Sample 27FPA and (n) cross-section Sample 27FPA.
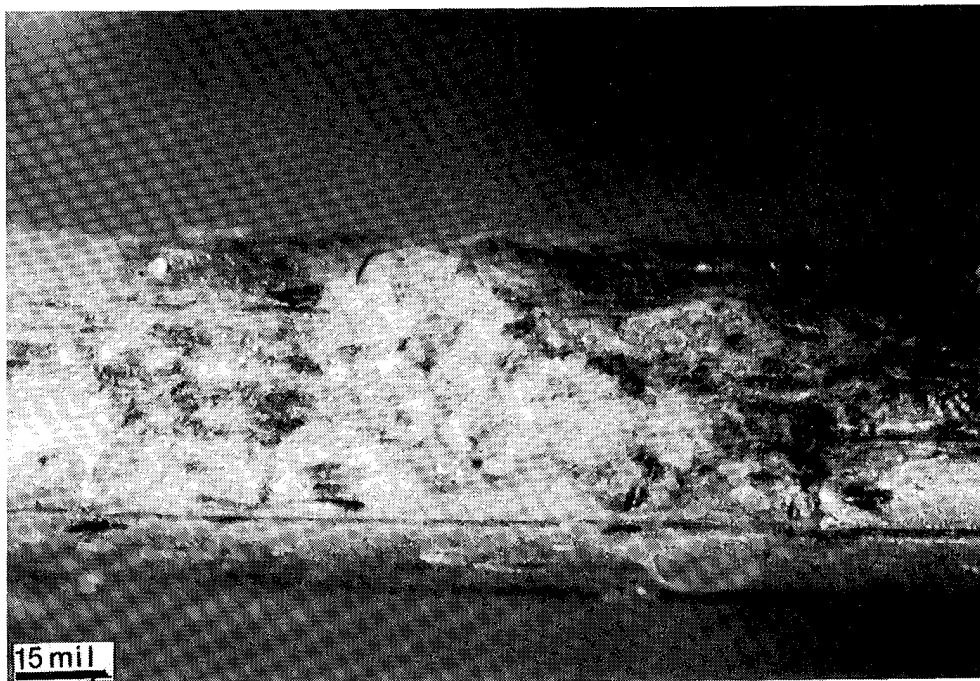
(o)
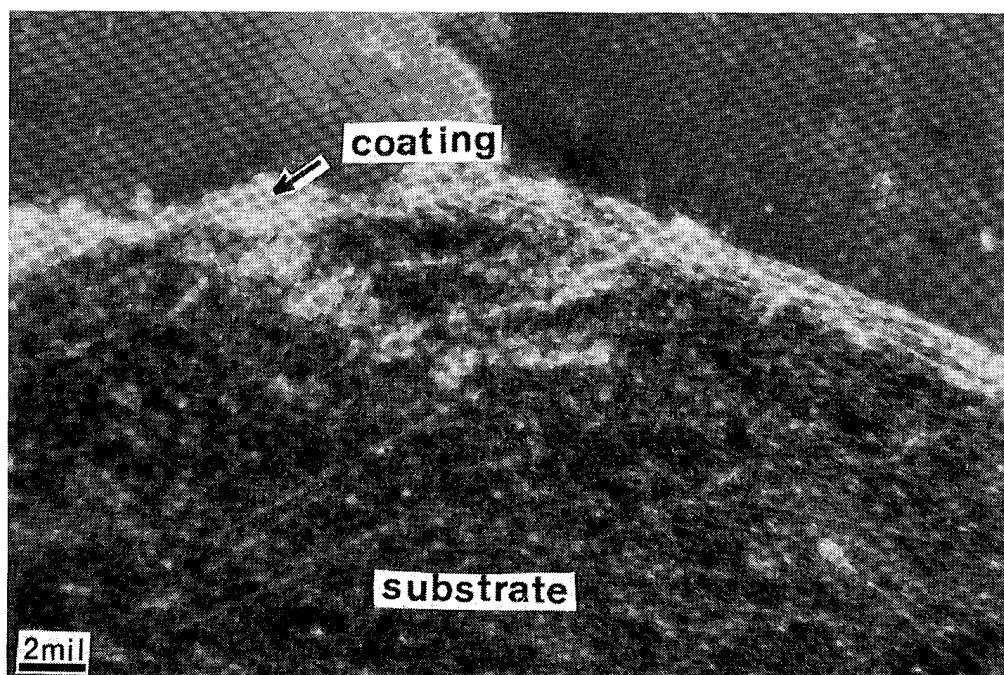
(p)

Figure 3.3. (Cont'd). Optical micrograph of knife-edge (o) Sample 27FPB and (p) cross-section
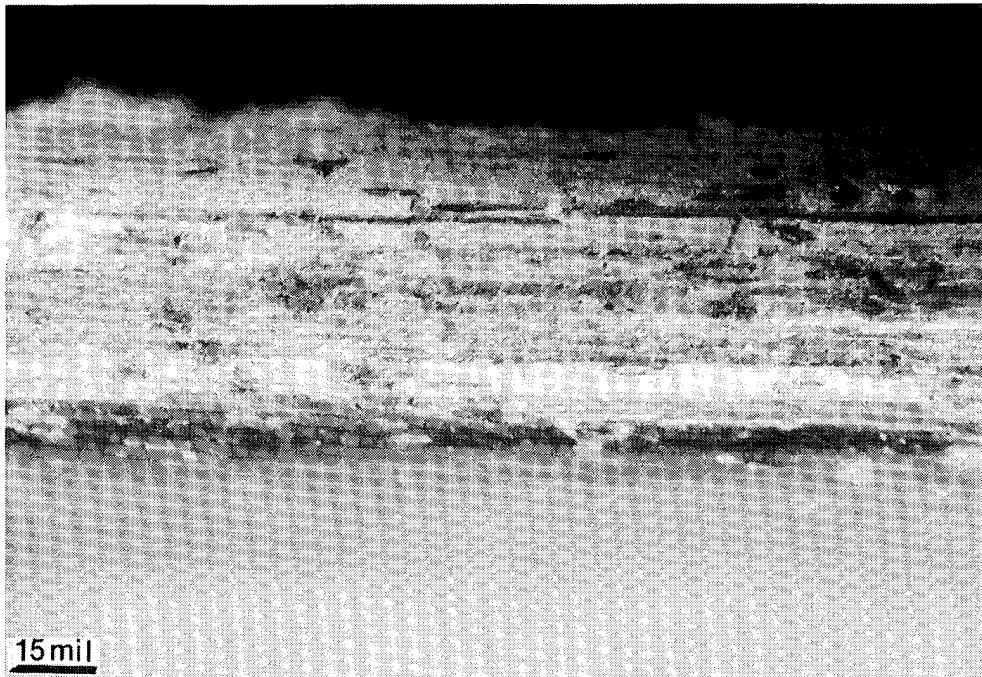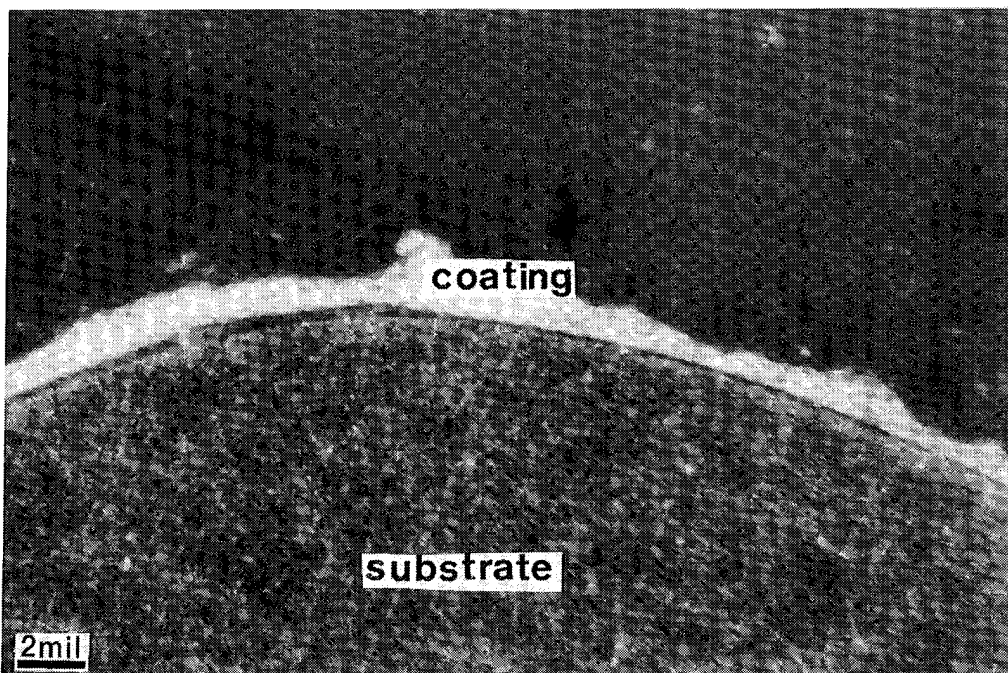Sample 27FPB.
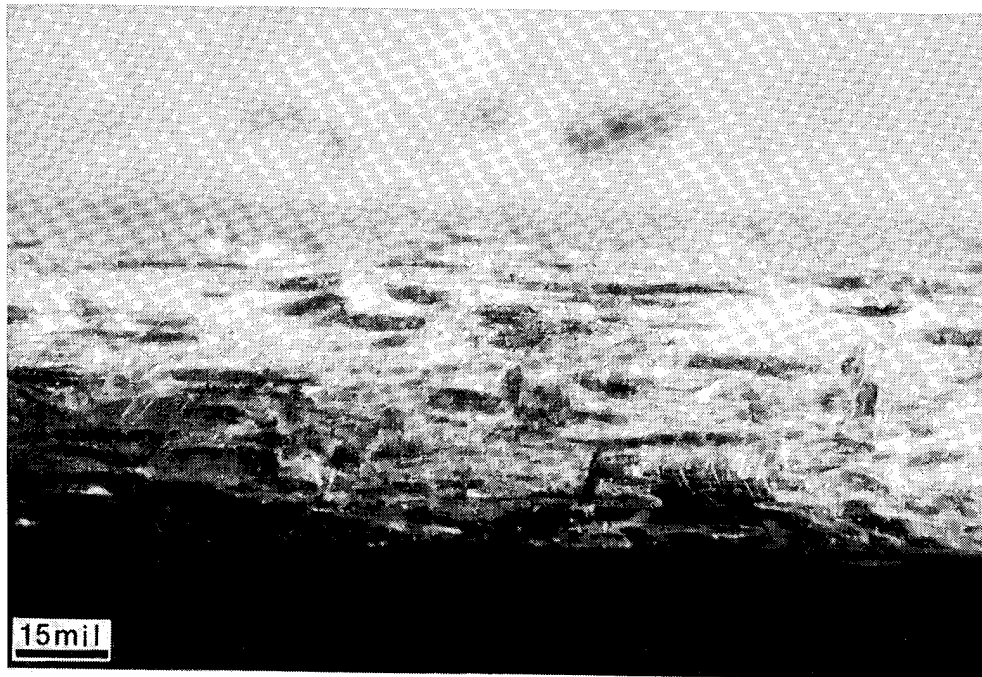
(q)
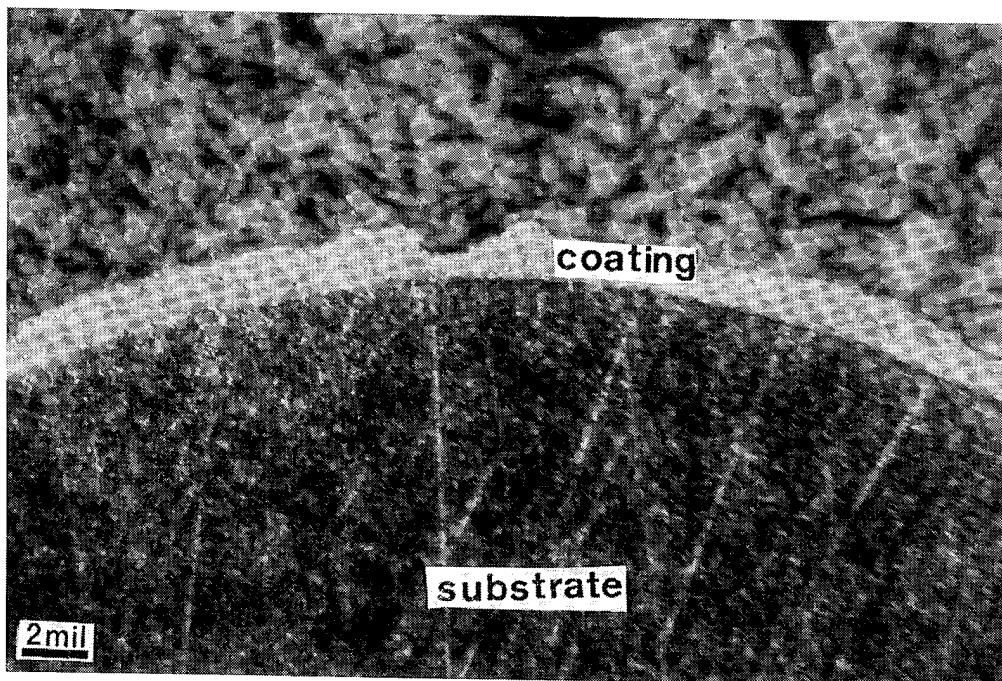
(r)

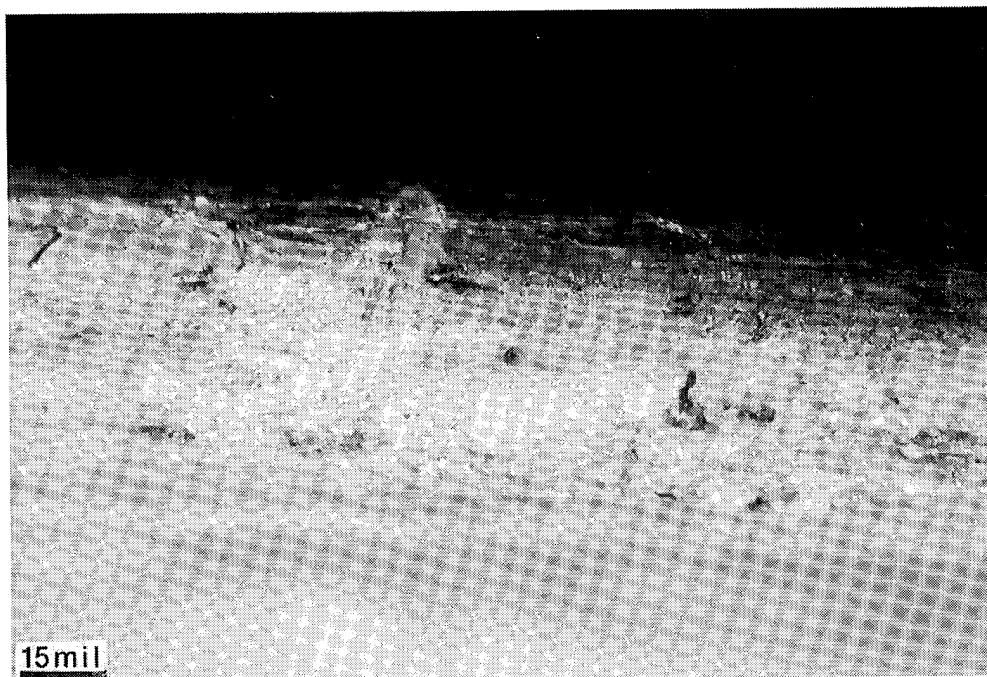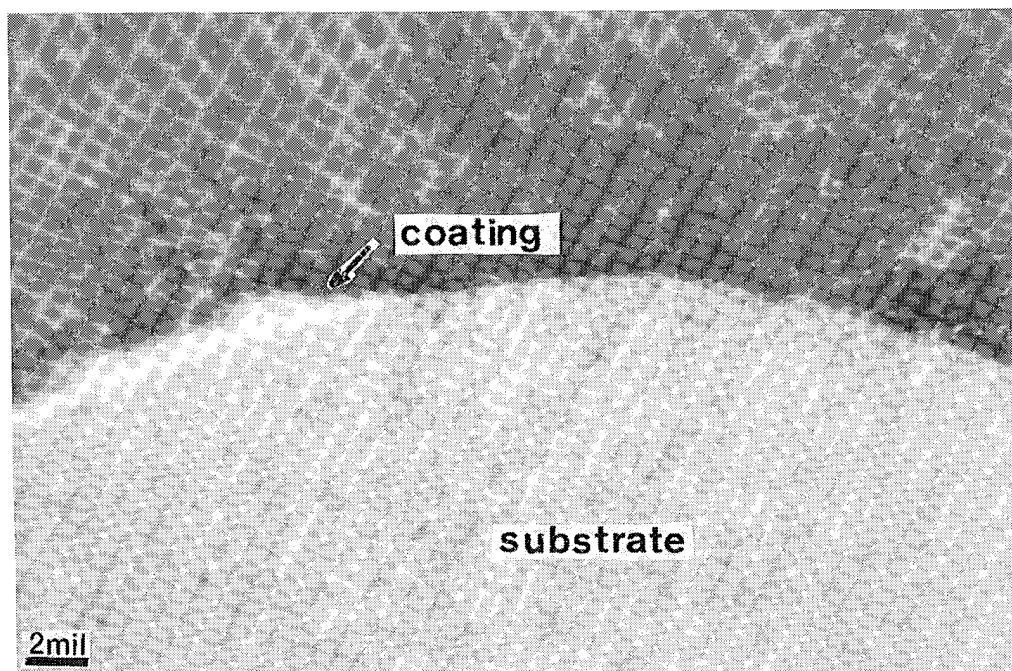Figure 3.3. (Cont'd). Optical micrograph of knife-edge (q) Sample 28FPA and (r) cross-section Sample 28FPA.
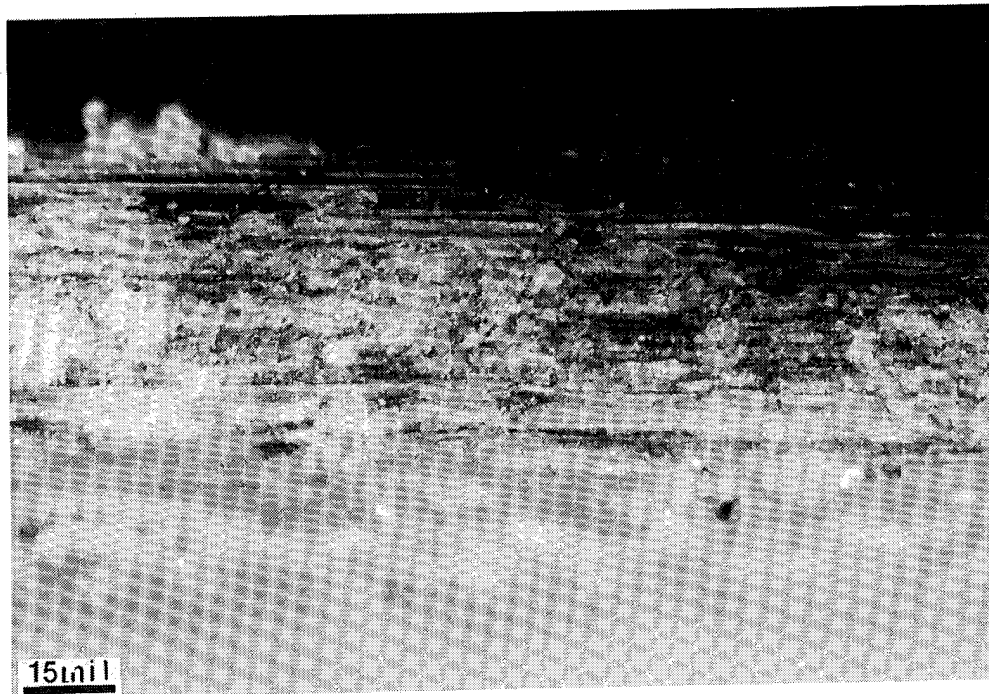
(s)
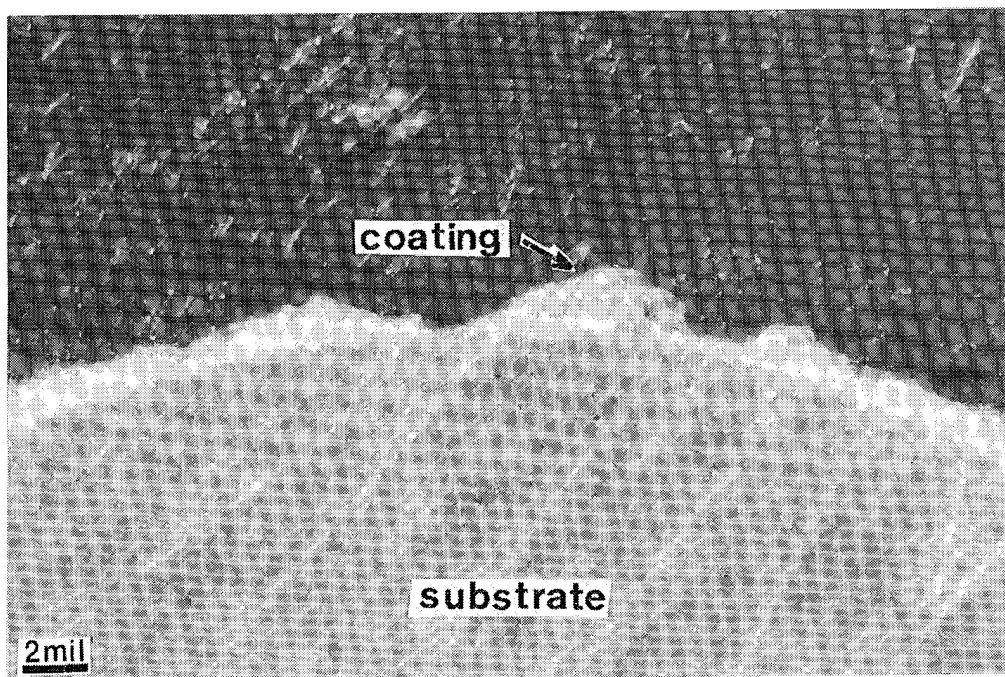
(t)

Figure 3.3. (Cont'd). Optical micrograph of knife-edge (s) Sample 28FPB and (t) cross-section
Sample 28FPB.

Table 3.7. Summary of findings on B-117 Salt Spray (Fog) tested stylus electroplated 6061 aluminum samples.

Sample #	Coating Description	Results of Salt Fog Tests
23 CF	Sn on Ni. Shiny w/ lines in the plate. No blisters.	Sparse corrosion product indicates a fair plate. Increase in thickness should yield good plate.
23 CF ACT	Sn on Ni. Shiny w/ lines in the plate. No blisters.	Same as above only less discoloration.
31 CF	Sn on Cu on Ni. Shiny, no blisters.	Maintained most of its shine; little discoloration. Almost no corrosion. One of three great plates.
32 CF	Sn on Cu. Shiny, with a hint of Cu color; NB.	Little discoloration; no visible corrosion. Best coating in terms of corrosion resistance.
33 CF	Cu on Ni. Cu in appearance with no visible blisters.	Very poor corrosion resistance. Cu both discolored and flaked away at substrate exposure.
34 CF	Sn on Ni. Lines in plate. Dull. No blisters.	Another very good coating(#2); very little and sparse corrosion. Slight discoloration.
35 CF	Sn on 60/40 Sn:Pb on Ni. Blisters. Dull.	A bit worse; sparse random product originating at surface flaws. Little discoloration.
36 CF	60/40 Sn:Pb on Ni. Very, shiny; no blisters.	Worst of the Sn(Sn-Pb) series. Discoloration and significant corrosion; however, still shiny.
37 CF	95/5 Sn:Pb on 60/40 on Ni. Very shiny; no blisters.	Also poor. Discoloration and random corrosion. Some shine is still present.
38 CF	95/5 Sn:Pb on Ni. Very, shiny; no blisters.	Same as above only with a great deal of shine retained.
39 CF	Ni: Dull, Ni color. No blisters; water spots easy.	Surface of coating greatly discolored. No significant buildup of salt of product.
40 CF	Ni: Dull, Ni color. No blisters; water spots easy.	Surface of coating greatly discolored. No significant buildup of salt or product.
Uncoated Al standard	N/A	No solid corrosion product. Discoloration - bronze with spots of light, dull Al present.

Other Comments: It appears that a great deal of what was initially considered to be corrosion product, is predominately solidified salts. Quantitatively, the ability of for the above coatings to resist sea salt corrosion is listed from best to worst as follows: 32 CF, 34 CF, 31 CF, 23 CF, 23 ACT CF, 35 CF, 38 CF, 37 CF, 36 CF, 40 CF, 39 CF, 33 CF.

02   04

NMA   S C   KS C
A G L   L   N A
CURSOR (KEV) =02.960   EDAX

(a)

Scratch

Corrosion
Prod.

Corrosion
Prod.

13mil
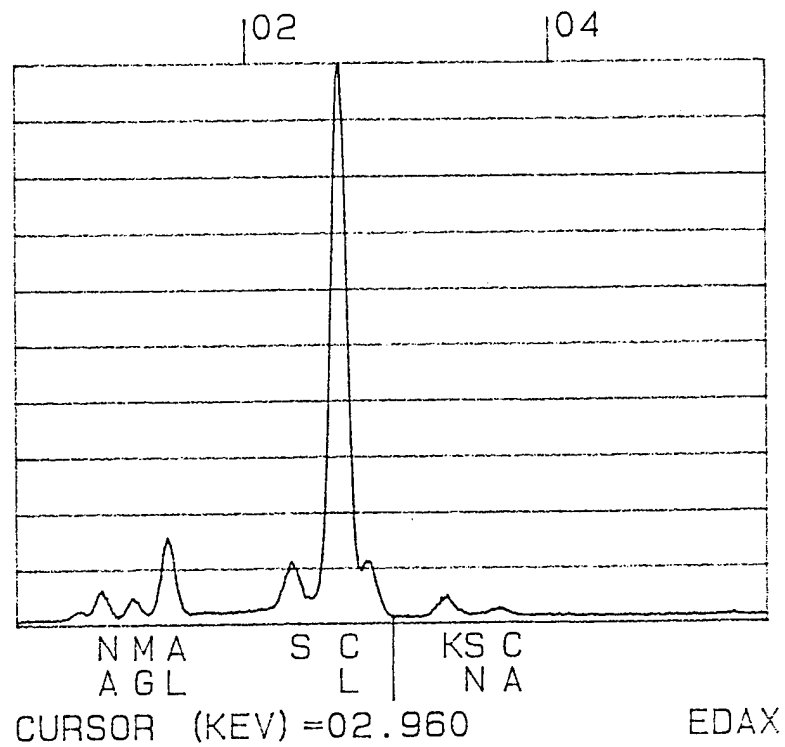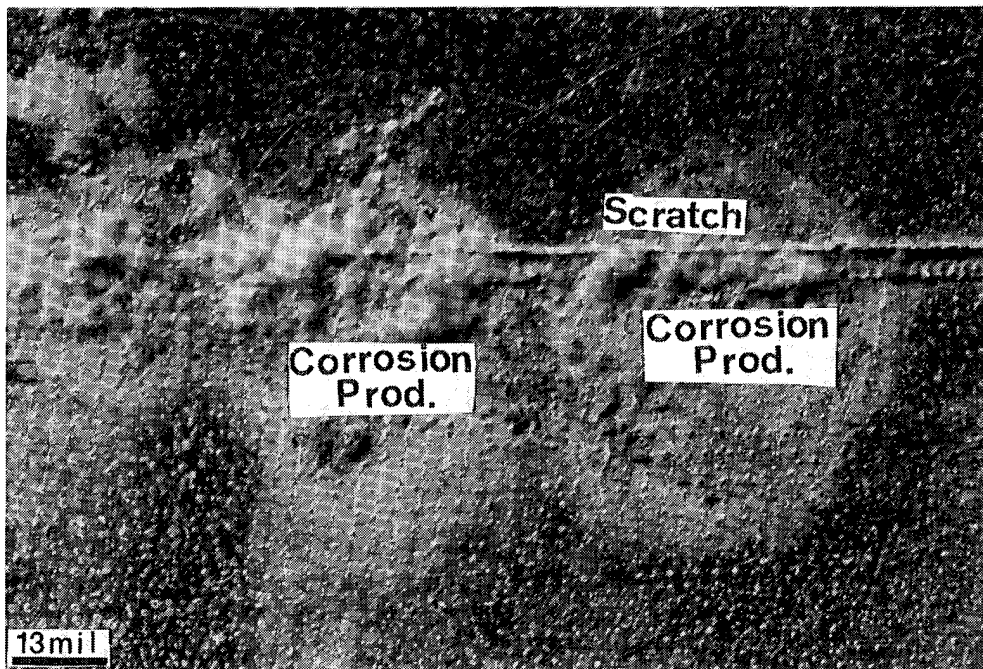
(b)

Figure 3.4. (a) Energy dispersive x-ray analysis of corrosion product and (b) Corrosion of
aluminum substrate exaggerated by high cathode (Sn coat) to anode (Al) ratio.
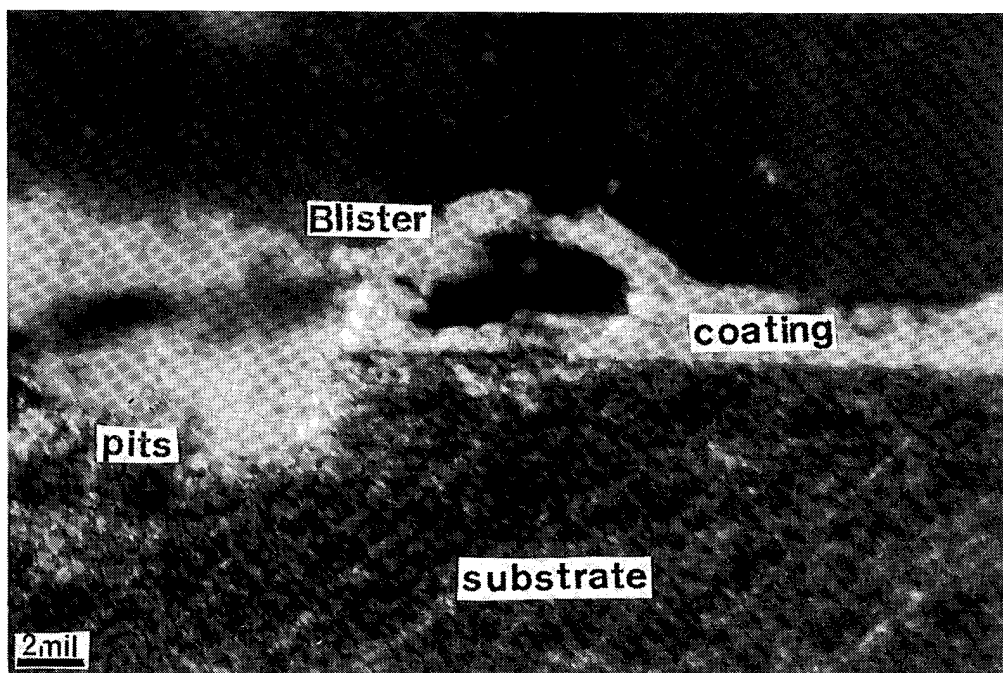
(c)
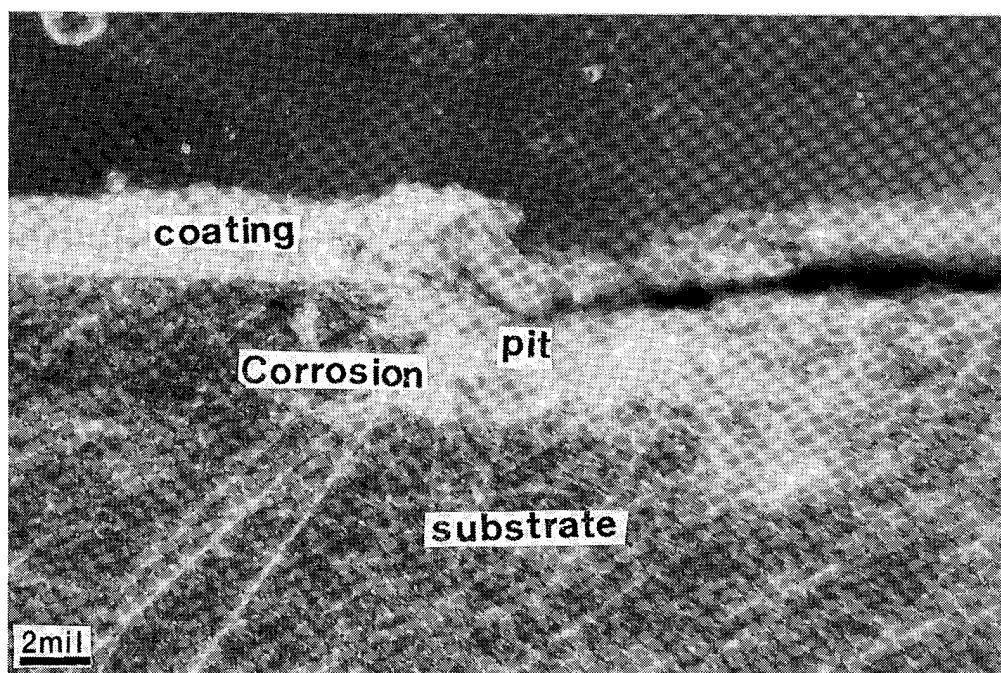
(d)

Figure 3.4. (c) Example of corrosion and salt product at defect (blister) on Sn plate and (d) same example with corrosion product removed.
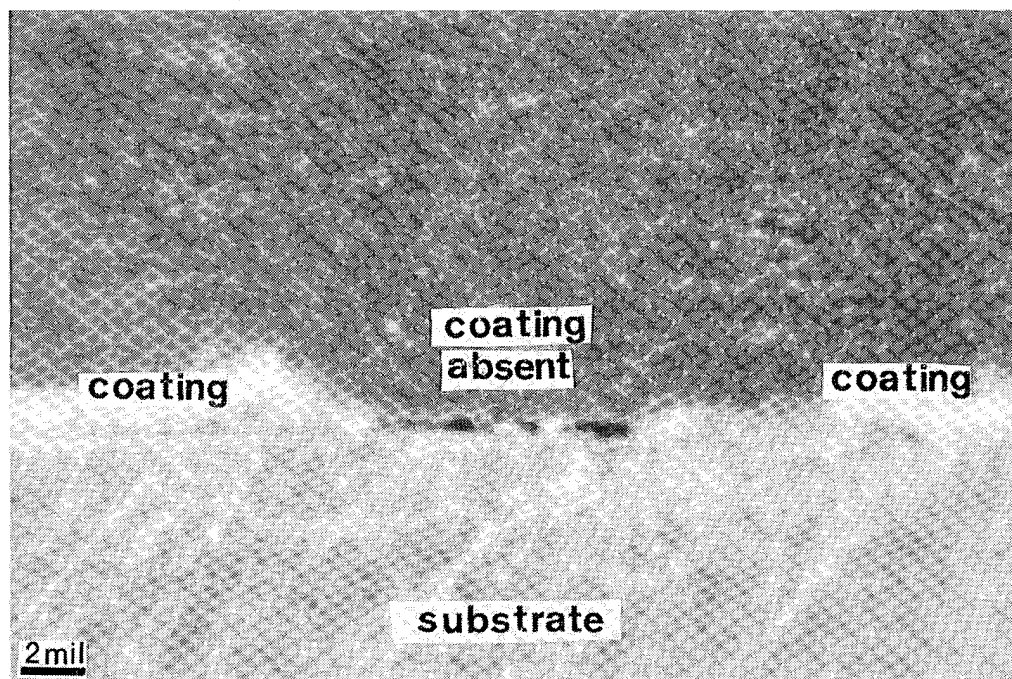
(e)
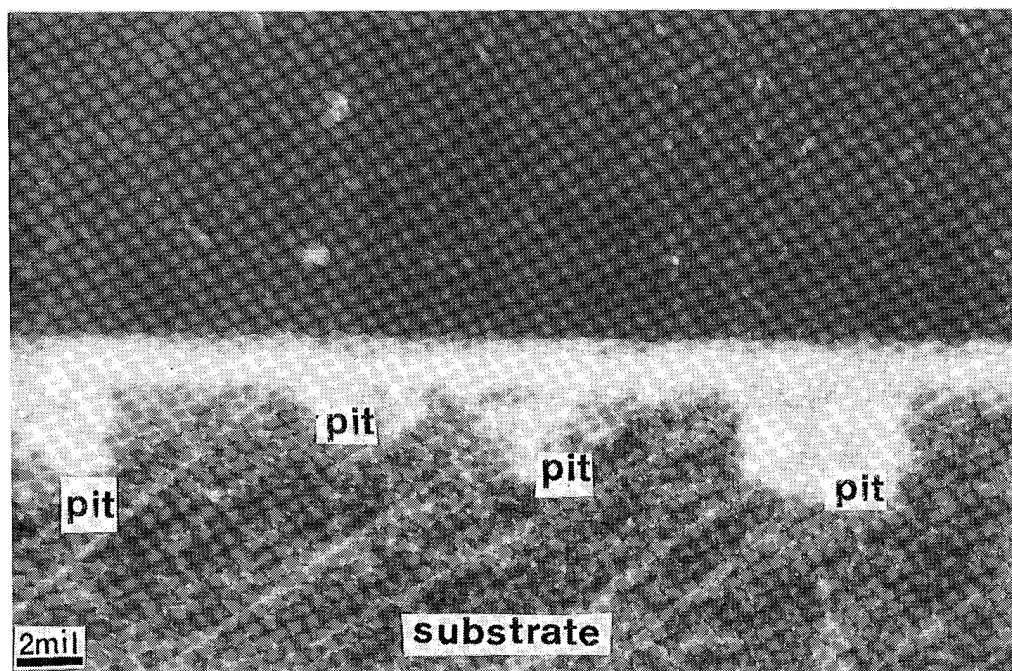
(f)

Figure 3.4. (e) Example of tin coating flaked away because of plating flaws that exaggerated corrosion of aluminum substrate and (f) pitting corrosion through tin coating and past nickel preplate.

Line A-B indicates depth of pitting into knife-edge.
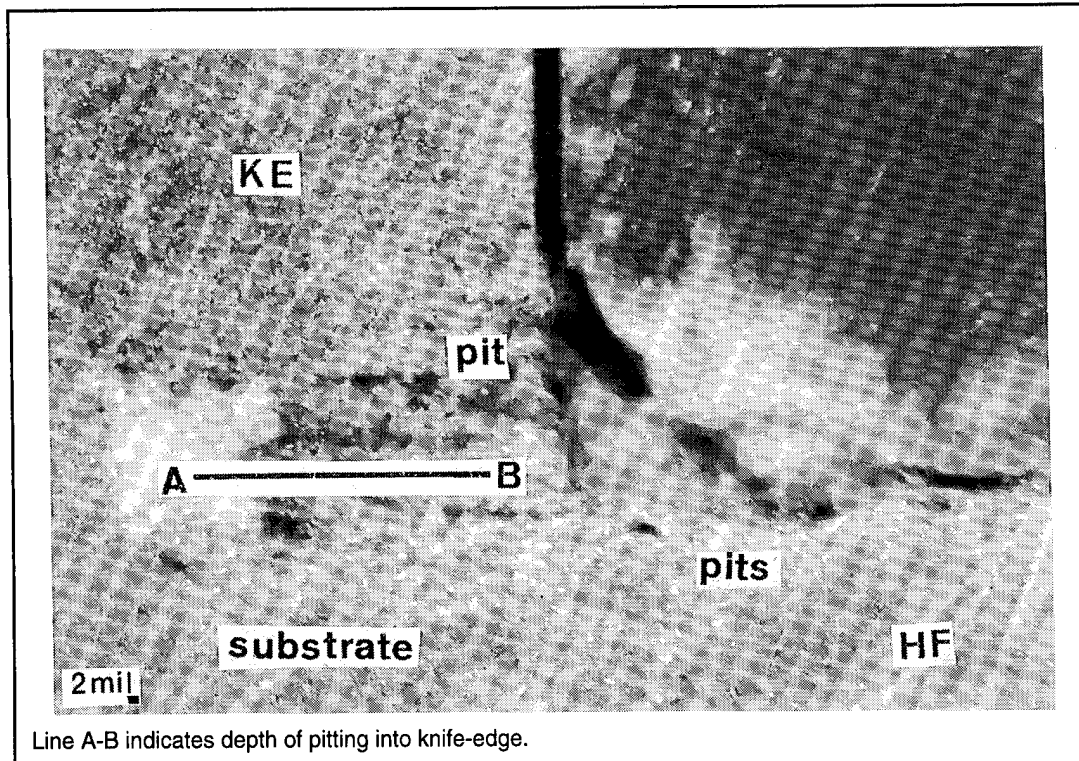
Figure 3.4. (g) Pitting corrosion in corner; cross-section shows knife-edge (KE) and half-face (HF) surfaces.

Scale: 1.5 in. _____
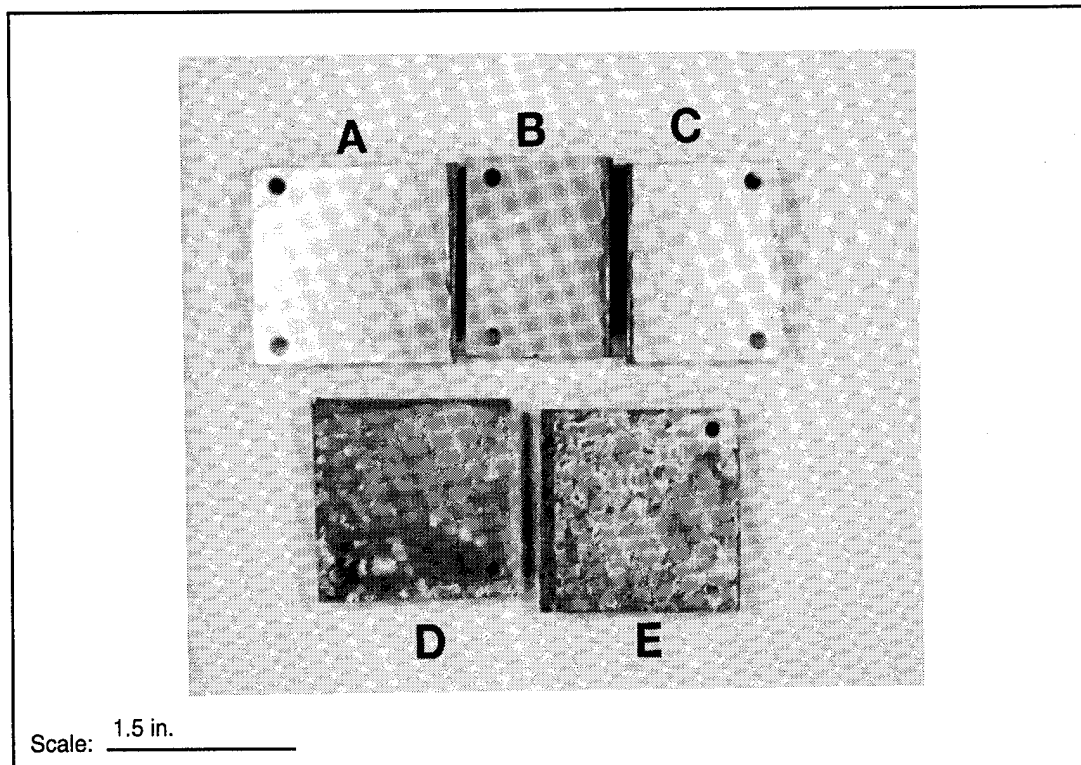
Figure 3.5. Post-salt fog test stylus electroplated samples of (A) tin coated; (B) uncoated; (C) tin coated; (D) nickel coated; and (E) copper coated.

4 Phase IV — New Anode Tool, Efficacy of Copper Underlayers, Adhesion, and Microhardness Testing

Phase IV of this research project addressed two major topics: (1) the utility of a special stylus electroplating anode tool custom-designed to "fit" the contours of the selected substrate (in this case the knife-edge sample substrate) and (2) the efficacy of the copper underlayer in filling in and smoothing out areas in the substrate that are scratched, chipped, or gouged, before application of the top layer coating.

Custom-Designed Electroplating Tool

As previously reported (USACERL, February, May, and August 1994), the standard plating tool is baton-shaped so the only way the "knife-edge" side of the sample can be plated is to divide the plating process into three sequences: (1) plating the knife-edge only, (2) plating one half-face only, and (3) plating the remaining half-face (Figures 1.4a,b). When new areas or sections of the sample are to be coated, the previously coated areas are protected from contamination (possibly arising from solution dripping) by applying Microstop to protect the parts of the sample already coated.

However, a custom-designed plating tool has been designed that allows plating of both half-faces and the knife-edges concurrently (i.e., the entire side where the knife-edge surface is located can be plated more easily and in one single plating sequence, instead of separating the plating sequence into a KE procedure and two HF procedures. The implementation of this tool (Figures 4.1a,b) provides better control of the plating process and better uniformity of the resultant coating, in addition to significantly reducing the total electroplating time for one side. This tool also circumvents problems of possible interference with previously deposited areas and allows cul-de-sacs in complex geometries to be coated (such as the corners at the intersection of the knife-edge and half-face). It is important to realize that the electroplating tool must be

custom-designed for each configuration to be plated. The major criteria for the design
of this tool are that it:

- must be an inverse-image of the substrate to be plated (e.g., if the substrate
  configuration is "male" then the stylus anode must be "female")
- must allow contact of the electroplating pad with the substrate, yet must be
  relatively easy to move across the substrate area to be plated.

Stylus electroplated samples were prepared using this tool according to parameters
listed in Table 4.1.

Samples prepared with this tool were subjected to the same test regimen used for
samples previously prepared with the standard baton-shaped stylus electroplating
tool.

Because of its relatively high microthrowing power, copper was investigated for
smoothing out and filling in surface defects. Copper was used as an underlayer in lieu
of, or in addition to, nickel underlayers. Note: Coatings number 71 through 74, and
76 in Table 4.1 were prepared with copper underlayers in lieu of nickel underlayers.
In each case, the top layers were tin.

Generally, the custom-designed anode tool performed very well. As predicted, it
facilitated the stylus electroplating process and reduced the process time required. The
resulting coatings appeared to be as good and possibly better than those coated with the
baton-shaped anode tool in earlier phases of this research. Of course, it must be noted
that all the knowledge and skill accumulated in the previous phases were applied in this
final research phase where the custom-designed anode was used. This "acquired
knowledge/skill" factor also may partly explain the improvement in the coatings
produced with the custom-designed anode tool. For example, in this last batch of
coatings (i.e., Samples 71 through 79), the stylus electroplating pad was kept wetter
than in previous coatings sessions. It is possible, however, that the use of greater
amounts of solutions to maintain a high degree of wetness during the coating process (to
reduce burning and blistering) may result in the production of softer coatings. Table 4.2
gives the pre-salt spray test appearance of coatings number 71 through 79.

Mitigation of Blisters, Burning, Flaking, Scarring, and Poor Adhesion of Coatings

In addition to the development of an optimum stylus electroplating procedure
discussed in Chapter 1, this research effort has culminated with the identification of
the parameters and phenomena that appear to critically affect the quality of the

coatings obtained. The following factors were identified as the most important contributors to the quality of the electroplated coatings, in general, and must be especially controlled to mitigate the occurrence of coating blisters, burning, flaking, scarring, and poor adhesion:

- current density and voltage
- pressure and speed of brushing motion
- wetness of applicator pad
- heat buildup
- cleanliness.

Each of these factors is addressed below.

Current Density and Voltage

Higher current densities often provide the best coatings. Recently, good coatings also have been obtained by starting with low voltages and current densities and increasing them during the plating of that particular metal (e.g., initially set the voltage to 20 percent of the highest voltage that will be used, and then increase voltage by the initial value per minute until the highest voltage is obtained). It was suggested by the manufacturer[*] of the coating solutions used for this research that 8 to 15 V and 3 to 5 amps per sq in. (0.465 to 0.775 amp/cm^2) is the optimum range. Recent experience indicates no reason to believe otherwise.

Brushing Motion and Burning of Deposit

In essence, the brushing motion is a form of pulse plating, so the highest current density and brush speed seem to affect coating quality. At 8 V, tin will not "burn" if the stylus is held stationary on a given area during electroplating. At 10 V, the coating will burn if the stylus is held stationary, but a slow brush motion will prevent burning. At higher voltages, a faster stylus brushing motion is necessary. Experience shows that one back and forth movement of the stylus over an area of 6 sq in. (38.7 cm^2) per second is a reasonable brushing speed at the suggested current densities of 3 to 5 amp/sq in. (0.465 to 0.775 amp/cm^2). Firm but not heavy pressure should be applied.

Amount of Applicator Pad Wetness

As metal ions are depleted, the concentration of the solution changes. No good correlation has been made as to how wet is wet enough; however, the current has been

---

[*]Liquid Development Corp., 3748 E. 91st Street, Cleveland, Ohio 44105.

observed to decrease as the pad gets dry, so perhaps a minimum current density could be established to indicate to the operator when to redip the pad. In general, the pad should be redipped in the plating solution at least once per minute. Some commercially available plating tools and pumps will provide a continuous flow of solutions to the stylus pads, but they were not available for this project. The disadvantages to using such a setup are: (1) the cost (since a separate pumping system must be used for each solution), (2) the time required for and difficulty of cleaning each system, and (3) the amount of solutions wasted by the pumping process. As an inexpensive alternative to dipping the stylus into the plating solutions, a small container of solution that feeds into the plating tool and can be hand-squeezed intermittently to allow proper pad wetness is suggested.

Thermal Effects

Excessive heat buildup during electroplating causes a concomitant volume change, which in turn is suspected to be a major cause of blistering. Therefore, heat should be extracted from the coating during electroplating. The volume change will still occur at room temperature, but it will not be as severe as the volume change from a higher temperature heat buildup. If the substrate to be coated is bonded to a large piece of high mass metal (as in the case of DSMDPS bars bonded to a tactical shelter), a good heat sink may form.

Cleanliness

Contamination of solutions and pads causes scarring, flaking, and poor adhesion of the coating; plating solutions and pads should be free of contamination. Electroplating tools must be scrubbed clean after each plating session. Stylus pads should be discarded after each use. Distilled and deionized water should be used (if available) for rinsing. Clean lint-free cloth or paper towels should be used for drying. As in the plating procedure, a water rinse is required between each plating step, including the final step; otherwise, a nonconductive and contaminating gel will form on the surface of the freshly applied coating. Also, proper preparation of the substrate before electroplating enhances adhesion.

It is not immediately obvious which factors are the most influential in causing blisters; however, implementation of the above recommendations mitigates the production of blisters. For this project, blisters were observed at the following times:

1.   During electroplating of tin coatings (blisters were never observed in the nickel or copper strikes).

2. Just after electroplating during the volume change that often accompanies electroplating (Kushner 1963).

3. Over longer periods (e.g., a week after plating). If blisters do not appear within a week, they are unlikely to form.

As-plated coatings have a dull gray finish; however, they can be buffed to a silvery luster with cotton balls or a soft cloth. Initially, the dull finish was believed to be the result of a reaction of the tin coating with oxygen or carbon. Auger electron spectroscopy (AES) is very sensitive to elements contaminating the surface of the electroplated substrate. AES of both buffed and as-plated surfaces showed that the as-plated surface composition had approximately the same atomic concentration of tin and oxygen as did the buffed surface. The buffed surface, however, contained more carbon contaminant, as is generally found on all types of AES specimens, because surfaces are extremely sensitive to carbon. The main difference in the appearance of the surface is believed to be caused by the removal of randomly oriented crystals on the surface. That is, only the texture (but not the chemistry) of the surface is modified by the buffing. Thus, the buffing action apparently removes only the loosely adherent randomly oriented topmost coating layers. Whether the as-plated or buffed coatings have any effect on the protective ability and EMI shielding performance of these coatings is unclear.

When coating larger area substrates, the resulting coatings are somewhat better, ostensibly due to the higher heat dissipation over the larger mass and reduced "edge effects"; that is, one can more easily brush over a large area without encountering substrate edges (where lower contact areas, and thus higher electric fields, dominate).

Testing of Tin Coatings With Copper Underlayers

Table 4.3 summarizes the post-salt fog test appearance of the coatings. The coated samples were then tested in the Gasket Cycler Test System. Tables 4.4 and 4.5 show the slopes of Resistance vs Number of Cycles plots for pre-salt fog and post-salt fog gasket cycling, respectively. Unfortunately, sea salt was not available for use in the salt fog testing chamber, as had been used for previous salt fog testing; therefore, a 3.5 percent sodium chloride salt solutions was used. Curiously, for most of these samples, the gasket cycling results revealed that the Resistance vs Number of Cycles slopes were actually lower for the post-salt fog samples than for the pre-salt fog samples. These anomalous results may be due partly to the use of sodium chloride salt rather than sea salt in the salt fog test. However, although sodium chloride is a less corrosive media than sea salt, exposure to it should not actually improve the contact resistance

of the knife-edge samples as suggested by these findings. More gasket cycling and salt fog testing is warranted for similarly prepared knife-edge samples.

As noted above, in the case of the *pre*-salt fog gasket cycling data, the average final resistances and quasi-slopes of the 71 through 79 series were higher than the average final resistances and quasi-slopes of the 23A,B through 28A,B series. However, for the *post*-salt fog results, the average quasi-slopes for the coated series 71 through 79 were somewhat lower than the average quasi-slopes of the 23A,B through 28A,B series. The average of the final resistance readings of the 71 through 79 series also were somewhat lower than the average of the final resistance readings for the 23A,B through 28A,B series.

Another significant observation: the uncoated aluminum samples generally show more erratic gasket cycling behavior than the tin-coated samples (Figure 4.2). Thus, the shielding effectiveness for *uncoated* knife-edge test pieces would be less predictable. Similar trends between the coated and uncoated samples were noted in the earlier phases of this research.

Figure 4.3a,b shows optical micrographs of a cross-section of a typical post-salt fogged sample (e.g., Sample 74) produced in this research phase. As seen in the figure, maximum thicknesses of 2 and 3 mils have been attained for the tin and copper layers, respectively. Note that this micrograph shows little coating or substrate degradation from exposure to the salt environment.

Intentional Substrate Defects (Flaws)

For each knife-edge substrate, two 0.0625 in. (0.1588 cm) long defects, two 0.125 in. (0.3175 cm) long defects, and two 0.1875 in. (0.4763 cm) long defects were intentionally cut into the top of the KE surface, which makes contact during gasket cycling. For any flawed substrate, the depths of the defects were held constant according to the following scheme:

Sample #	Depth mil (μm)
73	0.5 (12.7)
76	1.0 (25.4)
72	2.0 (50.8)
77	5.0 (127.0)
79	10.0 (254.0)
78	20.0 (508.0)

The results were similar to the results elaborated in Phase I. For example, the "repair" coatings always followed contours of the flaw. Thus, no matter how thick a coating is, a "dip" (taking the form of the original defect) in the final coating layer will always occur, unless a method is used to "fill in" this dip before applying the final electroplating layer. Figures 4.4a through 4.4f are selected micrographs showing relative resistance of coatings over flawed areas.

Each of the samples shown was electroplated with an underlayer of copper and a top layer of tin, subjected to 50,000 cycles on the Gasket Cycler Test System, 72 hr in the ASTM B-117 Salt Spray (Fog) Test, and another 50,000 cycle post-salt fog gasket cycling test. Figures 4.4a and 4.4b show pre- and post-salt fog micrographs of coated gouged substrates for Sample 76 with a 1-mil deep gouge. Very little degradation of the coating in the gouged area is from the salt fog exposure. Also, hardly any salt residue is in the gouged area. Note, however, that in the 5-mil deep gouged area on Sample 77 (Figures 4.4c and 4.4d), the post-salt fog coating shows considerably more degradation and slightly more salt residue. For these samples, the "repaired" areas have the same general appearance as the adjacent nondefected areas. Finally, in the 20-mil deep gouged area in Sample 78 (Figures 4.4e and 4.4f), the post-salt fog coating, although still intact, has begun to blister and pop in a few places.

It appears that coatings applied onto substrates with deeper gouges (e.g., Samples 77 and 78), may be more susceptible to concentration cell corrosion, because of the tendency of these gouged areas to retain salt and moisture. For this reason, either "filling in" or "machining out" deep gashes before electroplating the substrate is advised, as the gashes provide sites for contaminants to accumulate.

Results of Sebastian Adherence and Microhardness Tests

Adherence Tests

The results of the Sebastian Adherence Tests for this final set of coatings (Table 4.6), indicated that tin-coated samples with nickel underlayers usually had slightly greater adherence than those with copper underlayers. However, statistical analysis using Duncan's Multiple Range Testing (Walpole 1968) revealed that, with the exception of Sample 75, no significant difference is apparent in the adherence values. The one coating sample with the greatest adherence value was the tin coating with a nickel underlayer. Furthermore, when the adherence data from the previously coated samples (e.g., Tables 1.3 and 3.6) are considered, a significant difference is noted in the adherence of tin-coated samples with nickel underlayers compared to those with copper underlayers. All things considered, these data appear to indicate that nickel

underlayers promote better tin coating adherence. When compared with coatings made in earlier experiments (i.e., Samples 31 through 40 in Table 3.6), the recently fabricated coatings *with copper as the first layer directly deposited on the aluminum alloy substrate* do not exhibit the same degree of adherence as do coatings with *nickel underlayers directly deposited on the aluminum alloy substrates.* However, when nickel is the first layer directly deposited onto the aluminum alloy substrate *followed* by a layer of copper, and finally topcoated with a thick layer of tin, the adherence strength of the nickel underlayer dominates, and the coatings exhibit comparatively high adherence strengths. Apparently, copper does not bond as readily to 6061-T6 aluminum alloys as does nickel; however, copper bonds well to nickel, and tin bonds well to copper. In fact, the copper underlayers bonded so well to tin that, when the coatings failed during the adherence test, a larger area of coating was pulled off (usually 100 percent or more of the gouged-area) than was pulled off the tin coatings with nickel underlayers (see % Area Failed in Table 4.6).

Microhardness

Table 4.7 lists the microhardness values for the primary final set of electroplated coatings of tin on 6061-T6 aluminum alloy. The values were determined on a microhardness machine at the University of Illinois, Urbana-Champaign. The Knoop indenter was used. Due to substrate effects, in order for the microhardness values to be considered valid, the indenter must not penetrate any more than 20 percent of the coating thickness. ASTM standards recommend that the indentor not penetrate more than 10 percent of the coating.

It is doubtful that the aluminum alloy substrate affected the microhardness values; this was confirmed by optical microscopy by comparison of the depths of penetration with the coating thicknesses. It should also be noted that: (1) Knoop indenters are particularly sensitive to surface conditions and (2) the lighter the load, the higher the hardness value. For this research, coating surface conditions ranged from rough to smooth. All samples were measured at 10 grams per load. Samples 76 and 79 were so soft that the indentions they made were out of range for the magnification used for the other samples. For this reason, measurements of these two samples were taken at a different magnification and converted to the values reported.

Although no large differences in the microhardness values occurred among the coated samples tested, the microhardness values fell into three basic categories as determined by a statistical analysis using Duncan's Multiple Range Testing (Walpole 1968): "extremely low" for Samples 76 and 79; "low" for Samples 77 and 75; "medium" for Samples 71, 78, and the control cast tin sample; and "high" for Samples 72 and 73. Ironically, the results of the microhardness test indicated that the tin-coated samples

with nickel underlayers were actually slightly softer than those with the copper underlayers. In fact, one of the tin coatings with a nickel underlayer was too soft for measurement of microhardness. One plausible reason for this anomaly may be credited to several physical properties of copper that allow slightly harder tin coatings to be deposited onto copper. Of course, if a different indentor load is used, the results may vary. This hypothesis warrants more investigation. The aluminum control sample registered a very high microhardness value, as expected.

Results and Comments

Figures 4.5 and 4.6 graph the adherence and microhardness data for Samples 71 through 79 (including the uncoated aluminum substrate and the cast-tin sample). The relevance of the adherence and microhardness tests must be evaluated in terms of the service environment to which the coatings will be subjected. If the coatings are to be subjected to cyclic loading similar to that simulated in the Gasket Cycler Test System where they are loaded in compression (i.e., pushed against some wire mesh mating gasket in such a way that the mating surfaces scrape against and wear down the coating), then the microhardness test may be a reasonable indicator of which coatings offer more wear resistance. On the other hand, the adherence test may be a better indicator of the ability of the coatings to resist being torn and pulled off their substrates in cases where they are snagged at some holiday (or break in the coating) by the mating wire mesh.

(a)

1.5 in.
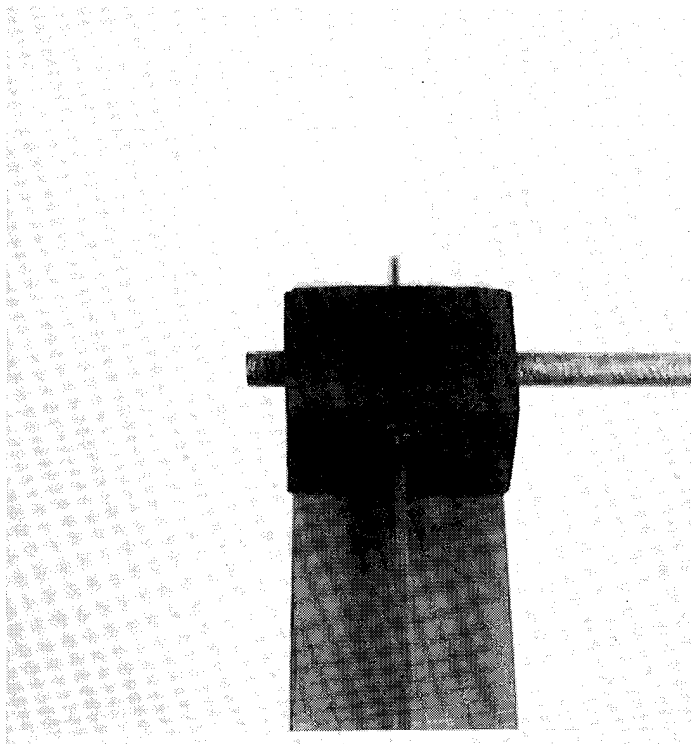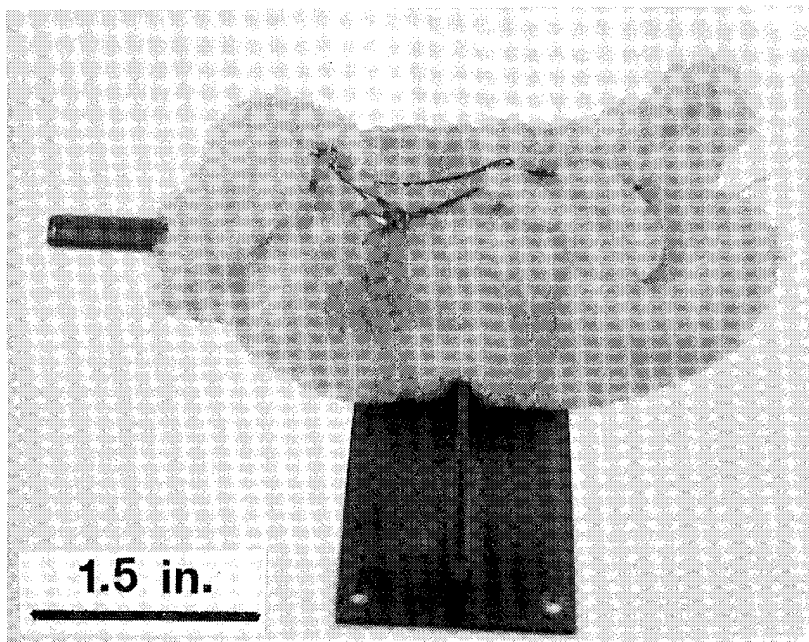
(b)

Figure 4.1. Custom-made graphite tool anode mounted on knife-edge substrate (a) bare and (b) wrapped with Dacron® pad.

Table 4.1. Stylus electroplating parameters for Samples 71 – 79.

Sample #	Solution	Volts	Current	Time
71	Etch	10 V	165 A	1 min
	Cu	10 V 7 V	5-6 A 3-5 A	1 min 3 min
	Sn	10 V 7 V	5-6 A 2 A	1 min 4 min
72	Etch	10 V	165 A	1 min
	Cu	10 V 7 V	5-6 A 3-5 A	1 min 3 min
	Sn	10 V 7 V	5-6 A 2 A	1 min 4 min
73	Etch	10 V	165 A	45 sec
	Cu	10 V 6 V	5-6 A 3-4 A	1 min 3 min
	Sn	9 V	2-3 A	5 min
74	Etch	10 V	165 A	45 sec
	Cu	10 V	7-9 A	3 min
	Sn	18 V	7-9 A	5 min
75	Etch	10 V	165 A	30 sec
	Ni	11 V	4-5 A	3 min
	Sn	11 V	2-4 A	5 min
76	Etch	10 V	165 A	30 sec
	Cu	11 V	4-5 A	3 min
	Sn	12 V	4-6 A	5 min
77	Etch	10 V	165 A	30 sec
	Ni	11 V 9 V	5-7 A 4-5 A	1 min 2 min
	Sn	13 V	4-8 A	5 min
78	Etch	10 V	165 A	30 sec
	Ni	11 V	4-5 A	3 min
	Sn	14 V	4-75 A	5 min
79	Etch	10 V	165 A	1 min
	Ni	11 V	4-5 A	2 min
	Sn	14 V	4-7 A	5 min

Table 4.2. Appearance of coatings for Samples 71 – 79 (pre-salt fog).

Sample 71: Slight blisters on HFs. Slight ridges are also evident. KE also appears to be ridged.
Sample 72: Good* coating; blisters are only slight. Coating is shiny, but KE is somewhat ridged.
Sample 73: Coating looks good and is very slightly blistered on one HF. KE contains no blisters, but is dull in appearance.
Sample 74: Slight blisters near the holes (on the ends). Outside of slight blisters on KE, the coat on the HFs and KE seem to be fairly good.
Sample 75: Very shiny, excellent coating. No blisters. KE and HFs are equally shiny.
Sample 76: Shiny with no blisters but badly ridged on HFs especially near the ends and the holes.
Sample 77: One HF is shiny while the other is dull. KE looks good. No blisters.
Sample 78: Very shiny and no blisters on HFs. KE contains slight blisters; otherwise excellent coat.
Sample 79: Ridged near the ends of the sample and near the holes. Also ridged on the KE. Slight blisters are visible on the sides of the KE and in the ridges.
* "Good" means not visibly ridged or blistered and fairly shiny.

Table 4.3. Appearance of coatings for Samples 71 – 79 (post-salt fog).

Sample 71: Very little corrosion product on sample. Even product often found in right angle is at a minimum.
Sample 72: Very little corrosion product on sample found at the right angle; still shiny.
Sample 73: A few exaggerated blisters due to salt fog. Outside of this and slight discoloration, the sample remains unaffected.
Sample 74: Severe discoloration. No corrosion product at all except in right angle. Discoloration includes oil or soapy colors. Large blisters on HF which previously did not have any blisters. Product on KE is minimal.
Sample 75: Spotted corrosion product on HF's and KE. A few large blisters not present before; shiny where product is missing.
Sample 76: Corrosion dominates in ridges and blisters on both HF's. Slight tan discoloration, but still remains shiny where product is absent.
Sample 77: Corrosion on one HF is very bad; dulling, discoloring, and corrosion product dominating at ridges and blisters. Other HF contains some product but is mostly shiny.
Sample 78: Spotted corrosion product on the HF's but not on the KE. Product dominates at small blisters. Where no product is visible, the sample remains shiny.
Sample 79: Severe discoloration of the specimen - oily color. Outside of that, Only slight amounts of corrosion product found on the side of the KE and at the few blisters that are present.

Table 4.4. Results of the pre-salt fog gasket cycling tests—resistance vs number of cycles.

Sample #	Slope (μΩ/cycle)	Initial Resistance (ohms)	Final Resistance (ohms)	r-Values of Line Fit
71; Pos. 1	0.6104	0.0005192	0.008656	0.85
72; Pos. 2	0.09530	0.0005458	0.002739	0.49
73; Pos. 3	0.2124	0.0006164	0.004107	0.79
AL(A)*; Pos. 4	0.3355	0.0003508	0.004469	0.39
79; Pos. 5	0.1929	0.0005590	0.003293	0.70
75; Pos. 6	0.8003	0.0006392	0.005893	0.73
AL(B)*; Pos. 7	0.5298	0.0006530	0.006755	0.65
76; Pos. 8	0.2072	0.0007758	0.003302	0.63
77; Pos. 9	0.1832	0.0006498	0.002376	0.64
78; Pos. 10	0.2005	0.0005566	0.003171	0.43

* Uncoated 6061-T6 aluminum substrates.
Note: 1 μΩ/cycle = 1 X 10^{-6} Ω/cycle.
Tests: 940926, 27, 28, and 29; each test was 10,000 cycles at 30-sec dwell time for 72 hr.

Table 4.5. Results of the post-salt fog gasket cycling tests—resistance vs number of cycles.

Sample #	Slope (μΩ/cycle)	Initial Resistance (ohms)	Final Resistance (ohms)	r-Values of Line Fit	Comments
71; Pos. 1	0.03040	0.0002922	0.0008786	0.12	
72; Pos. 2	0.2063	0.0003348	0.001821	0.64	
73; Pos. 3	0.3024	0.0004828	0.003390	0.92	
AL(A)[1]; Pos. 4	0.3572	0.0003724	0.002399	0.66	
79; Pos. 5	-0.0149	0.0003600	0.0005940	0.01	Note negative slope!
75; Pos. 6	0.09910	0.0003864	0.001159	0.88	
AL(B)[2]; Pos. 7	0.3495	0.0004246	0.004107	0.64	
76; Pos. 8	0.1665	0.0004942	0.001845	0.78	
77; Pos. 9	0.2823	0.0003740	0.002284	0.78	
78; Pos. 10	0.1007	0.001128	0.001830	0.62	

Note: 1 μΩ/cycle = 1 X 10^{-6} Ω/cycle.
[1] Uncoated 6061-T6 Aluminum substrate AL(A) was NOT subjected to Salt Fog Test.
[2] Uncoated 6061-T6 Aluminum substrate AL(B) subjected to Salt Fog Test.
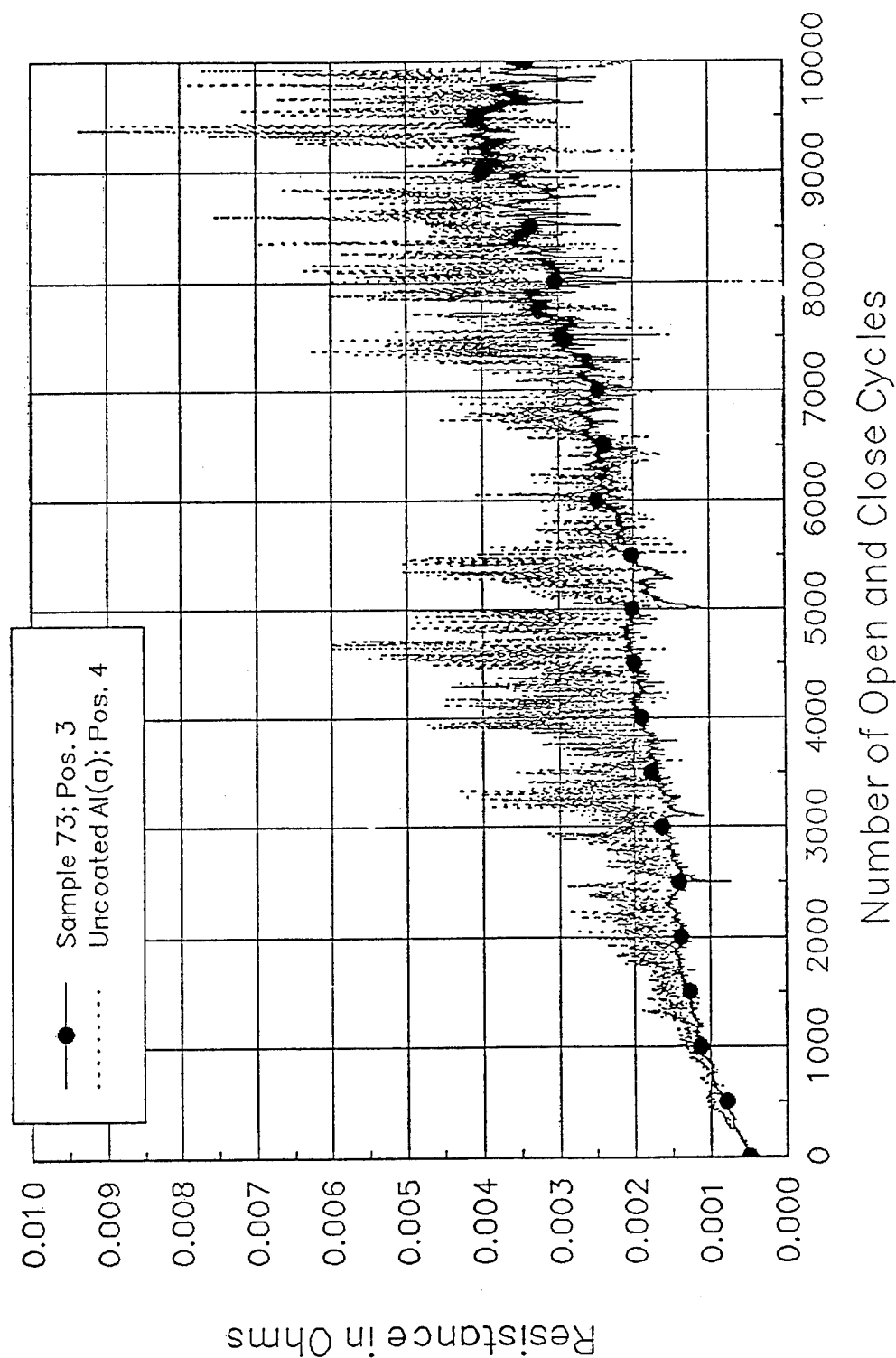
Figure 4.2. Resistance vs number of cycles plot for coated and uncoated knife-edge samples.
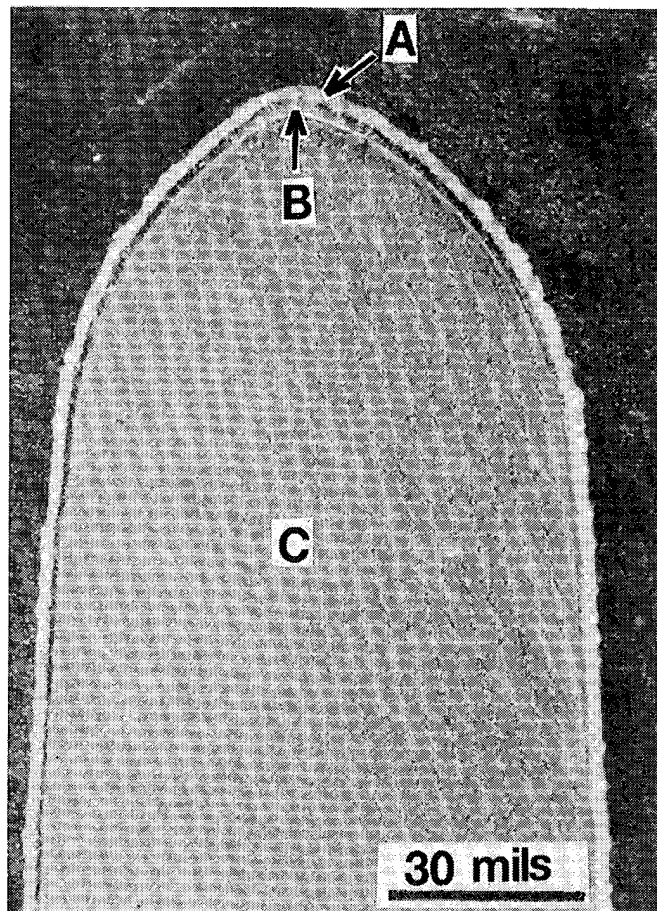
(a)
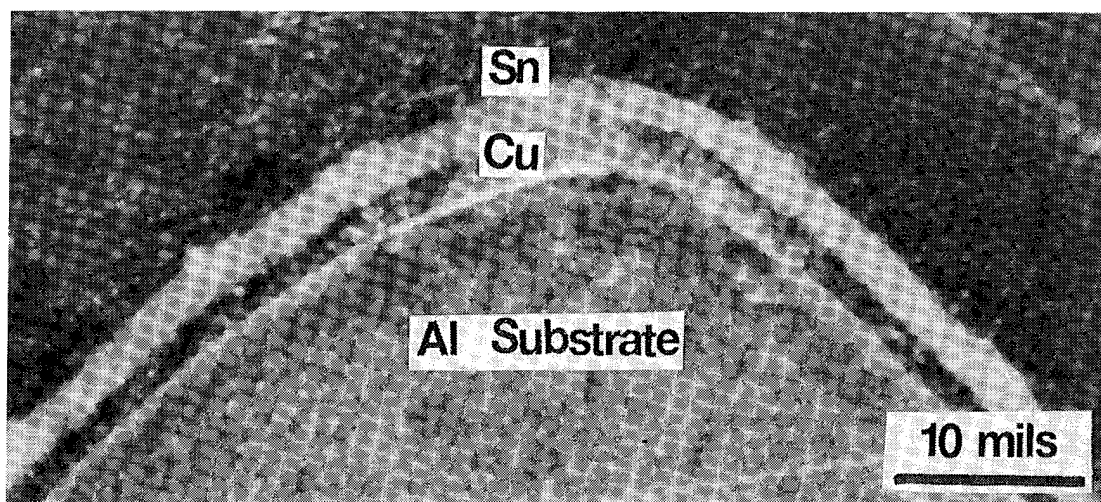
(b)

Figure 4.3. (a) Optical micrograph of KE portion of Sample 74 showing (A) tin top layer, (B) copper underlayer, and (C) 6061-T6 aluminum substrate; and (b) magnified view of same KE.

a) Sample 76, 1 mil deep gouge, pre-salt fog view.

b) Post-salt fog view of same area as in "a".

40 mils
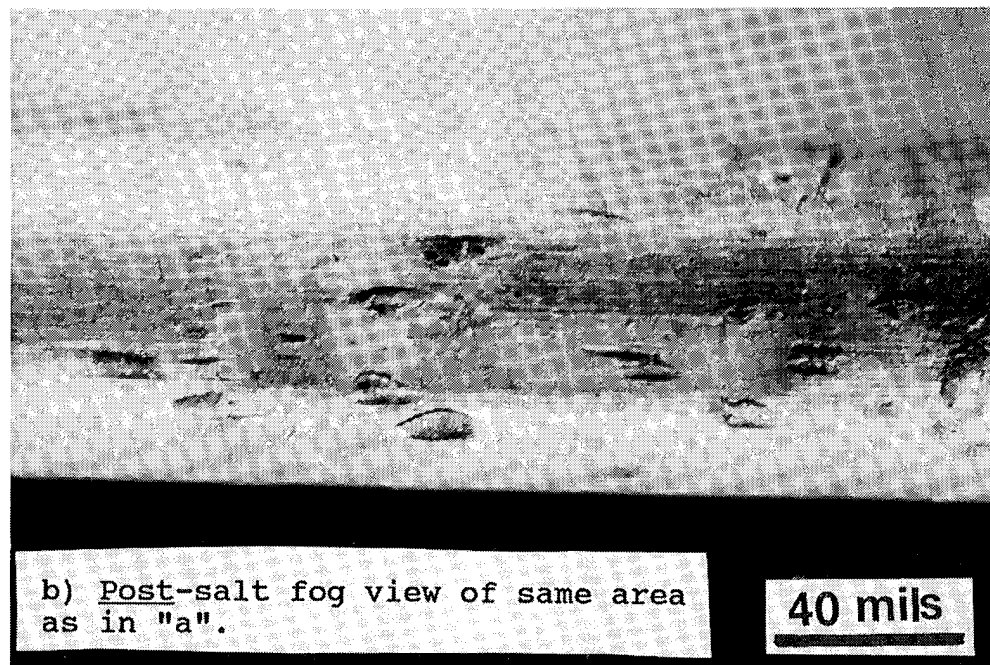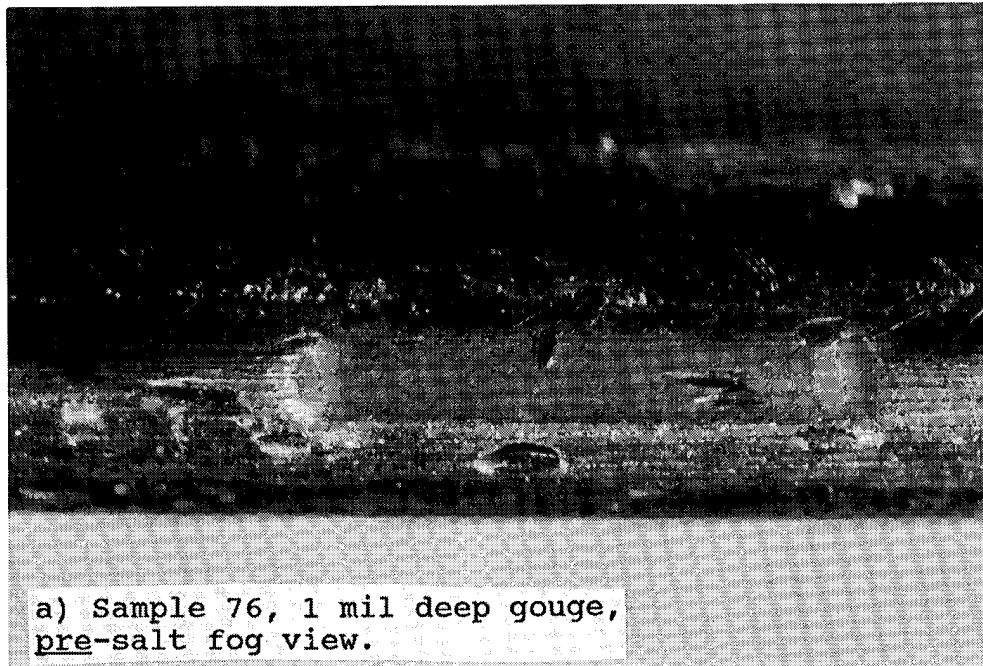
Figure 4.4. Micrograph of typical coated knife-edge samples showing the relative resistance of the coatings over intentionally gouged areas to salt fog degradation.

c) Sample 77, 5 mil deep
gouge, pre-salt fog view.

d) post-salt fog view of
same area as in "c".

40 mils

Figure 4.4. (Cont'd).

e) Sample 78, 20 mil deep gouge, pre-salt-fog view.

f) Post-salt fog view of same area as in "e".

40 mils

Figure 4.4. (Cont'd).

Table 4.6. Sebastian Adherence Test results for Samples 71 – 79.

Sample #	Adherence ksi	(MPa)	% Area[1] Failed	Average ksi	(MPa)	Stand. Dev. ksi	(MPa)
71	0.92	(6.34)	100				
Sn/Cu	0.28	(1.93)	110	0.603	(4.16)	0.320	(2.21)
	0.61	(4.21)	100				
72	2.11	(14.55)	100				
Sn/Cu	0.43	(2.97)	105	0.937	(6.46)	1.02	(7.03)
	0.27	(1.86)	115				
73	0.78	(5.37)	80				
Sn/Cu	0.44	(3.03)	100	0.726	(5.00)	0.264	(1.82)
	0.96	(6.62)	100				
75	10.42	(71.86)	15				
Sn/Ni	8.92	(61.5)	NF[2]	7.11	(49.1)	4.49	(31.0)
	2.00	(13.79)	25				
76	1.86	(12.82)	85				
Sn/Cu	2.34	(16.13)	100	2.04	(14.07)	0.260	(1.79)
	1.93	(13.3)	96				
77	0.36	(2.48)	100				
Sn/Ni	0.64	(4.41)	100	1.41	(9.75)	1.59	(10.9)
	3.24	(22.3)	100				
78	1.74	(12.0)	100				
Sn/Ni	2.67	(18.4)	100	1.72	(11.9)	0.960	(6.62)
	0.75	(3.45)	100				
79	0.76	(5.24)	90				
Sn/Ni	1.37	(9.44)	100	0.900	(6.21)	0.418	(2.88)
	0.57	(3.93)	100				
Uncoated	5.06	(34.9)	N/A[3]	3.77	(26.0)	1.58	(10.9)
6061-T6	2.01	(13.9)	N/A[3]				
Aluminum	4.25	(29.3)	N/A[3]				

[1]"Area" refers to gauge area (i.e., the area under the stud over which tension was applied). For the Sebastian Adherence Test, the gauge area was 0.106 in. (2.69 mm).
[2] NF = No Failure.
[3] N/A = Not Applicable.

Table 4.7. Microhardness test results for Samples 71 – 79.

Sample #	Microhardness	Average	Standard Deviation
71 Sn/Cu	6.76 6.73 6.83	6.77	0.0513
72 Sn/Cu	11.67 12.75 16.67	13.70	2.63
73 Sn/Cu	12.07 20.93 15.77	16.26	4.45
75 Sn/Ni	4.04 4.34 4.54	4.31	0.252
76 Sn/Cu	* * *	* * *	* * *
77 Sn/Ni	4.45 4.07 4.04	4.19	0.229
78 Sn/Ni	7.63 7.27 7.23	7.38	0.220
79 Sn/Ni	* * *	* * *	* * *
Al (uncoated)	N/A	N/A	N/A
Cast Sn	10.3 10.2 10.1	10.2	0.10
*Too soft.			

Figure 4.5. Adherence test results for Samples 71 – 79.

Figure 4.6. Microhardness test results for Samples 71 – 79.

5 Conclusions and Recommendations

Conclusions

Stylus Evaluation

Stylus electroplating experiments using tin-lead coatings were conducted to develop stylus electroplating for field application of adherent, electrically conductive corrosion-resistant EMI coatings. A baton-shaped anode stylus tool was used for flat surfaces or surfaces with simple geometries; otherwise, a custom-designed anode stylus tool worked best.

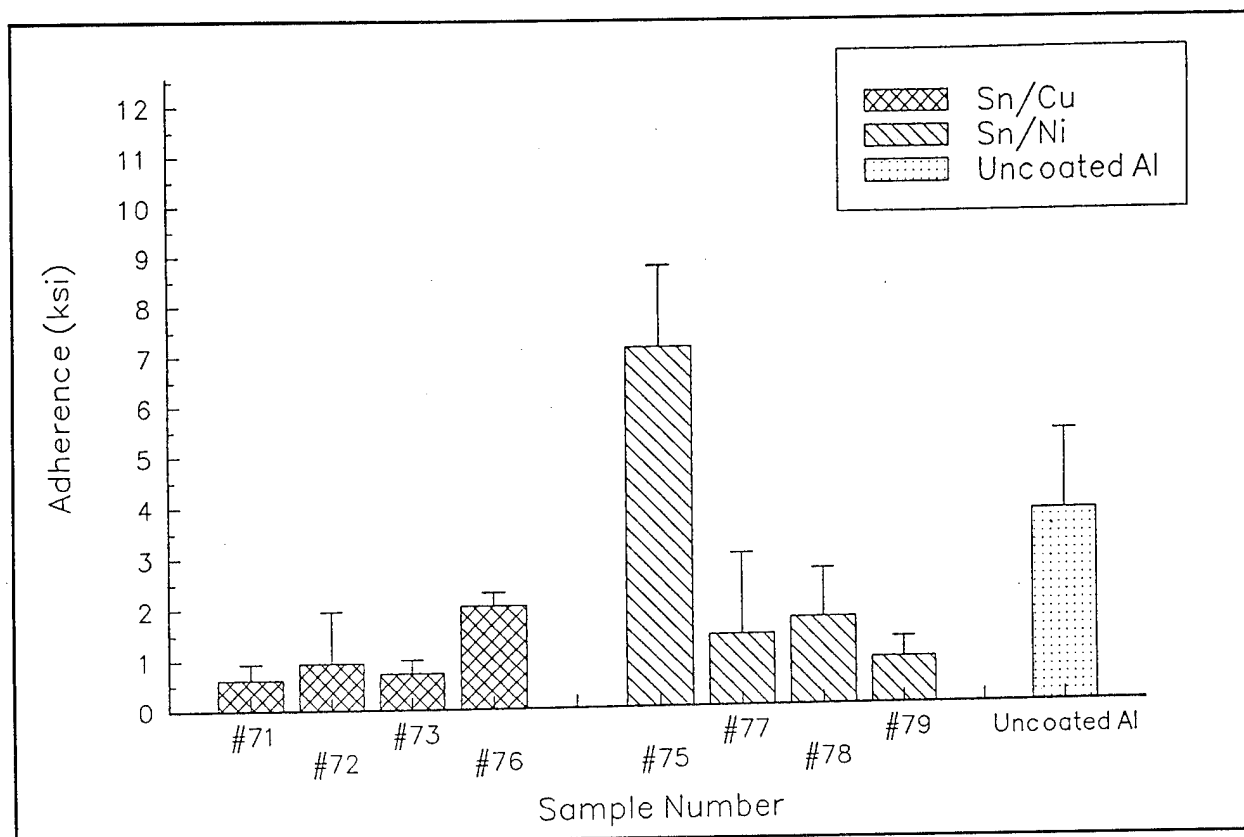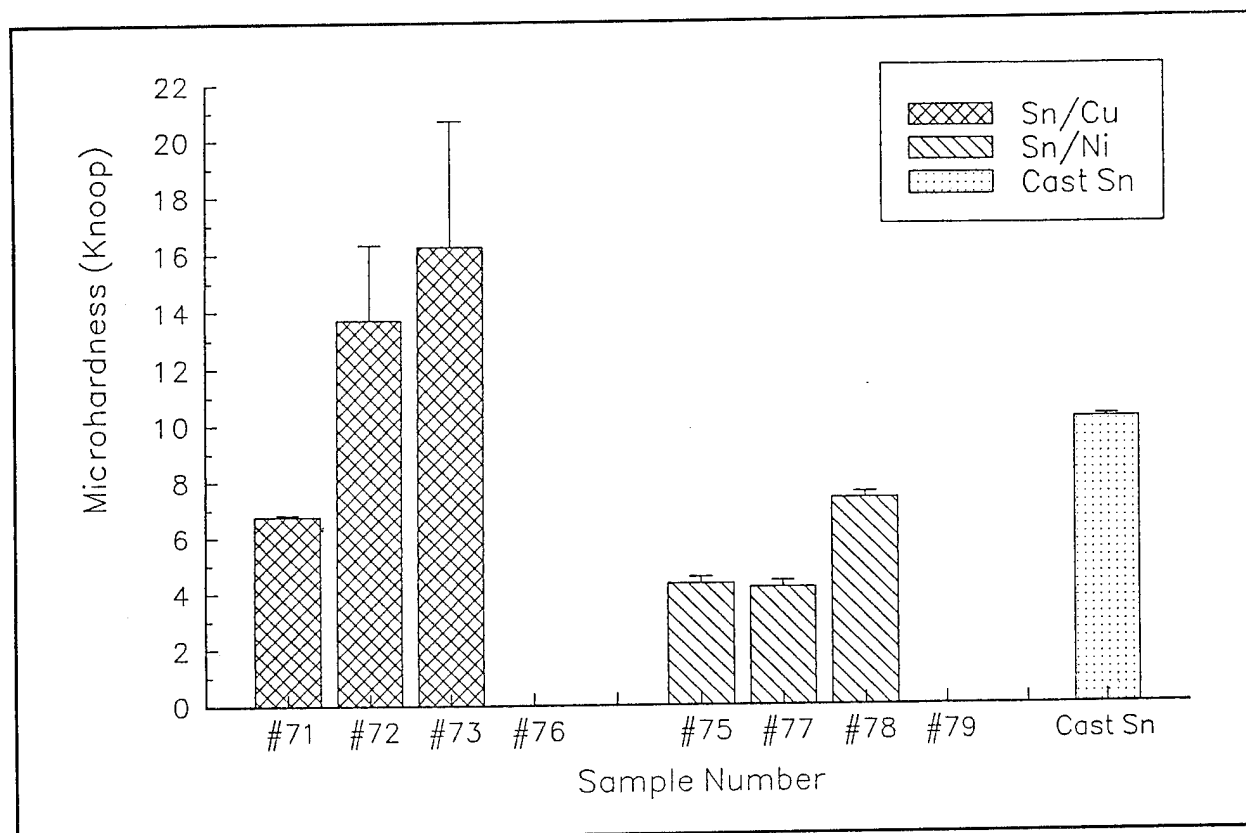The custom-designed tool allows concurrent coating of both knife-edge and half-face surfaces which allows for a much faster electroplating technique. It also reduces plating time for any given area to be coated, circumvents problems of possible interference with previously deposited areas, and allows cul-de-sacs in complex geometries to be coated (such as the corners at the intersection of the knife-edge and half-faces). It is important to note that the electroplating tool must be custom-designed for each given configuration to be plated.

Carbon anodes may be used for electroplating, but platinum-clad or stainless steel anodes are less subject to degradation. Whatever the anode used, it must be properly cleaned after every use to prevent contamination of plating solutions.

Coatings Evaluation

Research with coatings indicated that 100 percent tin or 95 percent tin - 5 percent lead coatings with either nickel or copper underlayers appeared to be useful in providing the corrosion-resistant electrically conductive surface necessary for long-term EMI shielding. Some recent field testing suggests that 95%Sn/5%Pb coatings provide better long-term shielding than 100%Sn top layer coatings (personal communication, Youn Lee, Joint Committee on Tactical Shelters, 2 February 1995). Gasket cycling testing in this research project revealed no such trends. It must be noted, however, that a smaller number of 95%Sn/5%Pb coating samples were available for gasket cycling tests than would be necessary to make valid statistical comparisons.

Some other possible advantages for the use of lead-tin coatings, in lieu of 100 percent tin coatings are summarized in Table 5.1. The decision to reduce, although not to

discontinue, testing of the lead-tin coatings was partly based on growing opposition to the use of lead as a result of environmental considerations.

Tests revealed that tin coatings with nickel underlayers had slightly higher adherence than did the coatings with copper underlayers. However, the copper underlaid coatings were slightly harder than the nickel underlaid coatings. Microhardness of the coating may actually be a better indicator than adhesion of coating durability because, in practice, the coating is subject to cyclic loading in compression rather than in tension. Copper was noted to be easily applied to high thicknesses and to be a good "filler" metal to cover flaws in the surface. It also exhibited better corrosion resistance than did the nickel underlayer.

This research identified these major factors for optimization of coating quality:

- current density
- speed of brushing motion during application of the coating
- pad wetness
- prevention of, or dissipation of, heat generated during the electroplating process
- cleanliness
- proper preparation of substrates prior to electroplating.

Attention to these details appears to mitigate blistering, burning, flaking, scarring, porosity, and poor adhesion of the resulting coating.

Parameters Evaluation

Some correlations between electroplating parameters and the resulting surface coating appearance, adherence, and contact resistance of coated knife-edge test pieces were ascertained. It appears that the coatings that exhibited fewer blisters were applied at either low current densities (less than 3 amp/sq in.) or high current densities (greater than 4 amp/sq in.), leading to less blistered and smoother coatings. Medium current densities (3 to 4 amp/sq in.) lead to larger blisters and more pronounced ridges.

The coated surface of the 6061-T6 aluminum alloy substrate can easily cover a defect or flaw, but very deep flaws (e.g., 10- to 20-mils deep) appear to be more susceptible to concentration cell corrosion, unless they are somehow "smoothed out." It may be possible to smooth out these flaws by allowing the electroplating stylus to dwell longer on the flawed areas than over the remainder of the surface.

Optimum Coating Strategy

Based on the results of this research, the optimum coating strategy suggested is:

1. Apply a thin layer or "strike" of nickel on the substrate to promote good adhesion.
2. Apply a thick layer of copper to help cover and smooth out surface flaws, increase thickness, enhance the electrical conductivity, and provide galvanic compatibility.
3. Apply a top layer of tin in a moderate thickness to help maintain a long-term low contact resistance.

Figure 5.1 shows this coating scheme.

Stylus electroplating appears to be more useful for depot-level maintenance than for field maintenance because of the complexity of equipment and operations involved, and the attention to detail necessary for its proper execution. However, stylus electroplating also may be useful in "touch up" electroplating applications in the field, where it can be used to repair damaged regions that are small in area on EMI shielding interfaces. To effect this repair process, the following course of action is suggested:

1. The corrupted area should be thoroughly cleaned of all oxides and corrosion products.
2. The old tin top layer, along with some of the underlayer, should be removed to expose metal atoms that are free of all contamination.
3. The cleaned area should be filled with copper.
4. A new tin top layer should be applied over the region to be repaired.

Recommendations

As a result of this study, the following recommendations are suggested for future research topics.

1. Investigate more fully the pre- and post-salt fog gasket cycling behavior of tin coatings with copper underlayers that were exposed to sodium chloride rather than sea salt fog.
2. Investigate more fully the differences in gasket cycling behavior of 95%Sn/5%Pb top layer coatings vs 100%Sn top layer coatings.
3. Investigate the efficacy of other electroplated coating materials (e.g., nickel-tin or copper-aluminum alloys).

4.   Develop field stylus electroplating "touch-up kits" and procedures for field repair of small areas on interfaces requiring coatings.

5.   Conduct long-term field tests and surveys on the shielding effectiveness of stylus electroplated coatings.

Table 5.1. Comparison of coatings.

	Advantages	Disadvantages
Nickel (underlayers)	- Very adherent - Hard - Very good electrical conductivity	- Low microthrowing power - Attacked by Cl⁻ - Only slightly more noble than Al
Copper (underlayers)	- Very noble - Excellent electrical conductivity - High microthrowing power - Easy to electroplate	- Low to moderate adherence - Softer than Ni - Attacked by S⁻
Tin (toplayers)	- Noble - Good electrical conductivity - Semiconducting thin oxide layer	- Slightly less noble than Sn-Pb - Subject to tin "pest" formation
Tin-lead (toplayers)	- Slightly more noble than Sn - Semiconducting thin oxide layer - Immune to tin "pest" formation	- Slightly less conductive than Sn - May produce more porous coatings - Environmental concerns

Tin (Sn):   Noble; moderate electrical conductivity; resistant to S⁻;
                 semiconducting oxide; soft; low amp/hr factor.
Copper (Cu):   Very noble; very high electrical conductivity; very high amp/hr factor
                 (easy to electroplate); moderate hardness; susceptible to S⁻.
Nickel (Ni):   Moderately noble; moderate electrical conductivity; high amp/hr factor
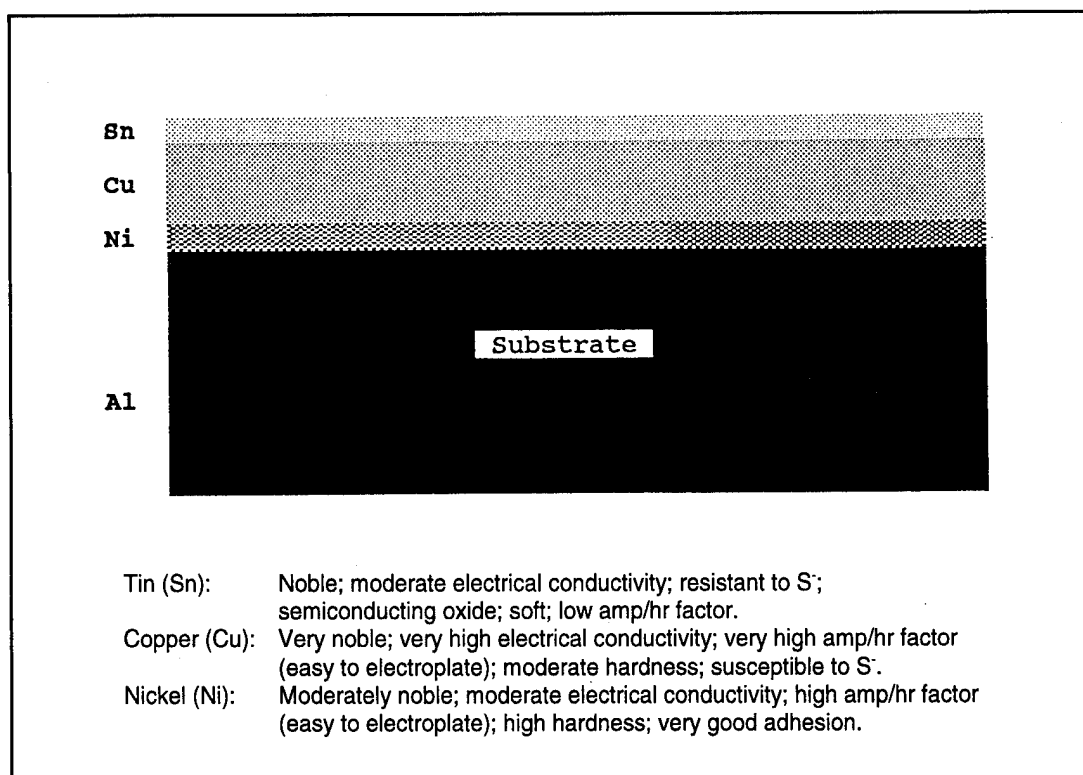   (easy to electroplate); high hardness; very good adhesion.

Figure 5.1. Diagram of optimum coating scheme based on research results.

References

American Society for Metals (ASM) International, "Plating and Electroplating," *ASM Handbook*, Vol 5 (Surface Engineering) (ASM International, 1994), pp 165-289.

Ben-Shalom, A.; Kaplan, L.; Boxman, R.L.; Goldsmith, S.; Nathan, M. "SnO$_2$ Transparent Conductor Films Produced by Filtered Vacuum Arc Deposition," *Thin Solid Films,* No. 236 (1993), pp 20-26.

Bunshsah, Rointan F., *Deposition Technologies for Film Coatings* (Noyes Publications, 1982), p 412.

Byrne, Garry F., "An Overview of Brush Electroplating and Present Technology & Expertise," *Proceedings of the Brush Plating Seminar*, American Electroplaters and Surface Finishers Society, Orlando, FL (January 1993).

Chemical Rubber Company, *CRC Handbook of Chemistry and Physics*, 52nd ed., 1971-1972, Robert C. Wear, Ed. (CRC), p D-53.

Department of Defense (DOD), Military Standard 865C (USAF), "Selective (Brush Plating), Electrodeposition" (DOD, 1 November 1988).

Hornbostel, Caleb, *Construction Materials* (John Wiley and Sons, 1978), p 249.

Kushner, Joseph B., *Electroplaters' Process Control Handbook* (Van Nostrand Reinhold Co., 1963), p 367.

Q-FOG™ Corrosion Chambers - Operating Manual (The Q-Fog Co., April 1991), p 16.

U.S. Army Construction Engineering Research Laboratories (USACERL), "Development of Stylus Electroplating Control and Materials Selection Protocol for Field Application of EMI Coatings," Phase I Progress Report for 1 October - 31 December 1993 (USACERL, 11 February 1994).

U.S. Federal Code of Regulations, 40 CFR Part 268.43(a).

USACERL, "Development of Stylus Electroplating Control and Materials Selection Protocol for Field Application of EMI Coatings," Phase II Progress Report for 1 January - 15 April 1994 (USACERL, 6 May 1994).

USACERL, "Development of Stylus Electroplating Control and Materials Selection Protocol for Field Application of EMI Coatings," Phase III Progress Report for 1 January - 15 April 1994 (USACERL, 31 August 1994).

Van Vlack, Lawrence H., *Elements of Materials Science and Engineering*, 3rd ed. (Addison-Wesley Publishing Co., 1977), pp 411-435.

Walpole, Ronald E., *Introduction to Statistics* (The MacMillan Co., 1968), p 300.

Abbreviations and Acronyms

AES   auger electron spectroscopy

AISI/SAE   American Iron and Steel Institute/Society of Automotive Engineers

BF   broadface

CBF   channel broadface

CF   channel face

DC   direct current

DSMDPS   Deployable Strategic Mission Data Preparation Shelter

EDX   energy dispersive x-ray

EMI   electromagnetic interference

EMP   electromagnetic pulse

HF   half face

KE   knife edge

MSDS   material safety data sheet

RCRA   Resource Conservation and Recovery Act

SEM   scanning electron microscope

SSD   sample standard deviations

USACERL DISTRIBUTION

Chief of Engineers
 ATTN: CEHEC-IM-LH (2)
 ATTN: CEHEC-IM-LP (2)
 ATTN: CEMP
 ATTN: CEMP-E
 ATTN: CEMP-C
 ATTN: CEMP-ET
 ATTN: CERD-L
 ATTN: CERD-M

CECPW 22310-3862
 ATTN: CECPW-K
 ATTN: CECPW-E
 ATTN: CECPW-FT
 ATTN: CECPW-ZC

US Army Engineer District, Omaha
 ATTN: CEMRO-ED-ST

US Army Materiel Command (AMC)
 Alexandria, VA 22333-0001
 ATTN: AMCEN-F

Fort Belvoir 22060
 ATTN: CETEC-IM-T
 ATTN: CETEC-ES 22315-3803

USA Natick RD&E Center 01760
 ATTN: STRNC-DT
 ATTN: AMSSC-S-IMI

US Army Materials Tech Lab
 ATTN: SLCMT-DPW 02172

CEWES 39180
 ATTN: Library

CECRL 03755
 ATTN: Library

US Army ARDEC 07806-5000
 ATTN: AMSTA-AR-IMC

Engr Societies Library
 ATTN: Acquisitions 10017

Defense Nuclear Agency
 ATTN: NADS 20305
 ATTN: HQ DNA/RAEE

Naval Facilities Engr Command
 ATTN: Facilities Engr Command (8)
 ATTN: Code 04C (NAVFAC 15C)
 ATTN: Public Works Center (8)
 ATTN: Naval Facilities Engr Service Center 93043-4328

Tyndall AFB 32403
 ATTN: HQAFCESA/CES
 ATTN: Engrg & Srvc Lab
 ATTN: HQAFCESA/CESE

Nat'l Institute of Standards & Tech
 ATTN: Library 20899

McClellan AFB, CA 95652-1027
 ATTN: SM-ALC/LHH

Hanscom AFB, MA 01731-2816
 ATTN: ESC/AVMS (2)

Keesler AFB, MS 39534-2634
 ATTN: 738 EIS/EEEF

U.S. Naval Air Systems Command 22243
 ATTN: AIR 3.6.4.1

U.S. Army Soldier Systems Command 01760-5018
 ATTN: SATNC-WST

U.S. Army Research Laboratory 20783-1197
 ATTN: AMSRL-WT-ND

Defense Tech Info Center 22060-6218
 ATTN: DTIC-O (2)

58
+1
2/96